UNIVERSITY OF SÃO PAULO POLYTECHNIC SCHOOL
HYDRAULIC AND ENVIRONMENTAL ENGINEERING

THE INFLUENCE OF THE NORTH ATLANTIC OSCILLATION AND ITS CENTRES OF PRESSURE OVER THE NORTH NORTHEAST BRAZIL RAINY SEASON

Thomas Fassi

São Paulo
2018

Thomas Fassi

THE INFLUENCE OF THE NORTH ATLANTIC OSCILLATION AND ITS CENTRES OF PRESSURE OVER THE NORTH NORTHEAST BRAZIL RAINY SEASON

Graduation project presented to the Polytechnic School of the University of Sao Paulo to obtain the degree of graduation in engineering

Concentration area: Atmospheric science

Advisor: Professor Doctor Tercio Ambrizzi

São Paulo
2018

FICHA CATALOGRÀFICA

Fassi, Thomas
THE INFLUENCE OF THE NORTH ATLANTIC OSCILLATION AND ITS CENTRES OF PRESSURE OVER THE NORTH NORTHEAST BRAZIL RAINY SEASON / T. Fassi, T. Ambrizzi -- São Paulo, 2018.
86 p.

Trabalho de Formatura - Escola Politécnica da Universidade de São Paulo. Departamento de Engenharia de Hidráulica e Ambiental.

1.Climatologia 2.Precipitações no Norte do Nordeste do Brasil 3.Oscilação do Atlântico Norte I.Universidade de São Paulo. Escola Politécnica. Departamento de Engenharia de Hidráulica e Ambiental II.t. III.Ambrizzi, Tercio

ABSTRACT

This study will investigate the influence of the North Atlantic Oscillation (NAO), the main teleconnection pattern of the Northern Hemisphere, over the Northern Northeast Brazil (NNE) rainy season. This relationship is analysed considering the average March-April-May rainfall to describe the NNE rainy season and the boreal wintertime NAO (December to March). The NAO teleconnection is represented by means of the classical NAO indices (station based and derived from principal component analysis) and considering the climatological displacements of its centres of pressure, obtained through a cluster analysis. Pearson's linear correlation coefficient and composite analysis are used to describe the relationship between the two phenomena. Winds and SST fields are presented to show the atmospheric-oceanic connection between the NAO related centre of pressure and the NNE rainfall. The results obtained in this work suggest that the NAO influence over the NNE rainy season is stronger if the teleconnection is not represented by the classical indices but if the area of action of the NAO centres of pressure is considered. Specifically, the area included between 60W-20W and 25N-40N present a significative relationship with the NNE rainy season. The composite analysis shows that high values of the SLP in this area during boreal winter (related to an anomalous displacement of the southern NAO centre of pressure) generate anomalies in the wind and SST field, thus forcing abundant precipitation over NNE. The northern centre of pressure seems to play a secondary role over the NNE precipitation. In the end, an index based on the SLP values in the above specified area is constructed. The index shows good statistical relationship with the NNE rainy season and can be used to improve the forecast in this region.

GLOSSARY

CP = Centre of pressure

ENSO = El Niño Southern Oscillation

EOF = Empirical Orthogonal Functions

ITCZ = Intertropical Convergence Zone

MJO = Madden-Julian Oscillation

NA = North Atlantic

NAO = North Atlantic Oscillation

NAOcp = North Atlantic Oscillation “Centres of pressure” Index

NAOpc = North Atlantic Oscillation “Principal Component” Index

NAOs = North Atlantic Oscillation “South” Index

NAOsb = North Atlantic Oscillation “Station-Based” Index

NEB = Northeast Brazil

NNE = North Northeast Brazil

ONI = Oceanic Niño Index

PCA = Principal Component Analysis

SLP = Surface Level Pressure

SST = Sea Surface Temperature

WES = Evaporation – Wind – SST

SUMMARY

1. INTRODUCTION 7

1.1. NNE and NEB characteristics 7

1.2. The "secas" of the nordeste 9

2. OBJECTIVES 10

3. LITERATURE REVIEW 10

3.1. The northern northeast rainfall 10

3.1.1. NEB rainy season characteristics 11

3.1.2. NNE rainfall variability – introduction 12

3.1.3. Factors influencing the rainfall variability in NNE 12

3.1.4. Circulation departures of wet and dry years 16

3.2. The North Atlantic Oscillation (NAO) 17

3.2.1. Introduction 18

3.2.2. The spatial signature of the NAO 20

3.2.3. Indices used to represent the NAO 24

3.2.4. Mechanisms that affect the behaviour of the NAO 25

3.2.5. NAO influence over the NH 26

3.2.6. NAO influence over the tropics 28

4. DATA, METHODOLOGY AND STATISTICAL TOOLS 29

4.1. Data 30

4.2. Methodology 31

4.2.1. NAO - NNE precipitation relationship 32

4.2.2. NAO's centres of action - NNE precipitation relationship 34

4.2.3. Wind and SST fields associated with NNE precipitation anomalies 34

4.2.4. NAOs and NAOcp index construction process 35

4.3. Statistical tools 36

4.3.1. Pearson correlation coefficient 36

4.3.2. Composite analysis 37

4.3.3. T-test 38

5. RESULTS AND DISCUSSION 39

5.1. NAO - NNE precipitation relationship 39

5.1.1. Monthly NAO - NNE rainy season correlation and composite 39

5.1.2. Analysis of the DRY- composite case 51

5.2. North Atlantic SLP field - NNE precipitation relationship 53
5.3. Surface wind and SST fields associated with NNE precipitation anomalies 61
5.4. NAOcp and naos index 74
6. CONCLUSIONS 81
6.1. Final remarks 81
6.2. Suggestions for future researches 83
REFERENCES 84

1. INTRODUCTION

1.1. NNE and NEB characteristics

The North of Northeast Brazil (NNE) is a region that comprehends the Ceará state, part of Rio Grande do Norte, Piauí and Maranhão and the western area of Pernambuco and Paraíba. It's approximately located between 44,5°-37,5°W and 3,5°-8,5°S. The region is divided in two natural regions, described by Carlos Garcia in his work "O que é o Nordeste Brasileiro" (1985, pp. 20-24): "O sertão" ("Backlands") and "O Meio-Norte" ("Midnorth"). The first region include part of Piauí, the whole Ceará, most of Rio Grande do Norte, Paraibá, Pernambuco and Bahia and a small area of Alagoas, Sergipe and Minas Gerais. This territory is characterized by a semi-arid climate and is almost totally covered by the "caatinga" vegetation ("white forest" in the local language), where xerophytes plants, that are resistant to water scarcity, are predominant. The rest of Piauí and the Maranhão state compose the "Meio-Norte", a transition region between the dry Northeast, the Center-West region and the Amazon. The average annual rainfall is 1000 mm/year, but the precipitations' spatial variability is very high: in the east part the climate conditions are similar to those of Sertão, while the North of Maranhão has rainfall amount comparable to those of Amazonia. The vegetation change with the climate conditions: in the South, the "cerrado" (a tropical savanna) is predominant, the east part is covered by caatinga and the north region is characterized by the dense vegetation typical of Amazonia.

NNE is included in the political 'Nordeste' region of Brazil (NEB), a densely populated area that counts 56.560.081 inhabitants (IBGE, 2015). Most of the population of the NEB lives along the coast, where most of the commercial, industrial and touristic activities are concentrated; the interior part is less populated, and the economy is based on agriculture and cattle ranching. The income distribution of the NEB is very unequal, and this gap increase in the interior sector, where a few number of people own the greatest amount of land. Evidences of this scheme were already reported by Carlos Garcia (1985, p.27), who wrote that in 1980 the 10% of richest people concentrated the 70% of the total revenue. Nowadays, the situation is going better but is still critical: looking at the POF (*"Pesquisa de Orçamento*

Familiar", Family Income Research) microdata of the year 2008/2009, the 10% of richest people own the 46,4 of the total income of the region and the Gini coefficient[1], that measure the degree of income distribution, is the highest among the Brazil's region (POF, 2008/2009). Overall, 58% of the population lives in poverty conditions, with a daily income below 2$ (Germany, 2011).

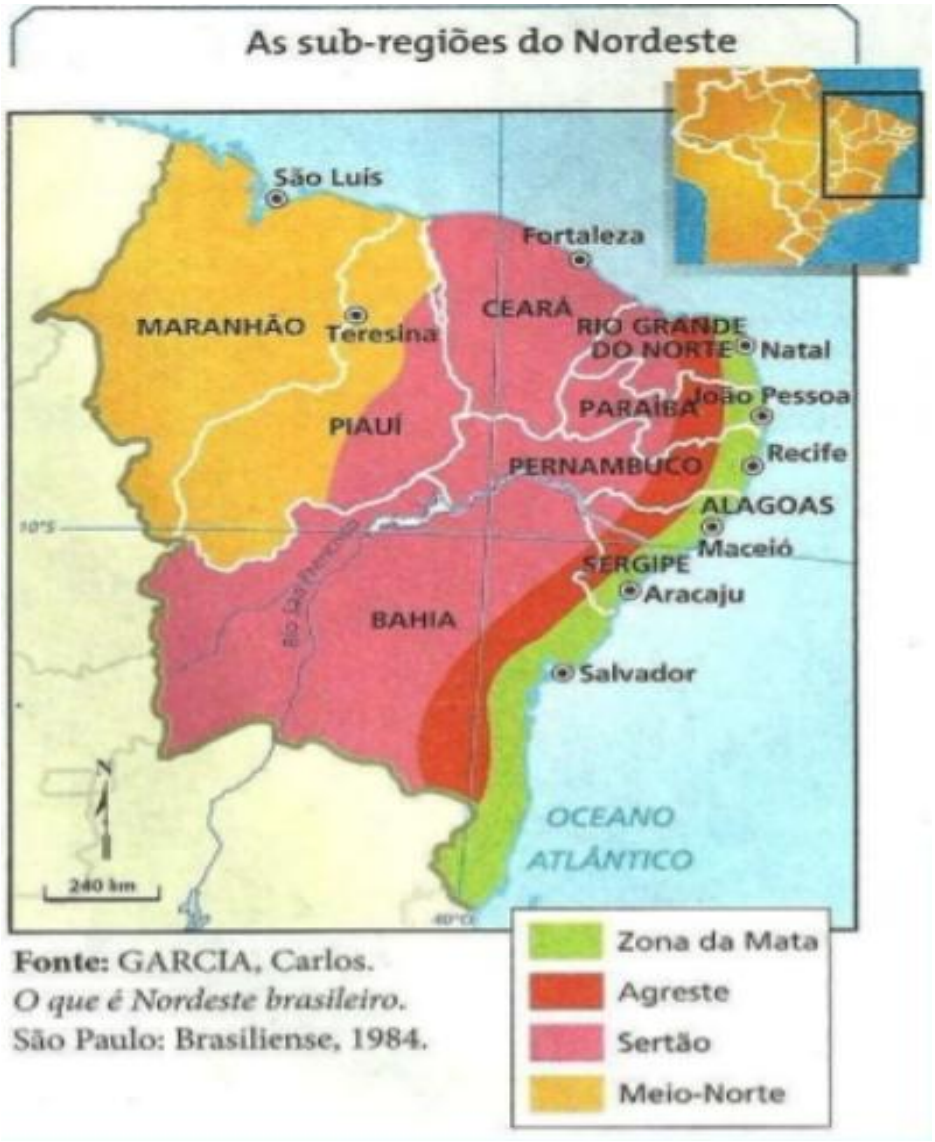

Figure 1. Northeast natural regions and NNE localization

[1] If the coefficient is equal to 0, it means that the income is perfectly the same for each person; if it's equal to 1, all the income is concentrated in one individual.

1.2. The “secas” of the nordeste

Except the Maranhão state, all the Northeast states have portions of their territories that can be reached by the Secas (Gonçalves de Souza, 1979). The Brazilian author Gonçalves de Souza (1979, p. 71) defined the Seca as the situation in which, during the rainfall season, the pluviometry indices are significantly below than normal, and the agriculture and cattle ranching activities become impracticable with the usual methods. He underlined that the phenomenon can continue for one year and might persist up to three years. According to G.T. Trewartha (1962, p. 50) the extension of the drought area varies in extent and location from year to year, thus complicating the definition of the dry region boundaries.

The Secas has ever affected the Northeast Brazil, since its Portuguese colonization. The worst Secas of the past centuries and its socio-economic implication were reported by Gonçalves de Souza (1979, pp. 71-76) in his book “O Nordeste Brasileiro: uma experiência de desenvolvimento regional”. The first seca that was registered happened in 1583, when thousands of “Indios” were forced by the dry condition to leave the interior part of the Pernambuco state to move in direction of the coast looking for food. Others drought events were reported in 1603, 1606, 1614, 1645, 1652 and 1692, and over the last three centuries, were recorded 40 Secas. Just to have an idea of the social impact of these events, during the Seca of 1877-79, half of the Nordeste population died and the total amount of demises between 1877 and 1913 is estimated in 2 million. Despite the government policies, the Secas continued to kill people also in recent times: according to the SUDENE data, during the Seca that starts in 1979 and ends in 1984 (it was one of the worst for time duration and spatial extension) 3,5 million of people died of hunger and diseases. Besides the deaths, others socio-economic consequences are related with droughts: the fall of agricultural and cattle productivity and the migration. For example, in the drought episode of 1778, as reported by the Senator Tomaz Pompeu, “the cattle of the Ceará Captaincy were reduced to less than one octave”; furthermore, during the Seca of 1958, the production value of alimentary cultures decreased by 65,4% compared to the previous year (MINTER, 1973). Migration is an indirect consequence of the Secas; the phenomenon was so intense that, according to

the 1940, 1950, 1960, 1970 demographic censa, the region present negative migration rates of 4%, 5%, 8%, 12% respectively (MINTER, 1973). In fact, the scarcity of food and the slowdown of the whole production chain force the people to emigrate to others Brazilian states as São Paulo or Minas Gerais, looking for new opportunities.

2. OBJECTIVES

The main objective of this work is to find and describe the relationship between the North Atlantic Oscillation teleconnection and the quality of the NNE rainy season, in order to deepen the knowledge over the factors that can act over the precipitation variability of this area.

To achieve this goal, four sub-objectives are defined and will be used as guidelines of the work:

1) Determine if exists a linear and/or nonlinear relationship between two classic NAO indices and the NNE rainfall.
2) Explore the regions of the North Atlantic, in which the NAO acts, that has a stronger relation with the NNE rainfall.
3) Validate the results found in the objective 2 using the Atlantic SST and wind field composites.
4) Construct an index for the NAO teleconnection that is better related to the variability of the NNE rainy season and possibly increase the NNE rainfall predictability.

3. LITERATURE REVIEW

3.1. The northern northeast rainfall

Looking to the uploaded world map of the Koppen-Geiger climate classification (Peel et al, 2007), the Nordeste is divided between “Tropical savanna” and “Hot semi-arid” climates, with a small region dominated by the “Hot Desert” climate (the same of the African Sahara Desert). One would expect to have an annual rainfall distribution typical of the equatorial regions, especially considering the

proximity to the Amazon rainforest but the mean annual rainfall is less than 800 mm/year in the most part of the Nordeste. For this reason, the NEB climate has ever been considered by the scientists as anomalous. In 1928, Sir Gilbert Thomas Walker had already perceived this peculiarity and so dedicated an article to the study of the air circulation system of the Ceará State and how it was influenced by pacific centres of action (Walker, 1928). Later, Trewartha included the Dry Region of Northeastern Brazil in his book "The Earth's Problem Climate", saying that in this zone there is an atypically located dry climate, whose extension is difficult to determine because of the great interannual variability of the dry climate (1962, p. 50).

3.1.1. NEB rainy season characteristics

The Northeast of Brazil is located approximately between 1°-18°S and 35°-47°W, and its general circulation is dominated by the ITCZ (*Intertropical Convergence Zone*), a near-equatorial trough of low pressure that acts between the subtropical highs of the two hemispheres. The ITCZ is characterized by a zone of convergence and maximum cloudiness and rainfall (Hastenrath 1990, p. 302). The latitudinal ITCZ position across the year is the main responsible for interannual rainfall variability over NEB.

The Nordeste has an extension of approximately 1.558.000 km^2. Despite the heavy influence of the ITCZ on the whole area, climate conditions change within the region. Quantitatively, Northeastern precipitations are characterized by amounts that vary from 2000 mm in some coastal areas to 600 mm in sectors of the interior part (Kousky, 1979). It's possible to divide NEB in three sub regions that are characterized by a great time variability of the rainy season (Strang 1972; Kousky 1979; Moura and Shukla 1981). This monthly variability is related to the different rainfall systems that cause precipitation over each sub region (Kousky, 1979). The eastern part of NEB has its rainy season between May and August; the southern part of the region has maximum precipitation in November–December. The NNE rainfall is concentrated in a few months, from February to May (Uvo et al., 1998) and exhibit monthly maximum cantered in March/April (Hastenrath, 2011; Kousky, 1979). Each sub region is influenced by different factors that determine the time location of the rainfall peak. The eastern Northeast climate is particularly affected by land-sea

breeze circulations (Kousky, 1979). This circulation has a nocturnal maximum due to the formation of a convergence zone between the land breeze and the background wind field. The author noted that the land breeze circulation is stronger during Autumn and Winter, when the thermal difference between land and sea is higher than normal. Moreover, Ferreira et al. (1990) identified the occurrence of easterly wave disturbances in the wind field that propagate westward over the Tropical South Atlantic Ocean during the austral autumn and winter. When these disturbances interact with local circulations, low-level convergence increases, causing strong rainfall on the eastern and northern NEB coasts (Torres and Ferreira, 2011). The precipitation in the Southern NEB is controlled by frontal influences of the Southern hemisphere (Kousky, 1979; Chu, 1983). These frontal systems can initiate and organize tropical convection (Kousky, 1985), that leads to the formation of the South Atlantic Convergence Zone, a band of cloudiness oriented in the northwest-southeast direction, from the Amazon basin to Subtropical Atlantic Ocean (Kousky, 1988; Kousky and Cavalcanti, 1988). This configuration holds heavy precipitations in the southern NEB area.

3.1.2. NNE rainfall variability – introduction

There are at least three factors in the surface circulation that are responsible to the time location of the narrow NNE rainy season: the convergence band over the Atlantic is closest to the Nordeste; the surface waters of the Equatorial South Atlantic upstream from the Nordeste are least cold, which serves to enhance the instability and possibly the moisture content of the boundary layer flow; the contrast between warm North equatorial waters and cold waters to the South of the equator is weakest (Hastenrath 1990, p. 302).

3.1.3. Factors influencing the rainfall variability in NNE

a) ZCIT position and intensity

The main factor that influences the duration and amount of NNE rainfall is the position and intensity of the ITCZ during the NNE rainy season (hastenrath and Haller, 1977). Considering the ITCZ displacement, more the convergence band is close to the NNE, more precipitation is expected over NNE (Hastenrath 1990, p.

302). The ITCZ reaches its southernmost position (around 2ºS-4ºS on average) during March and February (Hastenrath and Lamb, 1977), starting the rainy season over NNE. The return of the ITCZ to its more northern position determines the end of the rainy period (Uvo, 1989; Uvo and Nobre, 1989). The timing of this return affects the quality of the NNE rainy season: in near-normal precipitation years, the ITCZ starts its northward displacement around middle April; in wet years, during early May; in dry years, the ITCZ either doesn't reach positions south of the equator at all or retreats northward early, often during March (Hastenrath and Heller, 1977; Uvo, 1989; Uvo and Nobre, 1989).

b) Atlantic SST

Tropical Atlantic SST plays a fundamental role in the mechanism that control the low-pressure trough and the ITCZ displacement. In fact, the annual motion is induced by variation in the interhemispheric SST gradient: during the boreal summer the gradient is steep; the system composed by the band of warmest SST, the low-pressure trough and the ITCZ is located far North. In the progression from boreal summer to winter, the interhemispheric gradient weakens, and the system migrate southward, reaching his southernmost position around the beginning of boreal spring. After that, the waters of the tropical North Atlantic warm, the interhemispheric SST gradient steepens, and the complex of SST maximum, pressure trough and ITCZ migrate northward (Hastenrath, 2011). At this point, the annual cycle restart. The three "actors" mentioned above move together because the SST maximum hydrostatically controls the low-pressure trough, into which flow the airstreams from the two hemispheres, and thus the ITCZ position, as referred by Hastenrath and Druyan (1993) and Hastenrath and Greischar (1993).

The tropical Atlantic SST - NNE precipitation relationship was investigated from a spatial and temporal point of view by many authors: Hastenrath and Haller (1977) identified positive departures "extending from the real of the Canary current across the North Atlantic to the northeast coast of South America and the Caribbean" during a deficient rainy season; at the same time, most of the South Atlantic waters are anomalously cold. They also observed that the departure patterns are approximately inverted in drought years. Moura and Shukla (1981) made an

observational analysis of 25 years of SST anomalies over the tropical Atlantic and rainfall over selected stations of the Northeastern Brazil. They found that the simultaneous occurrence of warm SST anomalies in the north of the equator and cold SST anomalies in the south intensify the ITCZ to the equator, thus reducing moist convection and rainfall. Uvo et al. (Uvo et al., 1998) studied the simultaneous and time-lagged relationship between monthly normalized SST anomalies and monthly normalized NNE rainfall anomalies from January to May. They found a strong relationship between Atlantic SST in March and seasonal precipitation, due to the strong persistence of SST anomalies.

Nobre and Shukla (1981) hypothesized another mechanism that consider the tropical Atlantic SST as the driving force of the NNE precipitation: when tropical North Atlantic SST are warmer than normal during the NNE rainy season, a thermally direct local circulation which has its ascending branch at about 10ºN and its descending branch over Northeast Brazil and the adjoining oceanic region is established. Then, the combined effects of thermally forced subsidence, reduced evaporation and moisture flux convergence inhibits precipitation over NEB.

The tropical North Atlantic SST are influenced by variations in the intensity of the trade winds that, through the WES mechanism (Wind-evaporation-SST), can induce an anomalous increase or decrease of the SST. A wind stress relaxation (strengthening) is related to a tropical North Atlantic SST warming (cooling), and the time lag of this relationship is about two months (Nobre and Shukla, 1996).

c) Pacific SST and ENSO

El Niño–Southern Oscillation (ENSO) is the dominant mode of interannual climate variability observed globally (e.g., Ropelewski and Halpert 1987, 1989; Philander 1990). ENSO is originated by the strong coupling between the tropical ocean and the atmosphere (Bjerknes 1969; Zebiak and Cane 1987) and also contributes to large-scale teleconnections through the middle to high latitudes (Glantz et al. 1991). Already in 1928, Sir G.T. Walker associated Ceará rainfall with the “second group” of the Southern Oscillation; this “second group” is the way he

used to name la Niña events. More recently, Souza and Ambrizzi (2002) studied the impacts over South America rainfall of four ENSO episodes (two for each ENSO phase) in the decade of 80. During El Niño events, they observed a significant weakness of the ascending branch of the Hadley cell over South America tropics. This large scale sinking movement inhibits the convective activity associated to ITCZ and cause drought conditions in the rainy season in most of Northeast Brazil. In La Ninã events was observed a large-scale anomalous ascending movement going from Northeast brazil to the equatorial south Atlantic; this probably enhance the ITCZ activity, resulting in a abundant rainy season in these areas. These results are confirmed by the works of Hastenrath (2006 and 2011), that also identified, during El Niño events, an "atmospheric bridge" from the Pacific to the Atlantic: it consists of an upper-tropospheric wave train that affects the vertical motion over the Atlantic. This, in turn, weakens the meridional pressure gradient over the equatorial Atlantic and the equatorward trade winds from the tropical North Atlantic. This pattern confines the ITCZ anomalously far North and hold to drought conditions in the Nordeste. However, according to correlation analysis between tropical Pacific and Atlantic SST and NEB rainfall made by Uvo et al. (1998), the Pacific correlations were notably weaker than the Atlantic ones, suggesting that the Atlantic Ocean in more directly linked to the positioning and/or strength of the ITCZ precipitation.

d) Madden-Julian Oscillation (MJO)

MJO consists of a planetary-scale mechanism with disturbances in both tropical deep convection and atmospheric circulation, which propagates eastward along the equator in a complete cycle around the globe lasting approximately 30-60 days (Madden and Julian, 1994). De souza and Ambrizzi (2006) applied Wavelet, EOF and composite techniques on 15 years (1987-2011) daily data to describe the intraseasonal rainfall variability over tropical Brazil and its associated dynamical structure. They found that the MJO is the main atmospheric mechanism modulator of the regional rainfall variations over tropical Brazil on an intraseasonal time scale and it effectively contributes to a considerable fraction of the total precipitation over Northeast Brazil.

e) Extratropical North Atlantic

There aren't many studies that try to find a relation between the atmospheric circulation over the North Atlantic and the NEB rainfall. In 1972, Namias made a spatial correlation analysis between the rainfall at Quixeramobirim (Ceará state) station and the 700 mb circulation pattern over the North Atlantic. He found that stronger than normal cyclonic activity near Newfounfland is associated with more than normal rainfall in Ceará. He suggested that this cyclonic activity enhances the Hadley cell circulation thereby enhancing both northeast and southeast trade winds.

A recent study of Cavalcanti (2015) considered wet and dry cases over northern Northeast Brazil to analyse the atmospheric extratropical features in the Atlantic region that affects this area. The study was conducted removing the ENSO effect. They found that the extratropical centres of action displayed by the second mode of North Atlantic atmospheric variability have strong influence on the ITCZ position, thus affecting also the NNE precipitation. In particular, the author underline that high (low) pressure anomalies of the southern centre affect the tropical SST and trade winds, which result in ITCZ shifts and wet (dry) cases over NNE.

3.1.4. Circulation departures of wet and dry years

In this section is presented a resume of the general circulation pattern when NNE rainfall amount is particularly abundant or deficient. The following description is contained in Hastenrath (1984 and 1990). In wet years the near-equatorial trough of low-pressure, the interhemispheric trade wind confluence and the associated band of maximum convergence and cloudiness are displaced southward. Surface waters of the equatorial South Atlantic are anomalously warm, while negative SST departures prevail over the most of the tropical North Atlantic. At the same time, are registered statistically significant departures in positive/negative SLP over North/South tropical Atlantic, in the zonal wind field over the equatorial region and in the meridional wind field over the equatorial Atlantic adjacent to Northeast Brazil. During NNE drought years, the oceanic and atmospheric departure patterns are approximately opposite to those of the wet years. In the figure 2 is showed a simple scheme of the circulation pattern of the dry and wet years.

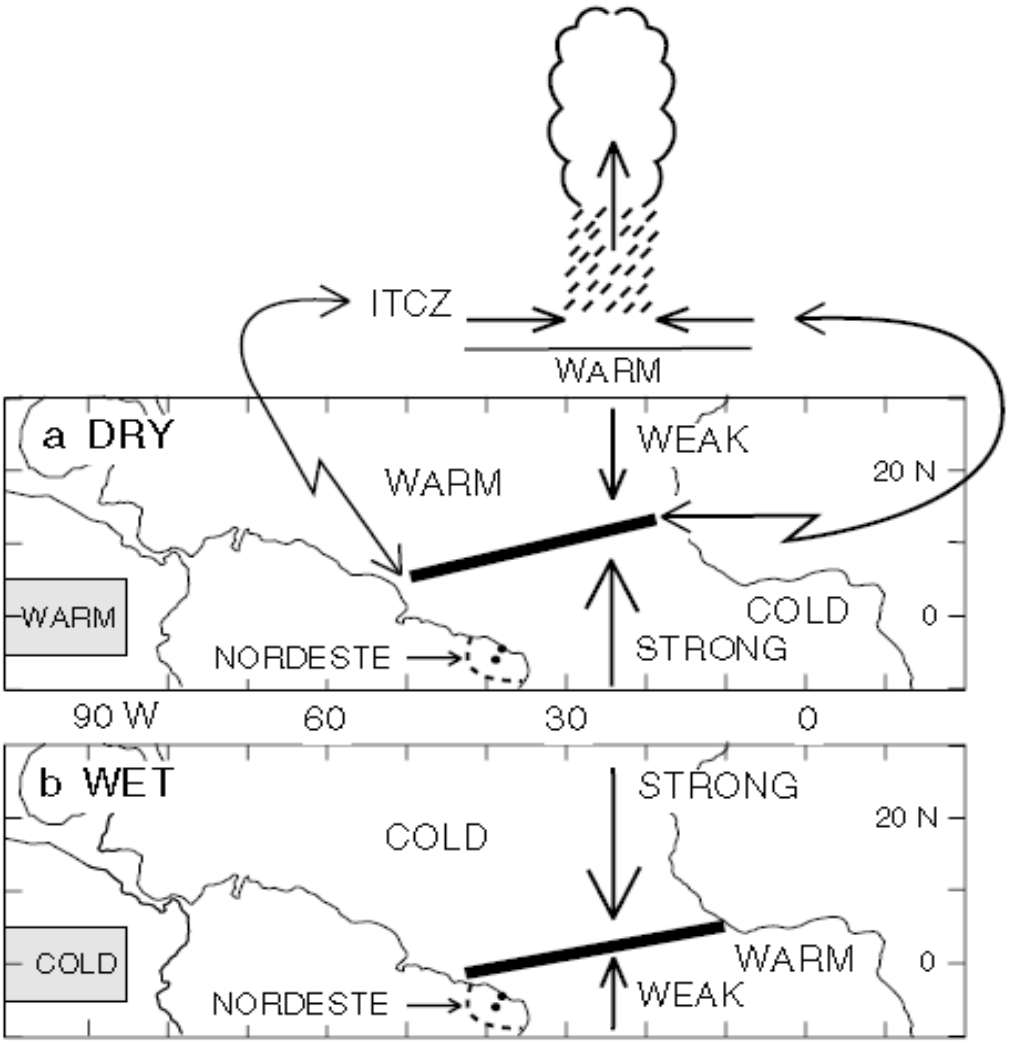

Figure 2. Schematic representation of the of the typical departure circulation in the tropical Atlantic region during NNE dry (upper panel) and wet (lower panel) years. Source: Hastenrath, 2006.

3.2. The North Atlantic Oscillation (NAO)

Most part of the literature review of this section is based on the first chapter "An overview of the North Atlantic oscillation" (Hurrell et al., 2003) of the book "The North Atlantic Oscillation: Climatic Significance and Environmental impact" (Visbeck et al., 2003)

3.2.1. Introduction

The North Atlantic Oscillation (NAO) is the most prominent and recurrent pattern of atmospheric variability over the Northern Hemisphere, especially during boreal winter. The NAO refers to a redistribution of atmospheric mass between the Arctic and the subtropical Atlantic. The shift of the NAO from one phase to another produces large changes over the Atlantic Ocean in:

- mean wind speed and direction;
- heat and moisture transport;
- intensity, path and number of storms.

In that way, this teleconnection influences agricultural harvests, water management, energy budget and fisheries of the neighbouring countries. However, despite the impacts that the NAO can hold to these countries, in the last decades was paid little attention to the prediction of its annual variability. In fact, NAO's annual changes in phase and amplitude were considered unpredictable (Hurrell et al., 2003). Recently, more researches were developed around the mechanisms that govern the NAO predictability, that is essentially related to the oceanic influence and to processes internal to the atmosphere.

The NAO is primarily a north-south dipole characterized by simultaneous out-of-phase anomalies between temperate and high latitudes over the Atlantic sector. It is responsible for large changes in the mean distribution of SLP over the NH from boreal winter (December-February) to boreal summer (June-August), as is represented in Figure 3. The annual cycle of the SLP's spatial distribution over the North Atlantic works as follow: during boreal summer, the subtropical Azores anticyclone cover almost all the North Atlantic; in wintertime this high-pressure system move equatorward and the Icelandic trough predominate. The circulation pattern described above, determines the occurrence of westerly winds across the middle latitudes of the Atlantic sector throughout the year. The intensity of these winds is enhanced when the meridional gradient between the two centres of pressure is stronger.

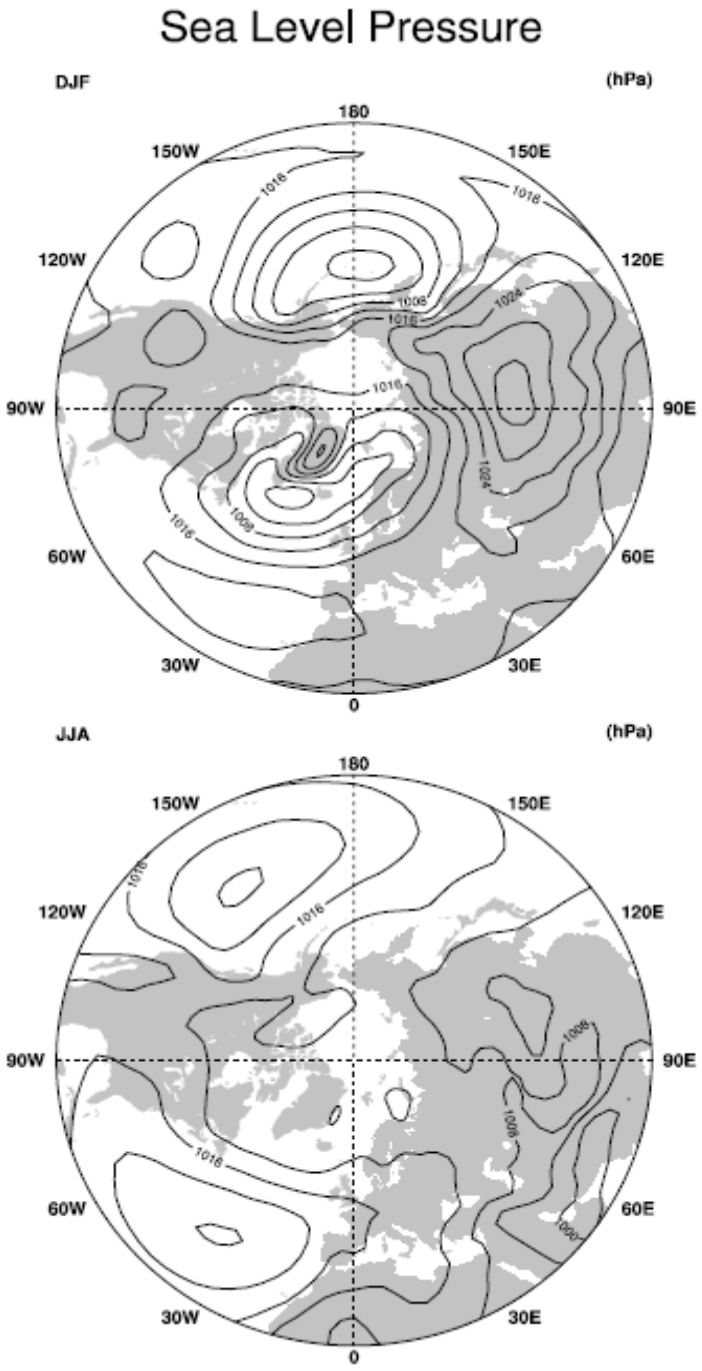

Figure 3. Mean sea level pressure for (top) boreal winter (December-February) and (bottom) boreal summer (June-August). The contour increment is 4 hPa. The maps represent the data from the NCEP/NCAR reanalysis project over 1958-2001 (Kalnay et al., 1996).

In wintertime, the so called positive phase of the NAO, characterized by higher-than-normal surface pressures south of 55º N, combine with a broad region of anomalously low pressure throughout the Arctic. When the NAO is in the positive phase, the climatological meridional pressure gradient is enhanced. In general, the

largest amplitude anomalies occur close to Iceland and Iberian Peninsula. The positive phase is also associated with stronger-than-normal surface westerlies across the middle latitudes of the Atlantic onto Europe, with anomalous southerly flow over the eastern USA and anomalous northerly flow across the Canadian Arctic and the Mediterranean.

3.2.2. The spatial signature of the NAO

There are many ways to determine the spatial structure of the NAO and different records can be used for this purpose. The NAO is the leading REOF of Atlantic Ocean in wintertime both considering 500 hPa height and SLP field. However, SLP charts of NH start in 1899 (Trenbeth and paolino, 1980), in contrast to 500 hPa height charts that are confined to after 1947. So, according to what Hurrell et al. (2003) did, the NAO spatial signature will be analysed using the SLP field records.

The NAO spatial signature can be identified in many ways. The easier method is through one-point correlation maps, with which is possible to recognize the NAO pattern by regions of maximum negative correlation over the Atlantic (Wallace and Gutzler, 1981; Kushnir and Wallace, 1989; Portis et al., 2001).

Another approach is EOF analysis: the NAO is identified from the eigenvectors of the cross-covariance matrix, computed from the time variations of the grid point values of SLP. The orthogonal eigenvectors are then scaled according to the amount of total data variance they explain. This linear approach assumes preferred atmospheric circulation states come in pairs, in which anomalies of opposite polarity have the same spatial structure (Hurrell et al., 2003, p. 8). Authors like Barnston and Livezey (1987), Hurrell and van Loon (1997), Portis et al. (2001), used this approach to identify the components that are responsible the SLP variance over the North Atlantic during boreal winter months. The leading eigenvectors of the cross-covariance matrix calculated from the seasonal (3-month average) SLP anomalies over the North Atlantic are shown in Figure 4.

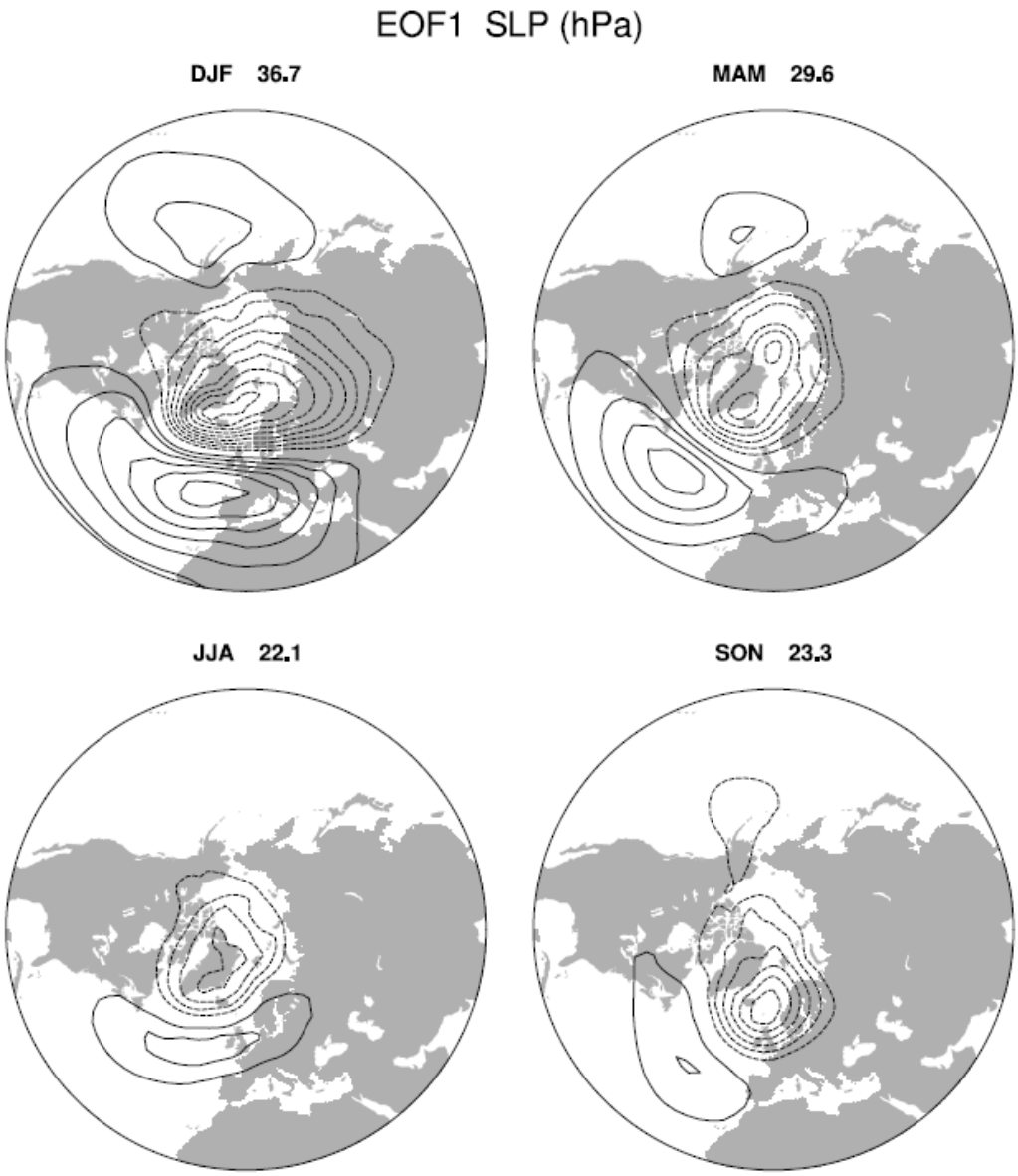

Figure 4. Leading empirical orthogonal functions (EOF 1) of the seasonal mean sea level pressure anomalies in North Atlantic sector (20º-70ºN, 90ºW-40ºE), and the percentage of the total variance they explain. The patterns are displayed in terms of amplitude (hPa), obtained by regressing the hemispheric sea level pressure anomalies upon the leading principal component time series. The contour increment is 0.5 hPa, and the zero contour has been excluded. The data cover 1899-2001. Source: Hurrell et al., 2003

They found that the leading pattern of variability is characterized by a surface pressure dipole that can be view as the NAO, although the spatial pattern is not stationary. From December to February, it accounts for more than one-third of the total variance in SLP over the North Atlantic. The second EOF resembles the East

Atlantic pattern during winter and spring months, and generally accounts for 15% of the total SLP variance. During boreal spring (March-May), the NAO appears as a north-south dipole with the southern centre near the Azores. Both the spatial extent and the amplitude of the SLP anomalies are smaller than during winter, but not by much, and the leading EOF explains 30% of the SLP variance. Boreal summer and autumn (from June to November) are the seasons in which the NAO less influence the NH dynamics. For this reason, most of the studies of the NAO focus on the NH winter months, when the atmosphere is most active dynamically and atmospheric circulation patterns show their largest amplitude. Consequently, the influence of the NAO on surface temperature and precipitation is also greatest at this time of the year; in this season, the NAO can also interact with the slower components of the climate system (the oceans, in particular) to leave persistent surface anomalies (Czaja et al., 2002; Rodwell, 2003). The EOF analysis shows a quite similar spatial pattern of the NAO throughout the year; in opposite, is not possible to say the same thing about the phase variability of this teleconnection, considering that the NAO index can shift from positive to negative values from one month to another.

The interannual spatial variability of the NAO can also be investigated through a nonlinear approach such as cluster analysis (Monahan et al., 2000; 2001). Following the procedures of Cassou and Terray (2001), which are based on the clustering algorithm of Michelangeli et al. (1995), were analysed 100 years (from 1900 to 2001) of December-March monthly SLP data applied over the Atlantic domain (20°-70°N; 90°W-40°E). Were identified four winter climate regimes in SLP (Figure 5): two correspond to the negative and positive phases of the NAO, the other ones display a strong anticyclonic ridge and a trough off western Europe (Wallace and Gutzler, 1981; Barnston and Livezey, 1987).

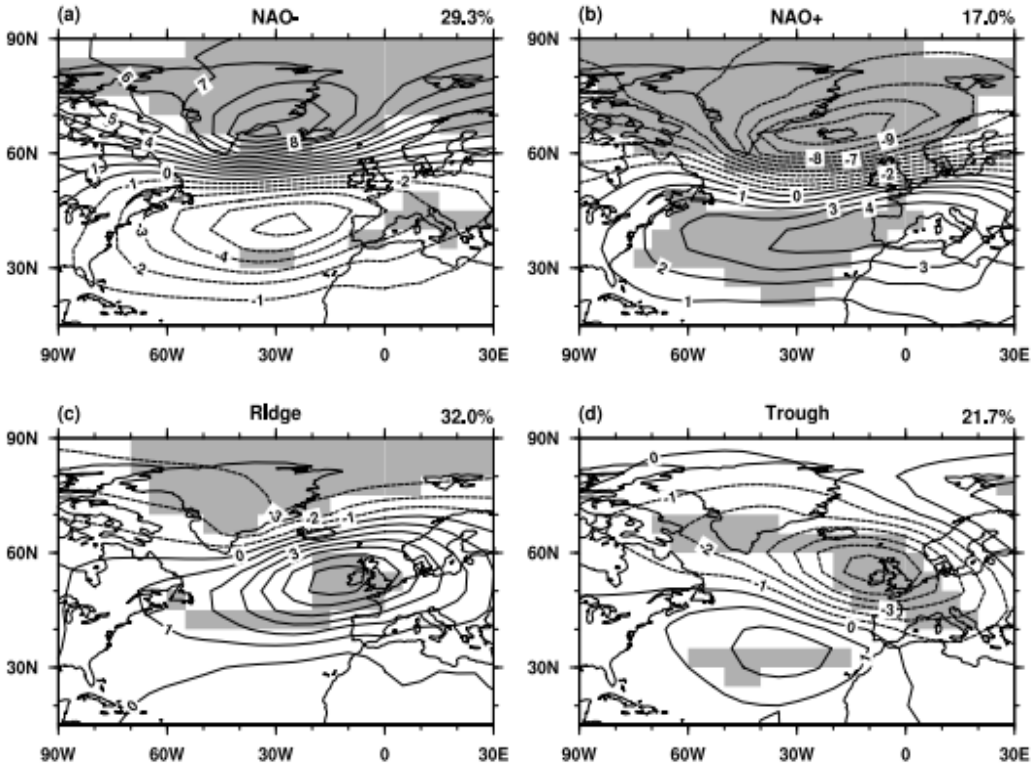

Figure 5. Boreal winter (December-March) climate regimes in sea level pressure (hPa) over the North Atlantic domain (20º-70ºN, 90ºW-40ºE) using monthly data over 1900-2001. Shaded areas exceed the 95% confidence level using T and F statistics [see Cassou, 2001]. The percentage at the top right of each panel expresses the frequency of occurrence of a cluster out of all winter months since 1900. The contour interval is 1 hPa.

Both the ridge and negative NAO regimes occur in about 30% of all winter months, while both the positive NAO and trough regimes are displayed in about 20% of all cases. This cluster analysis showed the most common monthly regimes: nevertheless, rarely one winter season was dominated by only one of the four regimes. This is because there is a large amount of within-season variance in the atmospheric circulation of the North Atlantic. Over the ~100-year record, for example, all four winter months are classified as the negative NAO regime for only four winters (1936,1940,1969, and 1977), only two winters (1989 and 1990) are classified under the positive NAO regime and nine winters in which neither the positive or negative NAO regimes weren't identified.

3.2.3. Indices used to represent the NAO

As it was illustrated, there isn't a unique way to define the spatial structure of the NAO; it follows that there is no universally accepted index to describe the temporal evolution of the phenomenon.

NAO indices are usually derived either from the difference in SLP anomalies between northern and southern locations (that can be stations or gridded analyses) or near to the climatological centres of action of the NAO, or from the PC time series of the leading (usually regional) EOF SLP. Each method has advantages and disadvantages. The major benefit of the station-based ones is their extension back to the mid-19th century or earlier. A disadvantage is that they are fixed in space, being able to capture the NAO variability only for parts of the year (Hurrell and van Loon, 1997; Portis et al., 2001; Jones 2003). Moreover, individual station pressures are significantly affected by small-scale and transient meteorological phenomena not related to the NAO and, thus, contain noise. Contrarily, the PC time series approach allows to capture the full NAO spatial pattern but the indices, based on gridded SLP data, can only be computed for parts of the 20th century.

When station-based indices are used, the location of the point of measure must be chosen with some criteria. After he had analysed the coupled modes of wintertime variability in SLP and surface temperature over the North Atlantic, Hurrell (1995) concluded that the southern-node station of Lisbon, Portugal, better captured the NAO-related variance. Jones et al. (2003) suggested that the specific location of the northern node (among stations in Iceland) is not critical but the choice of southern stations does make some difference. One graphical comparison between the most used indices is represented in Figure 6.

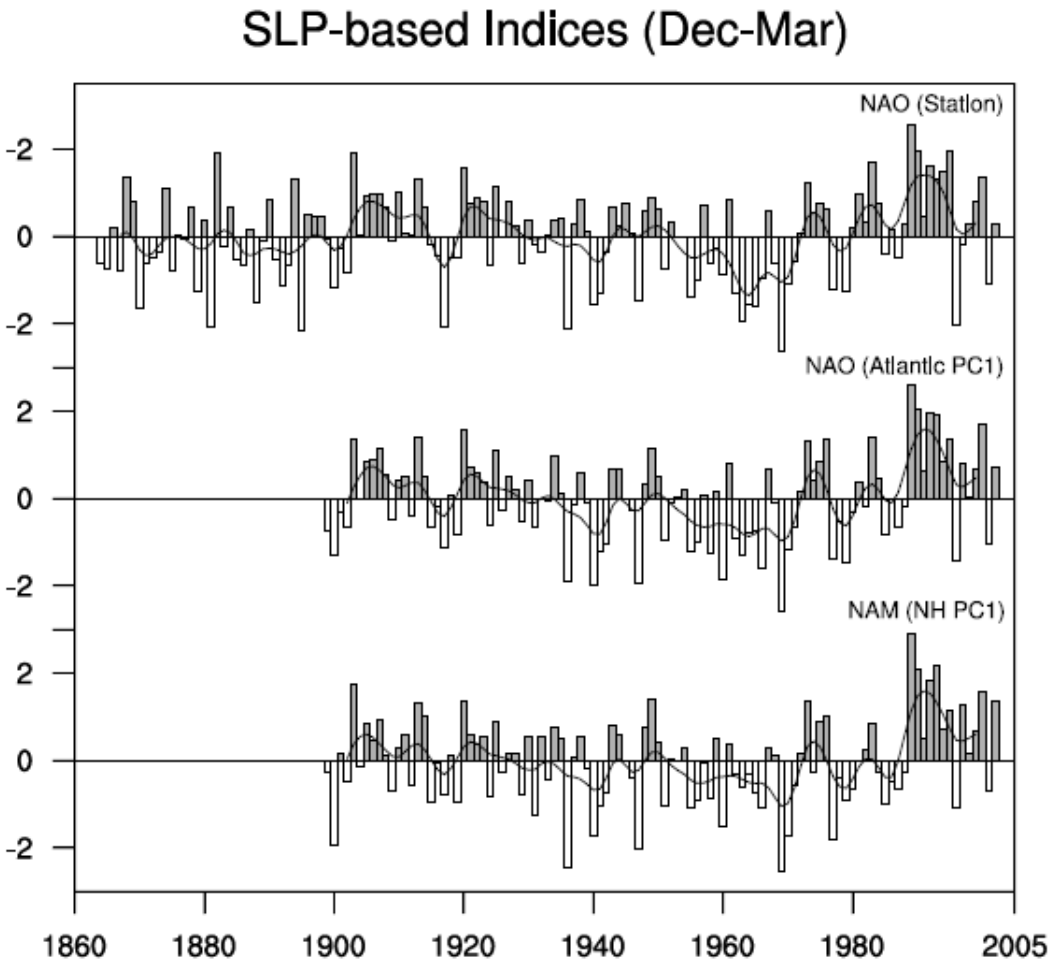

Figure 6. Normalized indices of the mean winter (December-March) NAO constructed from sea level pressure data. In the top panel, the index is based on the difference of normalized sea level pressure between Lisbon, Portugal and Stykkisholmur/Reykjavik, Iceland from 1864 through 2002. The average winter sea level pressure data at each station were normalized by division of each seasonal pressure by the long-term mean (1864-1983) standard deviation. In the middle panel, the index is the principal component time series of the leading empirical orthogonal function (EOF) of Atlantic-sector sea level pressure (bottom panel of Figure 8). In the lower panel, the index is the principal component time series of the leading EOF of Northern Hemisphere sea level pressure (top panel of Figure 8). The heavy solid lines represent the indices smoothed to remove fluctuations with periods less than 4 years. The indicated year corresponds to the January of the winter season (e.g., 1990 is the winter of 1989/1990). See http://www.cgd.ucar.edu/~jhurrell/nao.html for updated time series. Source: Hurrell et al., 2003

3.2.4. Mechanisms that affect the behaviour of the NAO

The NAO is considered a phenomenon whose predictability is limited. In fact, there is a shared assumption among the scientists that the NAO is a mode of

variability internal to the atmosphere. So, it is regulated by the interactions between the atmosphere and the underlying surface, and between the stratosphere and the troposphere. Nevertheless, there are other external factors that may influence the NAO, such as volcanic aerosols, the solar activity and the anthropogenic influence on the Earth's climate. Nowadays, there isn't a shared consensus about the relative effect over the NAO of each factor, especially considering the long (interdecadal) time scale variability.

The experts put great attention about the ocean's influence over the NAO. Though the effect of the extratropical SST field to the overlying atmosphere is considerably small compared to the influence of the internal atmospheric variability (Seager et al., 2000), Czaja et al. (2003) claim that the study of the ocean-atmosphere interaction could be important to understand the details of the observed amplitude of the NAO and its long-term temporal behaviour. Rodwell (2003) also suggest that these investigations are useful to improve the NAO predictability. With this purpose, many studies have investigated the relationship between the NAO and the tropical oceans, finding that NAO variability is closely linked to SST variations over the tropical Atlantic: the change of the equatorial meridional gradient can affect the middle latitude circulation over the North Atlantic (Xie and Tanimoto, 1998; Rajagopalan et al., 1998; Venzke et al., 1999; Robertson et al., 2000; Sutton et al., 2001). Nevertheless, there is already uncertainty about the relative influence of the tropical and extratropical oceans over the NAO.

3.2.5. NAO influence over the NH

During the boreal winter, the NAO influence heavily the NH SST and surface air temperatures over land. In fact, NAO variability is well correlated with precipitation and temperature of different areas of NH such as Eurasia, the Mediterranean basin, the North America, the Arctic and the North Atlantic Ocean. Below are presented the circulation patterns associated with a positive phase of the NAO during winter; in the negative phase, the variables behaviour is almost the opposite:

- Westerly winds are enhanced across the North Atlantic and transport moist and warm air over much of Europe; at the same time, strong northerly flows

over Canada and Greenland carry cold air southward, decreasing the surface temperatures over the northwest Atlantic. The increase of the flow associated to the clockwise rotation of the southern centre of action cause cooling in North Africa and the Middle East and Warming in North America. The differences in the wind intensity associated with the SLP deviation between the positive and negative NAO are shown in Figure 7.

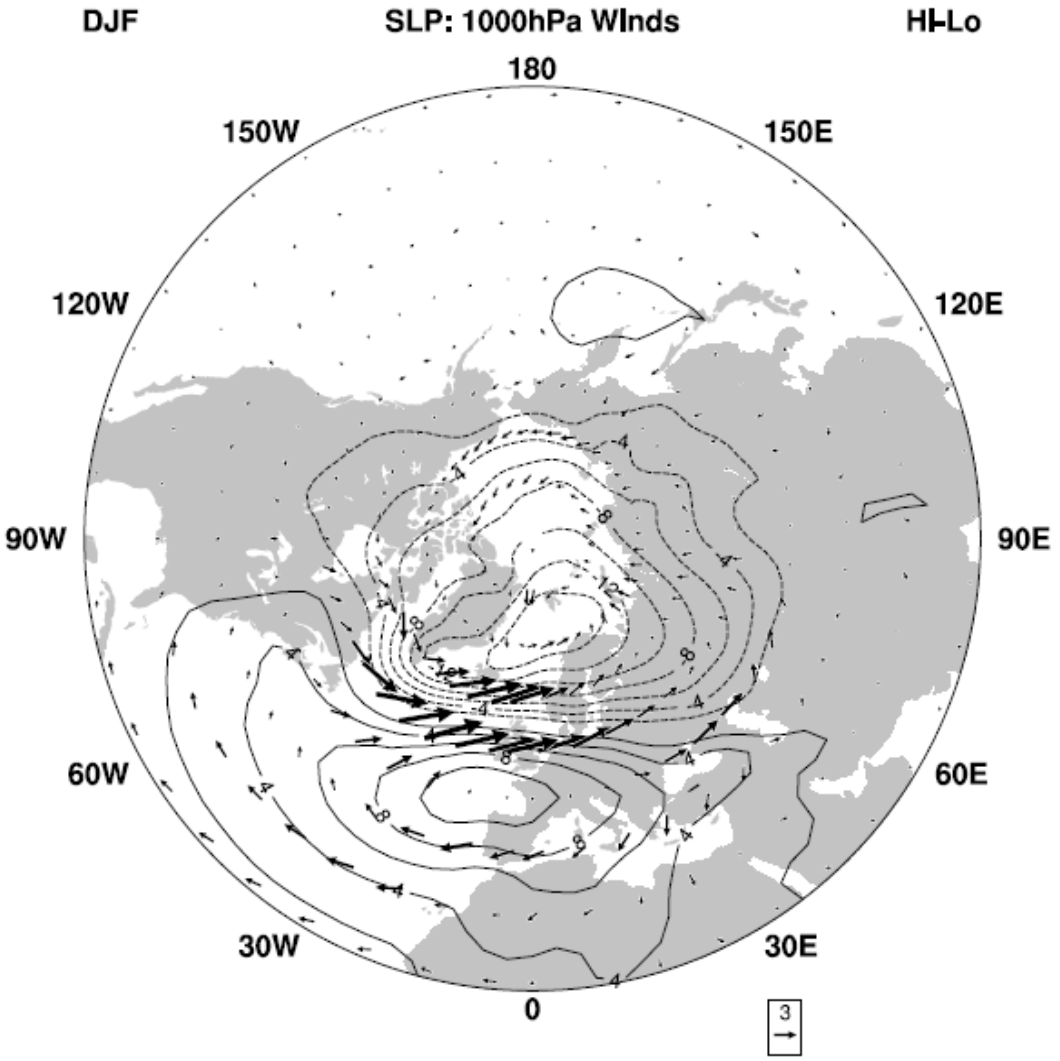

Figure 7. The difference in boreal winter (December-February) mean sea level pressure and 1000 hPa vector winds between positive and negative index phases of the NAO. The composites are constructed from winter data (the NCEP/NCAR reanalyses over 1958-2001) when the magnitude of the NAO index (defined as the principal component time series of the leading empirical orthogonal function of Atlantic-sector sea level pressure, as in Figures 6 and 10) exceeds one standard deviation. Nine winters are included in each composite. The contour increment for sea level pressure is 2 hPa,

negative values are indicated by the dashed contours, and the zero contour has been excluded. The scaling vector is 3 m s-1. Source: Hurrell et al., 2003

- The Atlantic storm activity shift north-eastward, with an increase in activity in the band from Newfoundland to the northern Europe and a modest decrease to the southern regions (Rogers, 1990, 1997; Hurrell and van Loon, 1997; Serreze et al., 1997; Alexandersson et al., 1998).

The changes in the surface winds and in the air-sea exchanges associated with the NAO affect the North Atlantic SST variability. The relationship between the NAO and the SST variability is stronger when the NAO index leads the one associated to SST by several weeks: this result, strengthen the theory that large-scale SST over the extratropical responds to atmospheric forcing (the NAO, in this case) on monthly and seasonal timescale (e.g., Battisti et al., 1995; Delworth, 1996; Deser and Timlin, 1997). However, Kushnir (1994) suggests that persistent SST anomalies seem to be related to persistent anomalous pattern of SLP (such as the NAO) even over longer timescale.

3.2.6. NAO influence over the tropics

As it was explained above, the NAO is the main mode of variability of the Northern Hemisphere and its shifts are largely explained by processes internal to the atmosphere. For this reason, it's still difficult for the GCM models to detect the noisy climate signals in the extratropics and consequently it's not possible to fully describe the teleconnection that links tropics and extratropics (Okumura et al., 2001).

Already in 1972, Namias discovered a link between the tropics and the NAO: he found a correlation between the southern centre of action of the NAO and the northeast Brazil rainfall in boreal winter and spring; he also pointed out that the subtropical/mid-latitude north Atlantic high often regulate the northeast trade winds. More recently, many scientists analysed the relation between tropics and extratropics focusing in the interaction between the NAO and the Cross-Equatorial SST Gradient (CESG) (Xie and Tanimoto, 1998; Chang et al., 2000; Czaja et al., 2002; and Kushnir et al., 2002). They suggested that the shifts in the Azores High and the Wind Evaporation SST (WES) feedback are the driven mechanisms that connect the two

elements. The Southern SLP centre of the NAO is responsible for changes in the strength of north-easterly trade winds that affect the northern tropical Atlantic SST. The WES feedback is a purely thermodynamic mechanism, whose description is reported from a paper of Mahajan and Chang (2010). The WES feedback works as follow in the tropics: consider an anomalous cross-equatorial northward positive SST gradient that generates anomalous northward cross-equatorial surface winds. These winds turn westward (eastward) in the southern (northern) side of the equator because of the Coriolis force, thereby enhancing (reducing) the background south-easterly (north-easterly) trade winds, leading to an increase (decrease) in evaporation, which in turn decreases (increases) the SST. The interaction between the surface winds, evaporation and SST thus forms a positive feedback amplifying the initial SST gradient. (Mahajan and Chang, 2010). Simulations made with coupled ocean-atmospheric GCM models, in which the air-sea feedback was alternatively added and removed, show that the NAO influence on the CESG requires the bridging effect of the air-sea interaction, that is responsible to drive the impacts of subtropical anomalies into the deep tropics (Xie and Tonimoto, 1998; Chiang and Bitz, 2005; Chang et al., 2001). Also, Yu and Lin (2016), using NCEP reanalysis data and SST observations, identified the anomalous meridional atmospheric circulation over the Atlantic Ocean as the mechanism that connect the NAO and the tropical American-Atlantic heating. However, also in this issue there isn't a complete agreement between the scientists: for example, Delworth and Metha (1998) reported that the NAO influence is limited to north of the equator.

4. DATA, METHODOLOGY AND STATISTICAL TOOLS

The first part of this chapter contains the description of the data used in this work; the second one holds the methodology adopted to develop the research; the last section presents the statistical methods used throughout the work.

Excluding the NAO data, all the data used are in NetCDF (network Common Data Form) format, that according to the UniData NetCDF page: "... is an interface for array-oriented data access and a library that provides an implementation of the

interface. The netCDF library also defines a machine-independent format for representing scientific data. Together, the interface, library, and format support the creation, access, and sharing of scientific data." The netCDF software was developed at the Unidata Program Center in Boulder, Colorado.

The datasets are obtained from the Earth System Research Laboratory (ESRL) section of the US National Oceanic and Atmospheric Administration (NOAA) website.

The analysis is performed using the software MATLAB, version 2017b.

4.1. Data

The data used for the precipitation is the monthly precipitation dataset "Full Data Product - V7" obtained from the Global Precipitation Climatology Centre (GPCC). It consists on a regular grid based on quality-controlled data from 67200 stations world-wide that feature record durations of 10 years or longer. A spatial resolution of 1.0 x 1.0 degree has been chosen.

The two datasets of the NAO index are obtained respectively from the projects "The Climate Data Guide: Hurrell North Atlantic Oscillation (NAO) Index (PC-based)" and "The Climate Data Guide: Hurrell North Atlantic Oscillation (NAO) Index (Station-based)", available on the <https://climatedataguide.ucar.edu/climate-data> website. The PC-based index is the time series of the leading Empirical Orthogonal Function (EOF) of SLP anomalies over the Atlantic sector, range from 20N-80N to 90W-40E. The monthly station-based index is constructed through the difference of normalized sea level pressure (SLP) between Ponta Delgada (Azores islands - 37.7428° N, 25.6806° W) and Reykjavik (Iceland - 64.1265° N, 21.8174° W) since 1864. The SLP values at each station were normalized by removing the long-term mean and by dividing by the long-term standard deviation. Both the long-term means and standard deviations are based on the period 1864-1983.

The Oceanic Niño Index (ONI) is obtained from the <http://origin.cpc.ncep.noaa.gov/products/analysis_monitoring/ensostuff/ONI_v5.php> website and is calculated as the 3 months running mean of ERSST.v5 SST anomalies in the Niño 3.4 region (5ºN-5ºS, 120º-170ºW).

The monthly Sea Level Pressure data come from the NCEP/NCAR Reanalysis 1 project, that use a state-of-the-art analysis/forecast system to perform data assimilation using part data from 1948 to the present. The data is available in a 2.5 x 2.5-degree global grid (144x73). The SLP variable is an instantaneous value at the reference time. It is an average of instantaneous values ate the four reference times: 0, 6, 12 and 18z over the monthly period.

The Sea Surface Temperature data is obtained from the COBE SST2 dataset. It includes monthly SST means from January 1950 to December 2015. The daily SST field is constructed as a sum of a trend, interannual variations, and daily changes, using in situ SST. All SST values are accompanied with theory-based analysis errors as a measure of reliability. More information about the dataset characteristics is contained in Hirahara, S., Ishii, M., and Y. Fukuda (2014). The dataset is available in the NOAA website <https://www.esrl.noaa.gov/psd/data/gridded/data.cobe2.html> in a 1.0 x 1.0 global grid.

The U (east-west direction) and V (north-south direction) wind component dataset is also obtained from the from the NCEP/NCAR Reanalysis 1 project and is computed with the same methodology of the SLP dataset. The data are also available within a grid of 2.5 x 2.5 longitude-latitude width.

4.2. Methodology

The analysis is performed in the 1981-2010 climatological period and all data have been downloaded at the monthly time scale. In that way, the starting dataset is constituted of 360-time step.

The NNE monthly precipitation values are calculated through the spatial average of the monthly precipitation recorded at each point of the grid that covers the NNE territory; in that way, at each month, there is a unique value of precipitation for the whole area. The boundaries of the grid adopted are the same as that used in De Souza and Ambrizzi (2006) (Figure 8) and the precipitation variability of the area inside the perimeter is determined by the same factors. The grid is 44.5W-38.5W width in longitude and 3.5S-8.5S in latitude.

The seasonal rainfall amount of the NNE area was calculated through the average of the monthly precipitation amount of March, April and May. The range of the rainy season was chosen including March and April months, in which the wet season peak is centred (Hastenrath, 1977; Kousky, 1979) and May, that also is important to detect the seasonal rainfall abundance due to the time variability of the northward migration of the ITCZ (Hastenrath and Heller, 1977; Uvo, 1989; Uvo and Nobre, 1989).

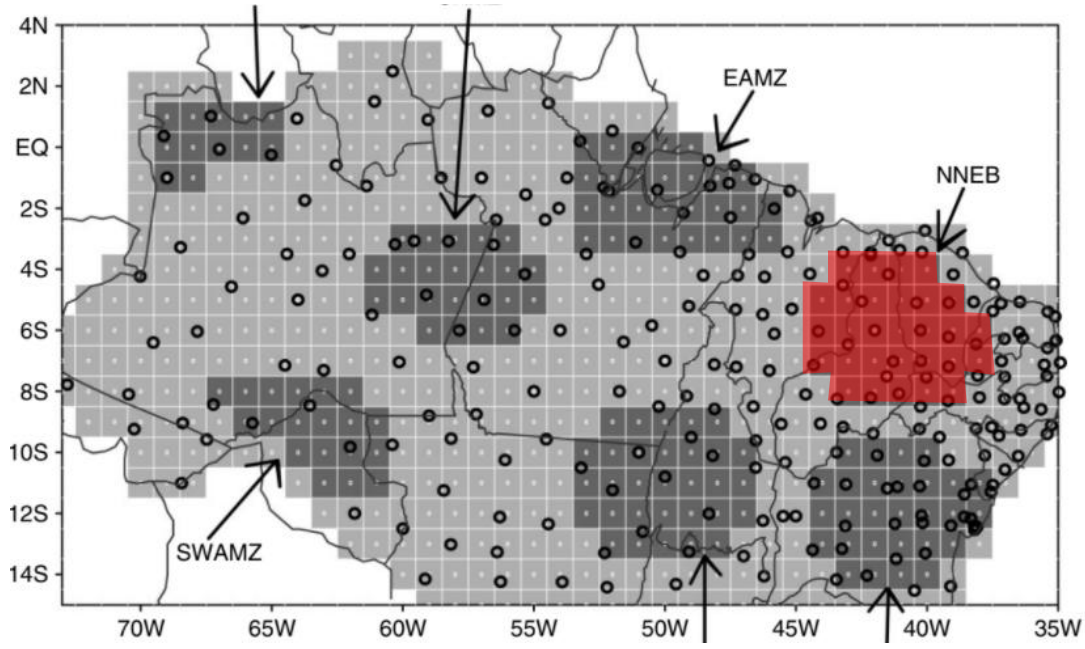

Figure 8. The figure shows the gridded map (1.0 x 1.0) of the North and Northeast Brazil. The red shaded area represents the subset of the grid used to calculate the mean precipitation amount over NNE. Each point of the grid contains one value of precipitation for each month. [Source: adapted from Souza and Ambrizzi, 2006]

4.2.1. NAO - NNE precipitation relationship

In this section are performed correlation and composite analysis to evaluate the NAO influence over NNE precipitation. These procedures are identically repeated for both the PC-based NAO index and the station based one.

The influence of the NAO over the NNE rainfall was studied during the boreal winter, from December to March, the months in which this teleconnection mostly influence the North Hemisphere SLP field (Hurrell et al., 2003). To assess the relative influence over the NNE rainfall of the NAO during the initial (December to February) and final (January to March) part of the boreal winter season, the analysis (both correlation and composite) were performed calculating the seasonal NAO

index with different time range. The time range used are: December to February (DJF), January to March (JFM), December to March (DJFM).

The first attempt to find some clue of the existence of the NAO-NNE rainfall relationship was performed through a correlation analysis. More details about this statistical method are reported in the section below "Statistical tools". Initially, a month to month correlation analysis was made, with the objective of explore the monthly influence of the NAO over the seasonal NNE rainfall. In practice, each monthly NAO index, from December to March, was separately correlated to the seasonal NNE rainfall; in this way, each correlation was made with a sample of 30 time steps. The Pearson coefficient was calculated for each month and the statistical significance was obtained through the comparison between the p-value and the significance level α. The second step of the correlation analysis was the calculation of the Pearson's coefficient for the wintertime NAO index, obtained through the average between the wintertime monthly NAO indices. Three seasonal indices, constructed with different months (defined above), were constructed and used in this analysis.

The second part of this section describe how the composite analysis was performed. Using the procedure reported in the "Statistical tools", the NNE rainy seasons of the 1981-2010 period were divided in four subsets. WET+ is the subset that collects the years in which the MAM rain amount was one standard deviation above than normal; DRY- is the name of the subset containing the years in which the seasonal rainfall amount was one standard deviation below than normal; WET contain the years in which the precipitation was above than normal where DRY contain the years with precipitation below than normal. Then, for each group, is calculated the seasonal NAO index anomaly of the data associated with each subset. The composite analysis is performed for each winter subperiod, and the significance of the difference between NAO anomalies of each group and the seasonal average NAO is test by mean of the t-Student test.

4.2.2. NAO's centres of action - NNE precipitation relationship

A spatial correlation analysis between the NNE precipitation and the North Atlantic SLP field during boreal winter is performed to collect information over the areas that can mostly influence the NNE rainfall variability. The grid used in that analysis ranges from 0N-80N to 100W-40E and the wintertime SLP field is constructed using the average of the monthly SLP values, from December to February. The spatial correlation map is obtained through the correlation between the NNE precipitation and each singular point of the SLP grid.

The same grid used in the spatial correlation analysis was adopted also for the spatial composite analysis. The only difference with the previous procedure is that the wintertime SLP field was constructed with the data from December to March, to verify the resemblance to the "trough" pattern of North Atlantic SLP field identified by Hurrell et al., (2003) using the cluster analysis method.

4.2.3. Wind and SST fields associated with NNE precipitation anomalies

To verify the wintertime influence of the NAO-associated centres of pressure over the tropical Atlantic and then over the NNE rainfall, a composite map of the wind and SST fields is constructed. The composite maps are realized with the same procedure as that used in the SLP case.

The SST and wind grids range from 30S-40N to 70W-20E. The SST extends southward until 30S in order to show the anomalous tropical Atlantic north-south SST dipole that affects NNE rainfall (Nobre and Shuckla, 1996). The same latitudinal extension was chosen for the wind map to check the connection between the North Atlantic wind flow and the deep tropics.

The wind's map velocity intensities are calculated through the square root of sum of squares of the u and v wind velocities components, as displayed in the underlying equation:

$$w_{uv} = \sqrt{u^2 + v^2}$$

The wind direction is obtained using the quiver function in MATLAB, that scale and plot one arrow for each cell of the map.

To describe the SST and wind time-response to the North Atlantic SLP forcing during wintertime and the persistence of this influence, were calculated four composites for each variable that includes different months across the boreal winter and spring. Each composite is based on the three-months average of the field considered, starting from December-January-February mean and ending at March-April-May; to give continuity to the results obtained in the previous parts, also the DJFM composite is presented. The reason that led to include also FMA and MAM three-months average is, in the wind case, to analyse the behaviour of the SST inducted cross equatorial wind stress that during NNE rainy season affect the ITCZ position; for the SST composite, the objective was evaluate the persistence of the temperature anomalies until the middle of the NNE rainy season.

4.2.4. NAOs and NAOcp index construction process

The NAOcp index is constructed starting from the DJFM SLP WET composite map above described (Figure 23, lower left panel). The index is constructed by mean of the difference between the seasonal SLP mean of the two centres of pressure associated with the anomalous displacement of the NAO teleconnection. The location and the width of the centres are identified using the statistical significance to the *t*-test as criterion: first, was considered the range of action of the southern CP and the area determined by the set of the SLP anomalies significant at the 0.10 confidence level was selected. However, the northern CP is not spatially defined as well as the southern one and is not possible to identify an area in which the p value drops below the 0.10 significance level. For this reason, to construct each CP with the same number of data, the number of cells contained in the southern CP area was calculated and used to fix the width of the northern centre of pressure area. After, the position of the cells was determined based on the minimum p-values recorded in the space of action of the northern CP. Each cell selected represent an anomaly value of the composite maps and it is associated to a dataset that contains the SLP data record associated with the cell position. For both the CP separately, a unique SLP vector is obtained through the seasonal mean of the SLP

vectors associated with the cells selected, to create one vector for each CP containing one value of SLP for each month. Then, each vector is separately standardized subtracting the mean and dividing by the standard deviation of its own CP and, finally, the difference between the two-standardized vector is calculated.

In the end, the NAOcp index performance is compared to that of the NAOs index. This last index is simply the normalized SLP value recorded in the area in which the southern NAO centre of pressure acts. The construction process is the same as the one used for the minuendo of the NAOcp index. The comparison is made considering two methods: the greater Pearson correlation coefficient between the seasonal index and the NNE MAM precipitation; the composite analysis between the index calculated in the DJFM season and the NNE MAM precipitation.

4.3. Statistical tools

4.3.1. Pearson correlation coefficient

The correlation coefficient of two random variables is a measure of their linear dependence.

Considering two variables, X and Y, with N scalar observations each, the Pearson correlation coefficient is defined as:

$$\boldsymbol{r\,(X,Y) = \frac{1}{N-1}\sum_{i=1}^{N}\left(\frac{x_i - \bar{x}}{s_x}\right)\left(\frac{y_i - \bar{y}}{s_y}\right)}$$

where $\bar{x}$ and s_x are the mean and standard deviation of X, respectively, and $\bar{y}$ and s_y are the mean and standard deviation of Y.

The values of the r coefficients can range for -1 to 1. with -1 representing a direct negative correlation, 0 representing no correlation and 1 representing a direct positive correlation. Values below 0 indicate negative correlation between the two variables while values above 0 indicate positive correlation.

To test the statistical significance of the Pearson correlation coefficient, a p-value is calculated. This p-value is used to test the null hypothesis that there is no

relationship between the two variables considered; it ranges from 0 to 1. If the p-value is smaller than a significance level α, than the corresponding correlation coefficient is considered significant. The p-value is calculated considering that the estimated Pearson coefficient (r) has Student's t-distribution, with N-2 degrees of freedom. Then, the test statistics is calculated in the following way:

$$t = r\sqrt{\frac{N - 2}{1 - r^2}}$$

where t is the test statistics, N is the number of the variable observations and r is the Pearson's coefficient estimation. From the result of the equation, is possible to obtain the p-value from a two-tailed Student's t-distribution table with N-2 degrees of freedom.

4.3.2. Composite analysis

Composite analysis is a simple and effective tool that permit to identify conditions observed during specific states of the climate. They can point to connections between a phenomenon and key surrounding regions and provide valuable information for hypotheses to be formed as to the physical mechanisms that may be involved in these connections (Boschat et al., 2016).

The composite analysis requires the calculation of the mean ($\bar{x}$) and the standard deviation (s_x) of the one of the dependent variable (X). Using these two statistical measures, the values of the variable considered is divided into four groups:

-the first group (X_1) comprehends the above-average values ($x_{1,i} > \bar{x}$);

-the second (X_2) the below-average values ($x_{2,i} < \bar{x}$);

-the third (X_3) the above average plus one standard deviation values ($x_{3,i} > \bar{x} + s_x$);

-and the last group (X_4) include the below average minus one standard deviation values ($x_{4,i} < \bar{x} + s_x$).

Each observation of the dependent variable is associated in time with another of the independent one (Y). In that way, other four groups are with the values of Y.

$$\mathbf{x_{1,i} \Rightarrow y_{1,i}, x_{1,i+1} \Rightarrow y_{1,i+1}, \dots, x_{1,n1} \Rightarrow y_{1,n1}}$$

$$\mathbf{x_{2,i} \Rightarrow y_{2,i}, x_{2,i+2} \Rightarrow y_{2,i+2}, \dots, x_{2,n2} \Rightarrow y_{2,n2}}$$

$$\mathbf{x_{3,i} \Rightarrow y_{3,i}, x_{3,i+3} \Rightarrow y_{3,i+3}, \dots, x_{3,n3} \Rightarrow y_{3,n3}}$$

$$\mathbf{x_{4,i} \Rightarrow y_{4,i}, x_{4,i+4} \Rightarrow y_{4,i+4}, \dots, x_{4,n4} \Rightarrow y_{4,n4}}$$

In which $x_{k,nk}$ are the elements of each group made from the data of the variable X and $y_{k,nk}$ are the values of each group filled by the data of Y. Then, the average of all the elements of the independent variable ($\bar{y}$) and of each of the four new groups ($\overline{y_1}, \overline{y_2}, \overline{y_3}, \overline{y_4}$) is calculated. Finally, the mean of Y is subtracted to the mean of the new four groups, thus obtaining one anomaly for each group.

The statistical significance of the anomalies is then assessed by means of a statistical test.

4.3.3. T-test

The two-sample t-test is a parametric test that compares the location parameter of two independent data samples. It is commonly used to test the significance of the composite maps, i.e. the difference between the means of the sample used in the composite analysis.

This procedure is used to test the null hypothesis that the data in vectors x and y are drawn from independent random samples, normally distributed, with equal means and common but unknown variances. The alternative hypothesis consists in the fact that the data in the x and y vectors comes from populations with unequal means.

The test statistic is:

$$\boldsymbol{t = \frac{\bar{x} - \bar{y}}{\sqrt{\frac{s_x^2}{n} + \frac{s_y^2}{m}}}}$$

where $\bar{x}$ and $\bar{y}$ are the sample means, s_x and s_y are the sample standard deviations, and n and m are the sample sizes.

If the data samples are considered to come from populations with equal variances, the test statistics under the null hypothesis has Student's *t* distribution with $n + m - 2$ degrees of freedom, and the sample standard deviation in the equation above are substituted by the pooled standard deviation:

$$s = \sqrt{\frac{(n-1)s_x^2 + (m-1)s_y^2}{n + m - 2}}$$

5. RESULTS AND DISCUSSION

5.1. NAO - NNE precipitation relationship

5.1.1. Monthly NAO - NNE rainy season correlation and composite

a) NAO index PC-based

The PC-based NAO index is constructed regressing the hemispheric sea level pressure anomalies upon the leading principal component time series. It allows the index to "follow" the two centres of pressure movement, thus detecting variations in strength and intensity of the teleconnection signal without dependence on the space location of the CP.

The first attempt is to find a monthly index - seasonal precipitation relationship using the linear correlation technique. Only boreal winter months and March were selected, and the correlation coefficient is calculated separately for each month. The results are displayed in the figure 9. There is no significant correlation between the two datasets, whichever month is considered. This means that, from a linear point of view, there isn't any relationship between the phenomenon that is statistically significant at the 0.05 confidence level. In fact, the p-value of each month doesn't go below the 0.05 threshold.

Secondly, the singular monthly NAO indices were aggregated to obtain a wintertime seasonal NAO index and, then, the Pearson's coefficient was calculated between this new index and the NNE precipitation. Three different seasonal indices

were individuated (DJF, JFM, DJFM) depending on the month chosen in the aggregation. Two of the seasonal indices correspond to the initial (DJF) and final (JFM) part of the boreal winter, whereas the third represent the whole extension of the season. This sensitivity analysis was made to assess if subperiods of the winter season influence in a different way the NNE precipitation. Also, in this case there were found no significant correlations between the data, but the Pearson coefficient are all negative. That is the opposite of what it was expected from the result. In fact, a positive NAO should have a positive effect (through the increasing of the northeasterly trade winds) over the NNE precipitation, acting as a forcing on the southward displacement of the ITCZ and contributing to the increase the negative SST anomaly over the tropical North Atlantic. These conditions, as reported by many authors (Hastenrath and Haller, 1977; Nobre and Shukla, 1981; Hastenrath, 2012; Uvo et al., 1989) are favorables to larger than normal precipitation during the NNE rainy season. The results of the composite analysis for each winter subperiod are displayed in the figures 11, 12. 13, for DJF, JFM, DJFM, respectively. In the first graph, none of composite groups is significantly different from the seasonal NAO mean, despite the DRY- p-value is just above the 0.05 significance threshold. In the other cases, it's possible to see how the composite mean is very close to the seasonal average, meaning that, in presence of fixed behaviour of the NNE rainy season, there aren't time-associated NAO events. The pattern identified in DJF are roughly repeated in the JFM and DJFM periods. The main difference is the fact that the DRY- mean is significantly different from the climatological seasonal NAO mean (the DRY- p-value is below the 0.05 threshold). This imply that the NAO+ phase might negatively affect the precipitation amount over NNE; one more time, this result is opposite of what it's expected from the theory. However, consider the influence that the ENSO teleconnection exerts over both the phenomenon can explain these unexpected results.

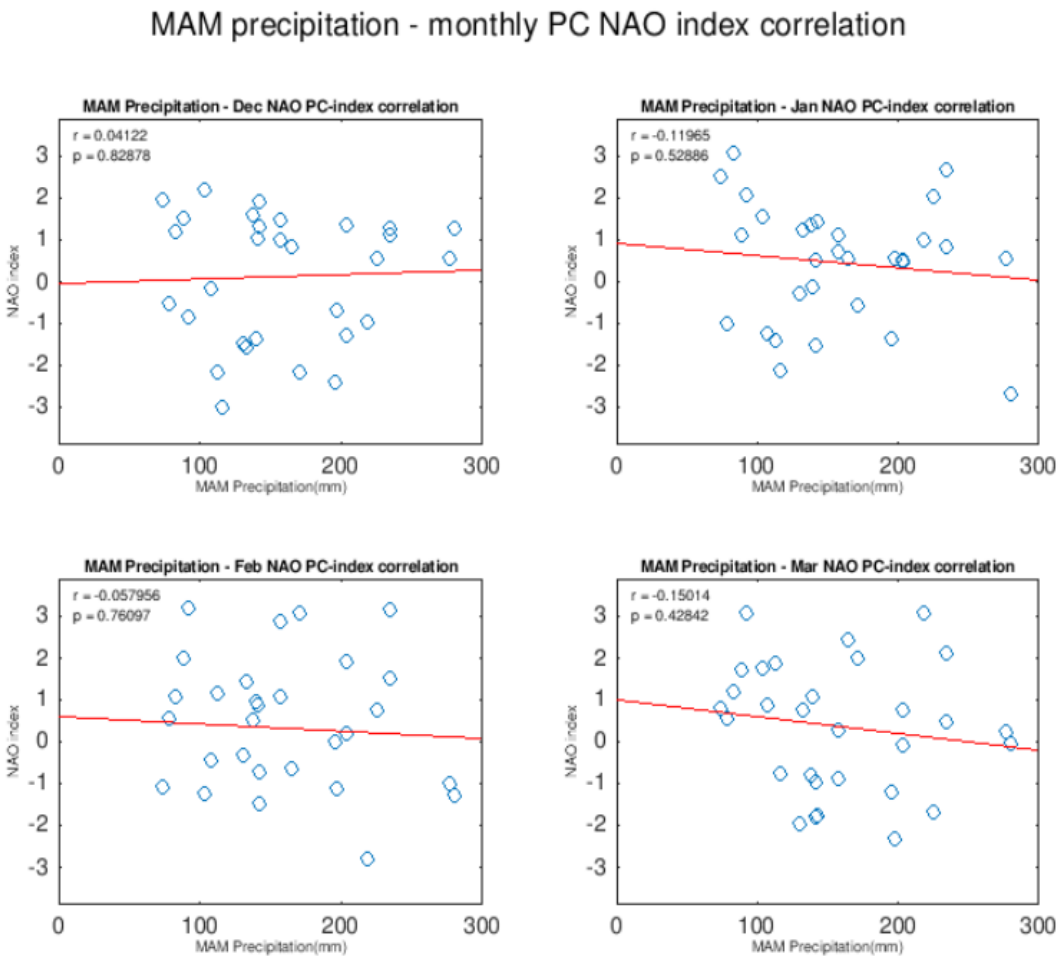

Figure 9: In the charts is represented the monthly (D-J-F-M) NAO PC index - MAM precipitation correlation. On the x-axis are represented the average of the seasonal NNE precipitation amount, calculated from March to May. On the y-axis it's shown the range of monthly NAO index. The monthly paired data are represented through blue circles. The red line represents the regression line among the data. r and p, in the upper left corner, are respectively the Pearson's coefficient value and the p-value.

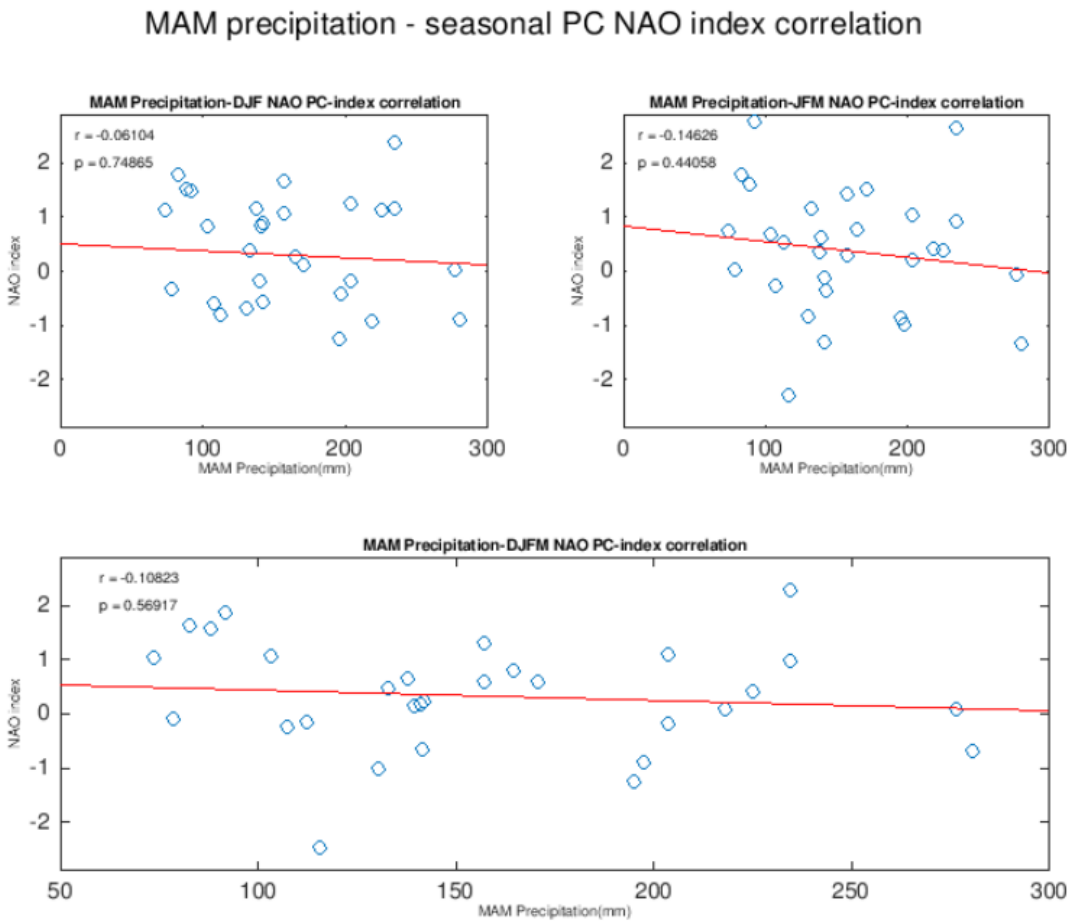

Figure 10: In the figure three correlation scatter plots of the MAM precipitation versus different seasonal PC NAO indices are displayed. DJF, JFM and DJFM NAO indices are represented, respectively, in the upper left, upper right and lower panels. The x-axis contains the MAM precipitation and the y-axis the seasonal NAO index. The paired data are represented through blue circles. The red line represents the regression line among the data. r and p, in the upper left corner, are respectively the Pearson's coefficient value and the p-value.

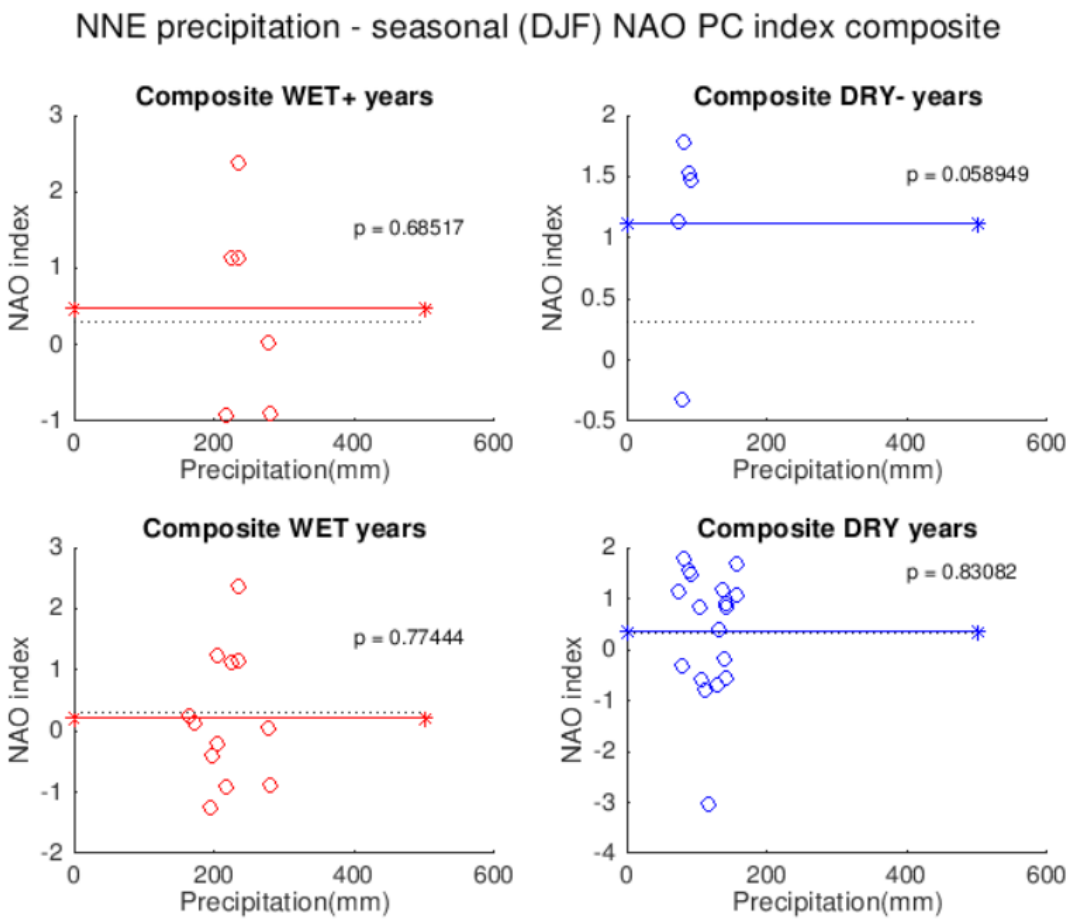

Figure 11: In the figure are displayed four panels representing the results of the composite analysis between NNE precipitation and seasonal (DJF) NAO PC index. WET+ and DRY- years are represented, respectively, in the left and right upper panels, while WET and DRY years are showed in the bottom panels. Blue colour is used in the graphs where precipitation below than normal is involved, red colour where precipitation is above than normal. On the x-axis the precipitation range is showed and on the y-axis the NAO index values are displayed. The blue/red dots represent the individual seasonal NAO index value, the blue/red lines represent the mean of the seasonal NAO index considering the years selected in each composite, and the black dotted line is the mean seasonal NAO index considering all the years from 1981 to 2010.

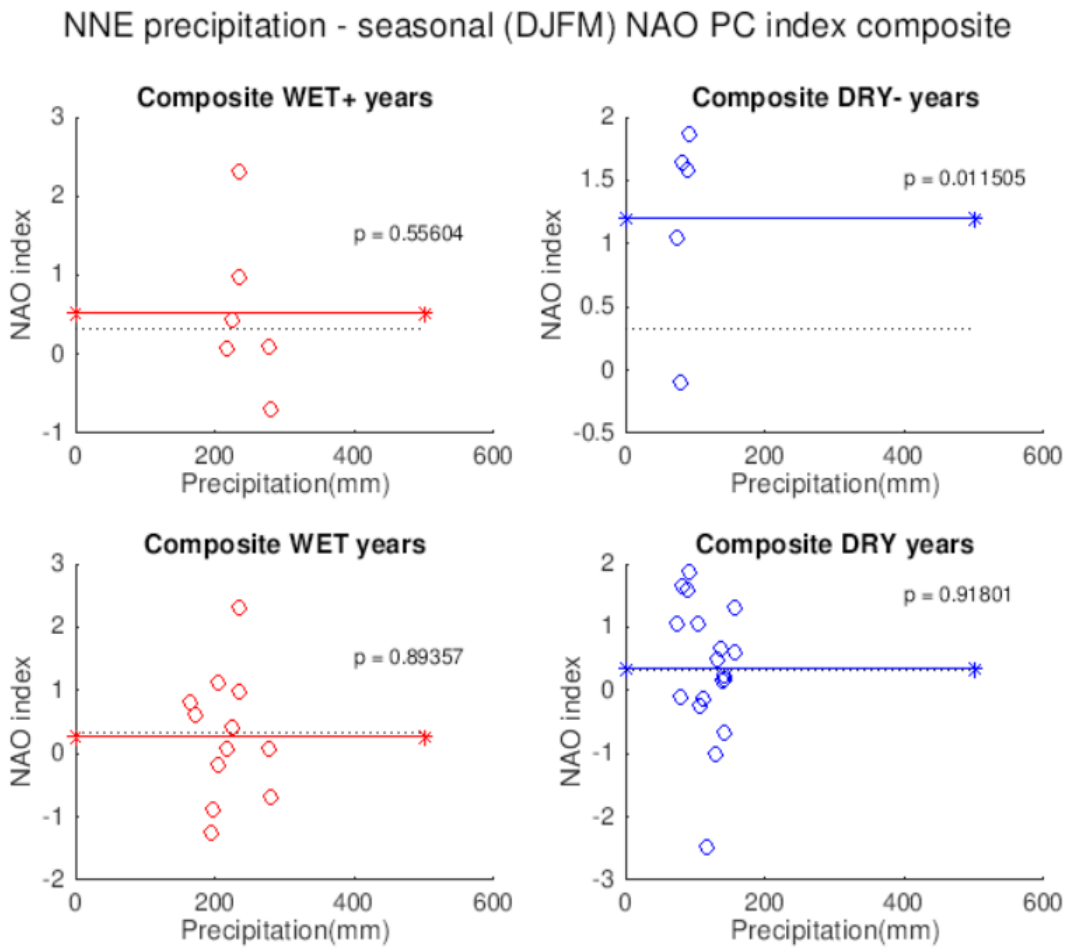

Figure 12: In the figure are displayed four panels representing the results of the composite analysis between NNE precipitation and seasonal (DJFM) NAO PC index. WET+ and DRY- years are represented, respectively, in the left and right upper panels, while WET and DRY years are showed in the bottom panels. Blue colour is used in the graphs where precipitation below than normal is involved, red colour where precipitation are above than normal. On the x-axis the precipitation range is showed and on the y-axis the NAO index values are displayed. The blue/red dots represent the individual seasonal NAO index value, the blue/red lines represent the mean of the seasonal NAO index considering the years selected in each composite, and the black dotted line is the mean seasonal NAO index considering all the years from 1981 to 2010.

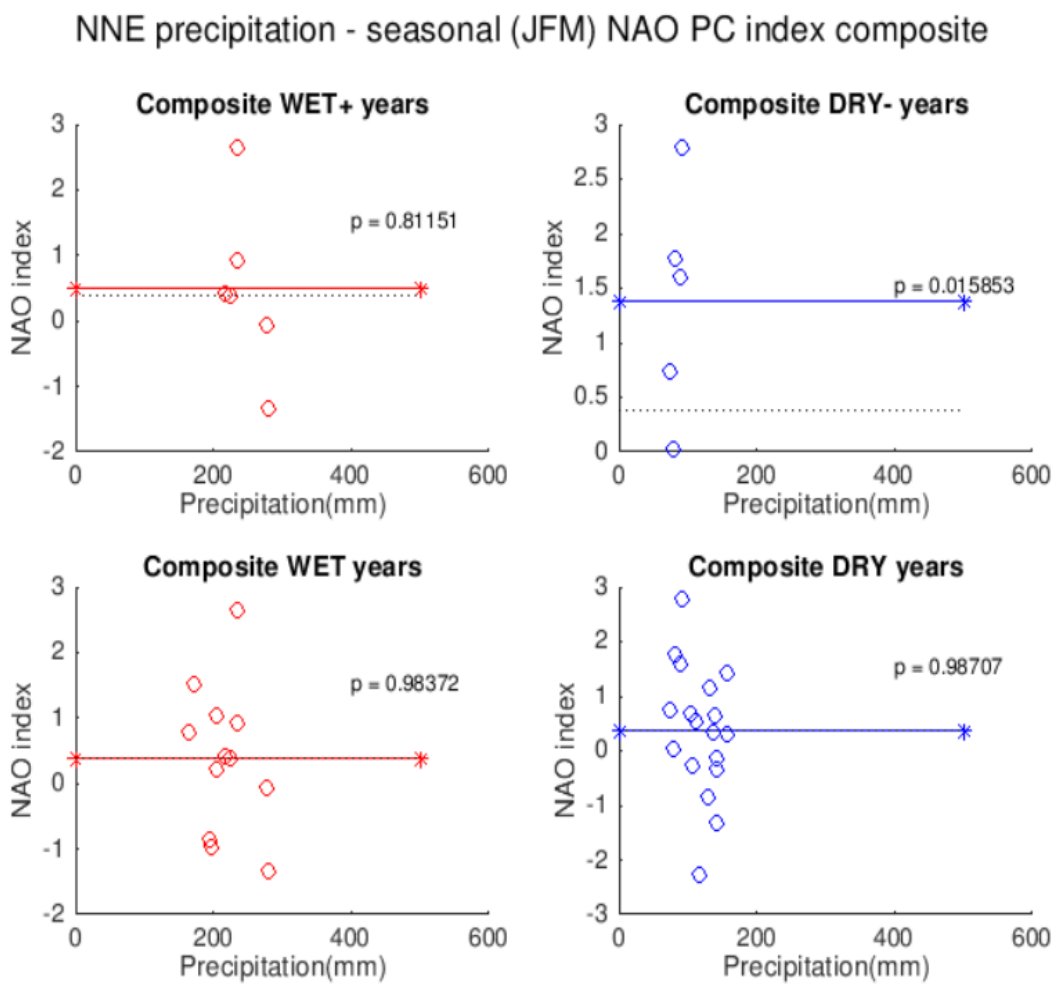

Figure 13: In the figure are displayed four panels representing the results of the composite analysis between NNE precipitation and seasonal (JFM) NAO PC index. WET+ and DRY- years are represented, respectively, in the left and right upper panels, while WET and DRY years are showed in the bottom panels. Blue colour is used in the graphs where precipitation below than normal is involved, red colour where precipitation are above than normal. On the x-axis the precipitation range is showed and on the y-axis the NAO index values are displayed. The blue/red dots represent the individual seasonal NAO index value, the blue/red lines represent the mean of the seasonal NAO index considering the years selected in each composite, and the black dotted line is the mean seasonal NAO index considering all the years from 1981 to 2010.

b) Station-Based NAO index

The station-based NAO index is calculated through the difference of the normalized Sea Level Pressure measured at the station of Ponta Delgada and Reykjavik. The bigger limitation of this calculation method is the fact that the

measures are fixed in the space and the movement of the NAO centres of pressure is not followed.

The procedure adopted in this part is exactly the same as that used in the PC-based NAO index.

Also when the SB NAO index is used in the analysis, both the monthly and seasonal correlations (showed in the Figures 13 and 14) with the NNE rainy season are not significant and all the p-values are very close to 1.

The SB NAO index composite analysis shower the same pattern of the PC ones. In all the graphs presented in Figures 14, 15 and 16, the composite means don't differ significantly from the climatological ones. As in the PC case, the DRY-composite is the situation in which the difference is more relevant but, in the SB case, no p-value goes below the 0.05 confidence threshold. Again, there are not remarkable changes in the results depending on the months chosen to construct the seasonal SB NAO index.

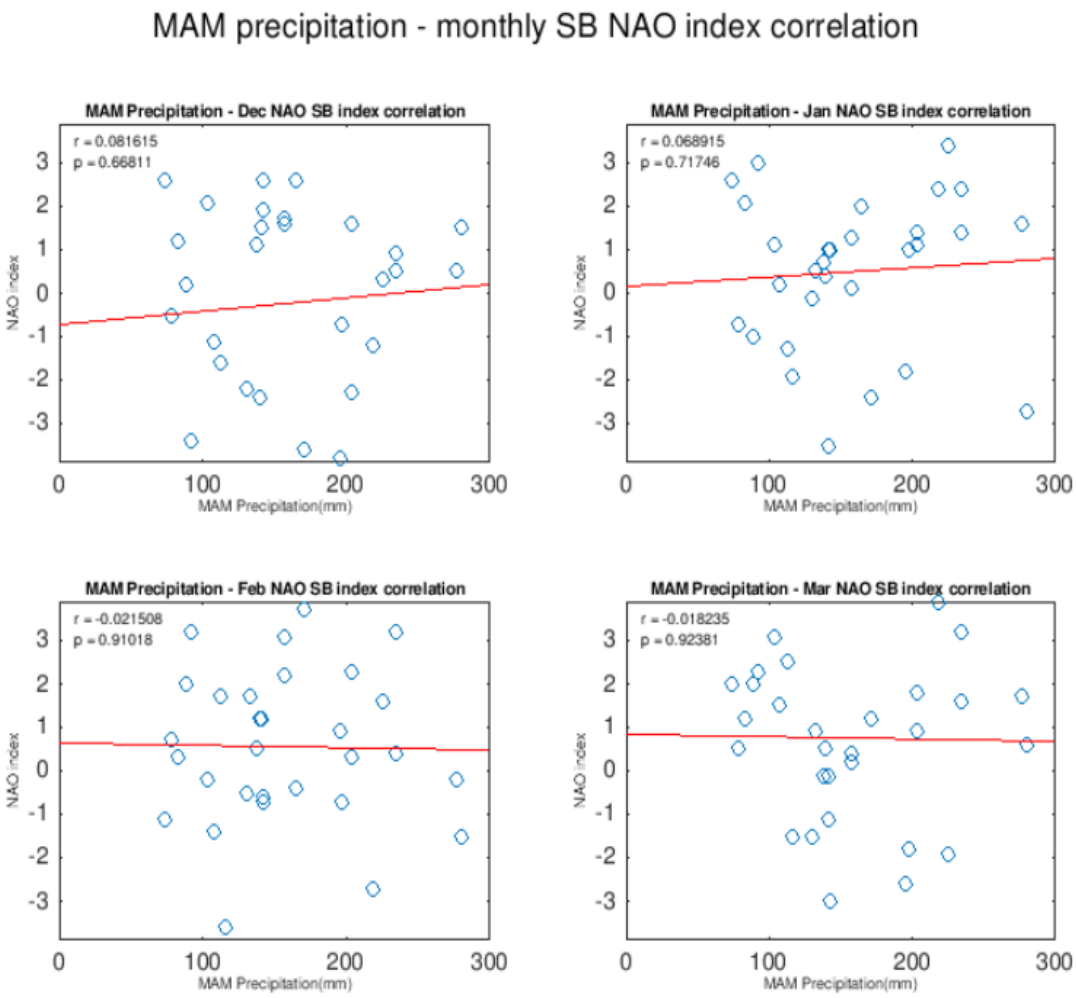

Figure 13: In the charts is represented the monthly (D-J-F-M) NAO SB index - MAM precipitation correlation. On the x-axis are represented the average of the seasonal NNE precipitation amount, calculated from March to May. On the y-axis it's shown the range of monthly NAO index. The monthly paired data are represented through blue circles. The red line represents the regression line among the data. r and p, in the upper left corner, are respectively the Pearson's coefficient value and the p-value.

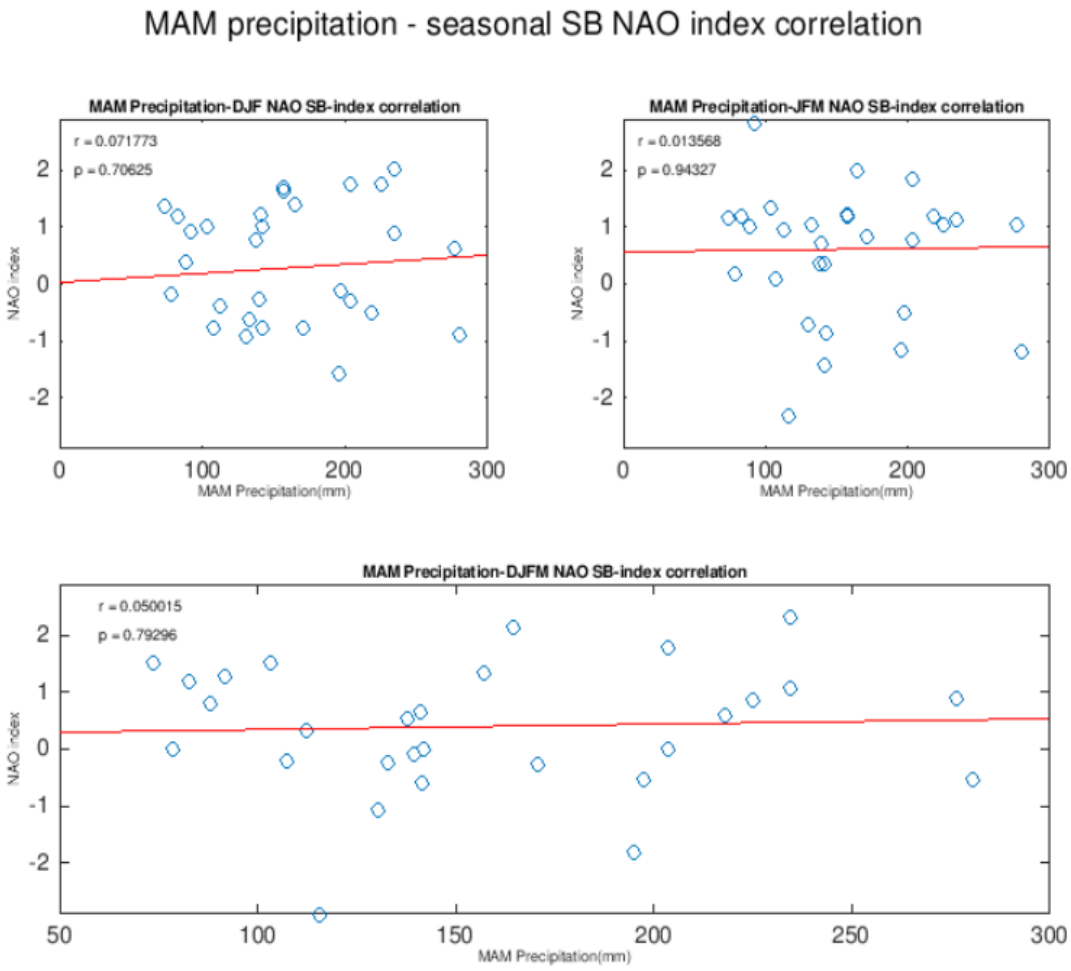

Figure 14: In the figure three correlation scatter plots of the MAM precipitation versus different seasonal SB NAO indices are displayed. DJF, JFM and DJFM NAO indices are represented, respectively, in the upper left, upper right and lower panels. The x-axis contains the MAM precipitation and the y-axis the seasonal NAO index. The paired data are represented through blue circles. The red line represents the regression line among the data. r and p, in the upper left corner, are respectively the Pearson's coefficient value and the p-value.

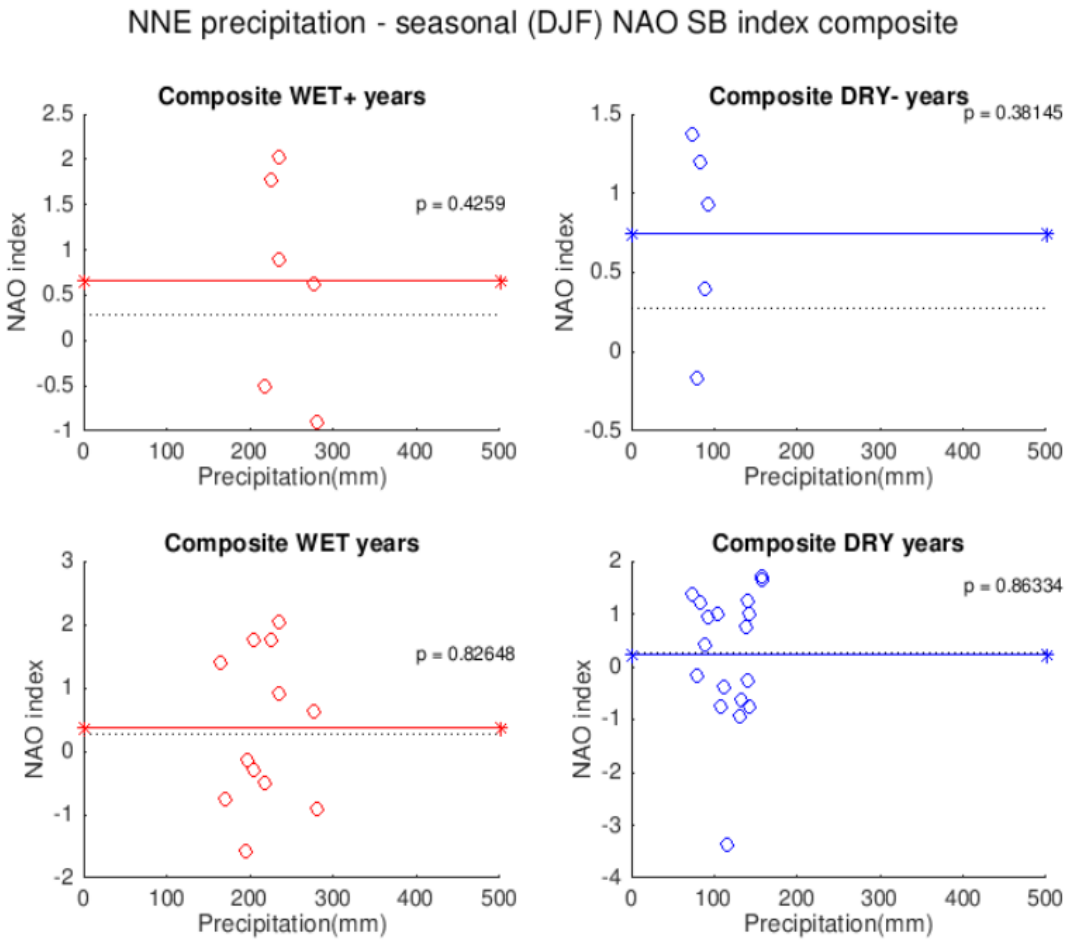

Figure 15: In the figure are displayed four panels representing the results of the composite analysis between NNE precipitation and seasonal (DJF) NAO SB index. WET+ and DRY- years are represented, respectively, in the left and right upper panels, while WET and DRY years are showed in the bottom panels. Blue colour is used in the graphs where precipitation below than normal is involved, red colour where precipitation are above than normal. On the x-axis the precipitation range is showed and on the y-axis the NAO index values are displayed. The blue/red dots represent the individual seasonal NAO index value, the blue/red lines represent the mean of the seasonal NAO index considering the years selected in each composite, and the black dotted line is the mean seasonal NAO index considering all the years from 1981 to 2010.

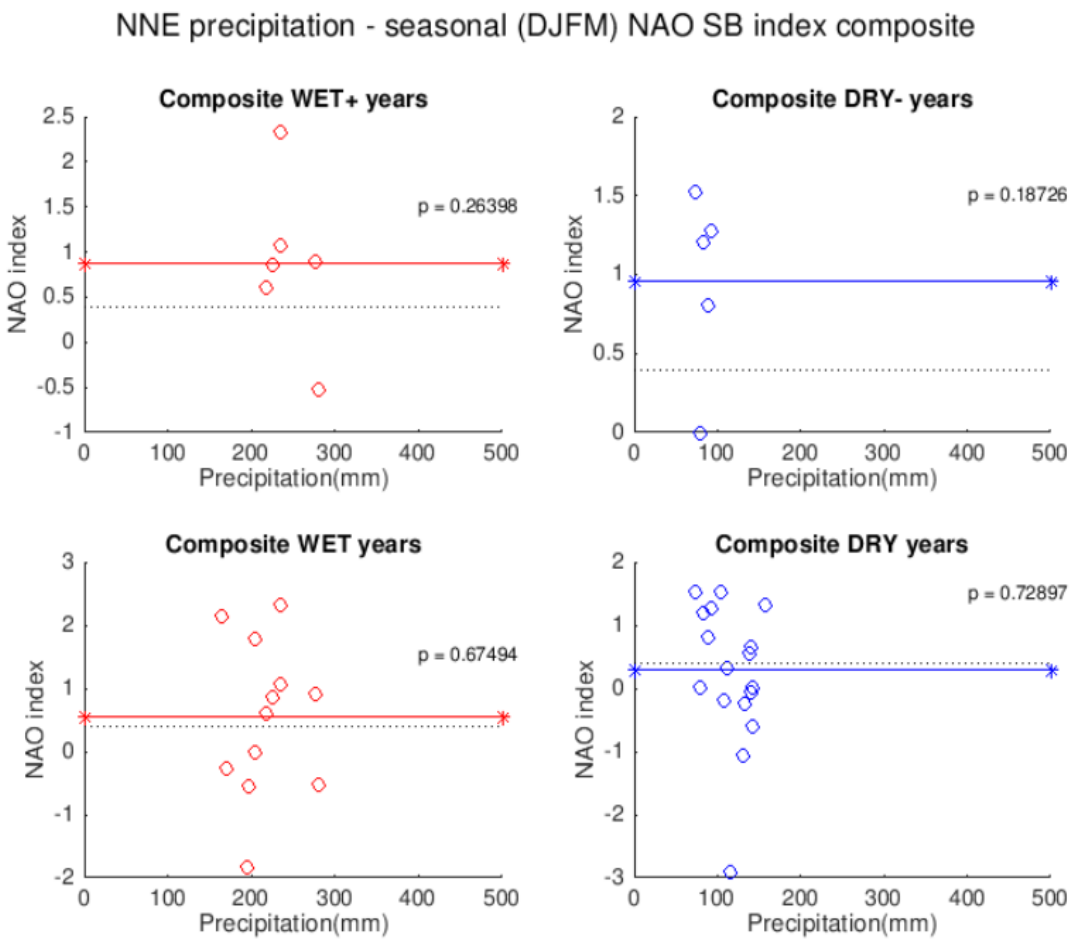

Figure 16: In the figure are displayed four panels representing the results of the composite analysis between NNE precipitation and seasonal (DJFM) NAO SB index. WET+ and DRY- years are represented, respectively, in the left and right upper panels, while WET and DRY years are showed in the bottom panels. Blue colour is used in the graphs where precipitation below than normal is involved, red colour where precipitation is above than normal. On the x-axis the precipitation range is showed and on the y-axis the NAO index values are displayed. The blue/red dots represent the individual seasonal NAO index value, the blue/red lines represent the mean of the seasonal NAO index considering the years selected in each composite, and the black dotted line is the mean seasonal NAO index considering all the years from 1981 to 2010.

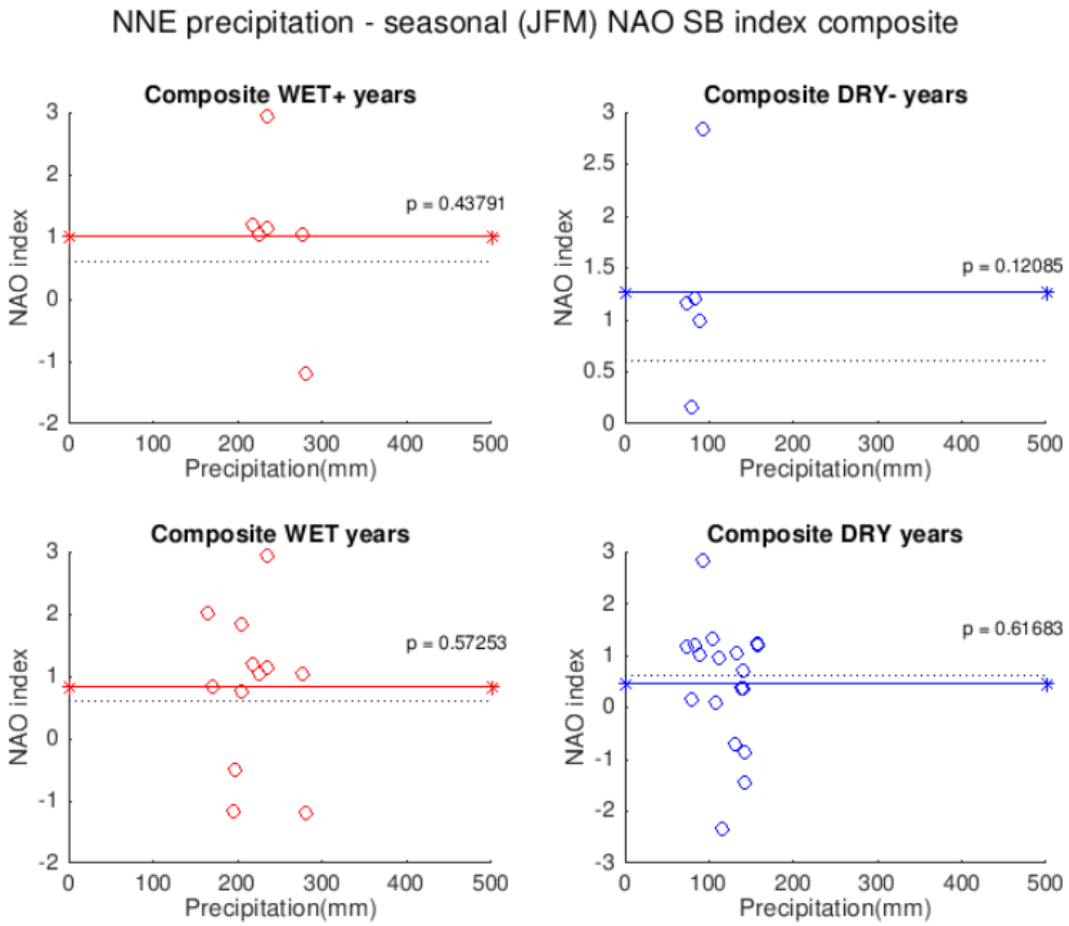

Figure 16: In the figure are displayed four panels representing the results of the composite analysis between NNE precipitation and seasonal (JFM) NAO SB index. WET+ and DRY- years are represented, respectively, in the left and right upper panels, while WET and DRY years are showed in the bottom panels. Blue colour is used in the graphs where precipitation below than normal is involved, red colour where precipitation is above than normal. On the x-axis the precipitation range is showed and on the y-axis the NAO index values are displayed. The blue/red dots represent the individual seasonal NAO index value, the blue/red lines represent the mean of the seasonal NAO index considering the years selected in each composite, and the black dotted line is the mean seasonal NAO index considering all the years from 1981 to 2010.

5.1.2. Analysis of the DRY- composite case

As it was shown above, the DRY- composite case result was unexpected. In fact, it was supposed that when the NAO is in the positive phase, the NNE should tend to be much abundant, due to the trade winds - SST mechanism. But in the DRY- case, i.e. when the NNE rainy season was extremely poor, it was find a significant positive difference (but only for the PC index) between the composite seasonal NAO

mean and the climatological seasonal NAO mean. However, if also the DRY case is considered, there is almost no difference between the two means, meaning that the signal recorded in the extreme dry years is not present in the years when the NNE precipitation is below the climatological mean. This issue can be explained introducing the ENSO forcing in the discussion. In fact, strong El Niño events are related to a stronger than normal Walker-type circulation with ascendant branch over the anomalously hot water in the equatorial pacific and sinking motion over the Northeast Brazil and equatorial Atlantic, this anomalous atmospheric circulation inhibits the formation of convective cells over the NEB and propitiate the creation of a positive northward topical SST dipole (Kousky et al., 1984; Coelho et al., 2002). Looking to the DRY+ years (1983, 1990, 1992, 1993, 1998), two of them (1983 and 1998) registered a Very Strong El Niño events, and 1992 is characterized by a Strong El Niño event, as it is showed in the Figure 17. These extreme positive El Niño events, as it is shown by Kayano et al. (1988) and Souza and Ambrizzi (2002) for the 1982/82 case, can cause droughts over the Northeast Brazil region. So, the El Niño forcing over the NNE precipitation may have been affected the DRY- composite, since the number of years involved is very low. This would explain the big difference found between the DRY and DRY- composites.

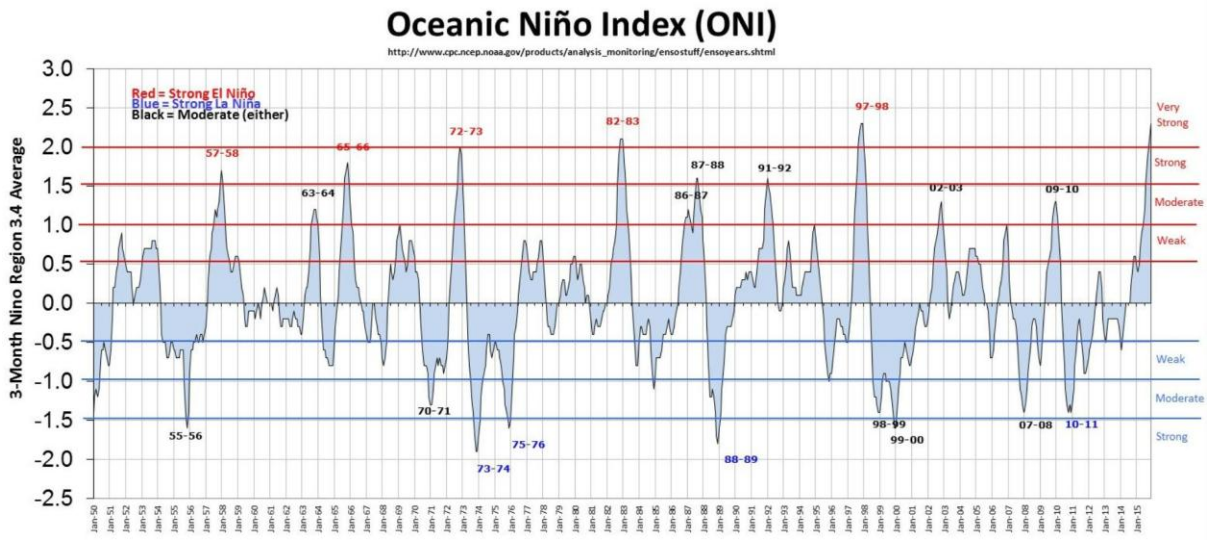

Figure 17: The ONI index is plotted in the time period from 1950 to 2015. Absolute values above 1, 1.5 and 2 define the El Niño/La Niña events as moderate, strong and very strong. The index is calculated using the 3-month running mean of ERSST.v5 SST anomalies in the Niño 3.4 region (5ºN-5ºS, 120º-170ºW). From: <http://origin.cpc.ncep.noaa.gov/products/analysis_monitoring/ensostuff/ensoyears.shtml>

5.2.North Atlantic SLP field - NNE precipitation relationship

In this section the relationship between the North Atlantic Oscillation and the NNE MAM rainfall is investigated under a different point of with. In fact, it won't be used the NAO index to represent the teleconnection behaviour but it's wintertime SLP field over the North Atlantic Ocean.

The first attempt is a spatial correlation analysis, whose results are displayed in Figures 18, 19 and 20. The maps are realized with the same method and only differ because of the months used in the seasonal SLP field construction. The main element that appears looking to the maps is the high correlation circle that appears across the middle and tropical latitudes of the North Atlantic and is situated in the same region where the southern centre of pressure of the NAO acts. This configuration is clear in all the maps, but is more pronounced in the DJF one, where the correlation is stronger and is significant at the 95% confidence level. So, it is likely that the NNE rainfall during MAM can be related to the pressure variation in this area. Another relevant fact is that, despite what it would have been expected, the area in which the northern NAO centre of pressure acts, is not characterized by significant values of the Pearson's correlation coefficient. It could mind that this region doesn't affect the NNE rainy season as much as the zone located in the middle of the North Atlantic between 25N and 40N.

Making a comparison between the maps obtained with different seasonal SLP field, it is possible to see that, in the whole area of study, the values of the Pearson's coefficient in the North Atlantic decrease between the beginning and the end of the winter season. It can be a clue of the fact that the SLP field can influence the NNE precipitation especially in the first part of the winter: probably, the Azores High-induced trade winds of this part of the year are fundamental to create the negative SST anomaly over the tropical North Atlantic and then, considering that the SST anomalies can persists up to six months, this anomaly can continue until the boreal spring.

Finally, it can be seen in the JFM map an area of negative and significant at the 95% level correlation in the Mediterranean area and another region of positive correlations in the east Europe. This configuration resembles the East Atlantic

teleconnection, that won't be analysed here but it can be the object of a future research.

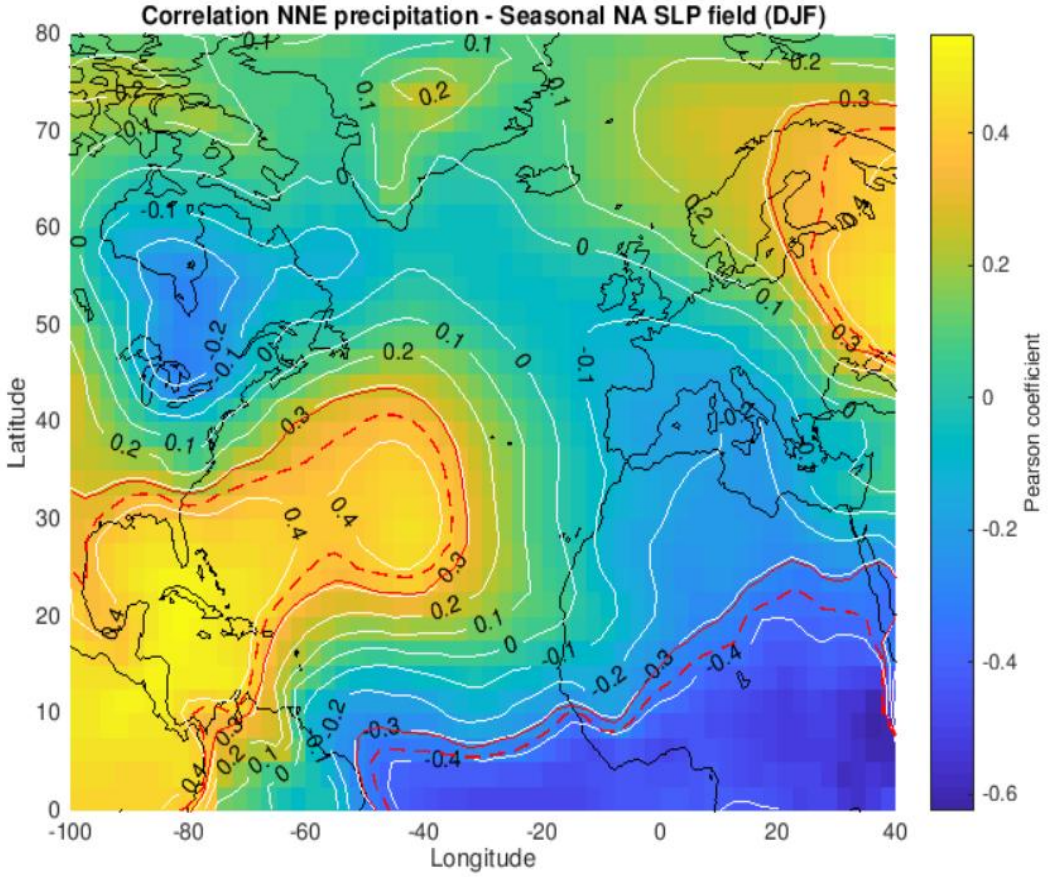

Figure 18. The correlation map between the MAM NNE rainfall and the seasonal SLP (DJF) field is displayed. The colours in the map represent the correlation level between the two variables in each point of the grid. Colours tending to blue indicate negative correlations while positive ones are shown using colours tending to red. White contours are used to represent the correlation levels. Red continuous and dashed lines surround the areas where the confidence level is above 90% and 95%, respectively.

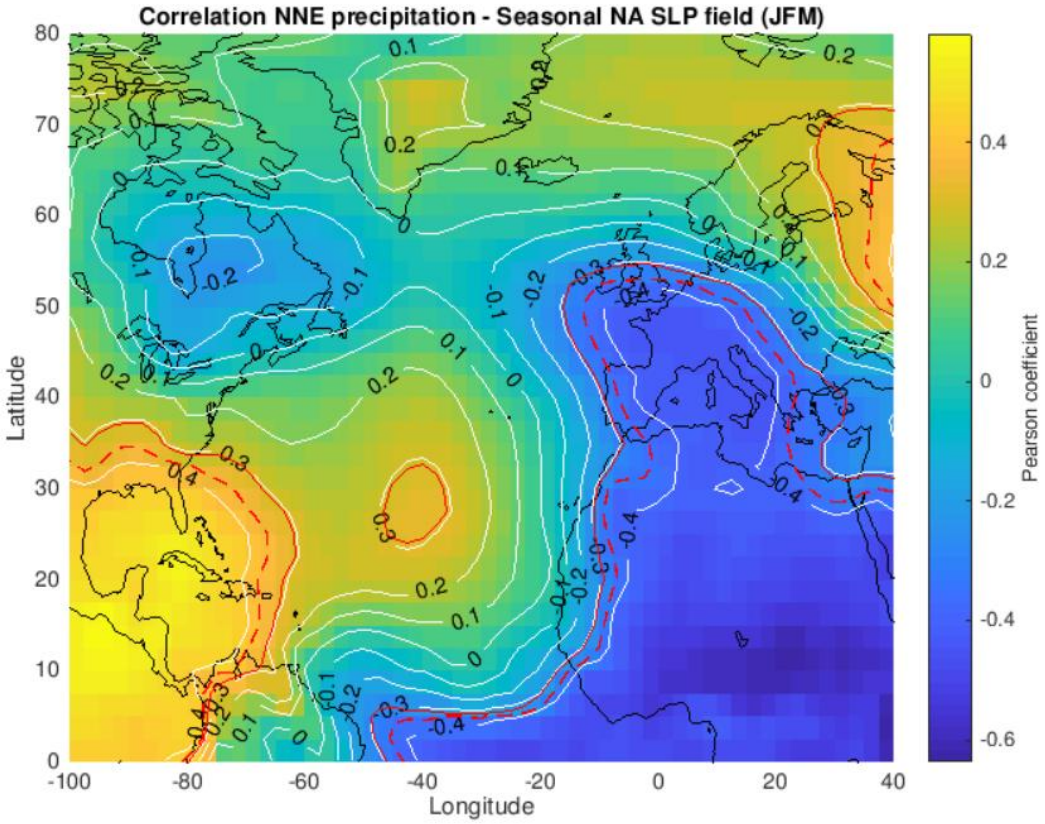

Figure 19. The correlation map between the MAM NNE rainfall and the seasonal SLP (JFM) field is displayed. The colours in the map represent the correlation level between the two variables in each point of the grid. Colours tending to blue indicate negative correlations while positive ones are shown using colours tending to red. White contours are used to represent the correlation levels. Red continuous and dashed lines surround the areas where the confidence level is above 90% and 95%, respectively.

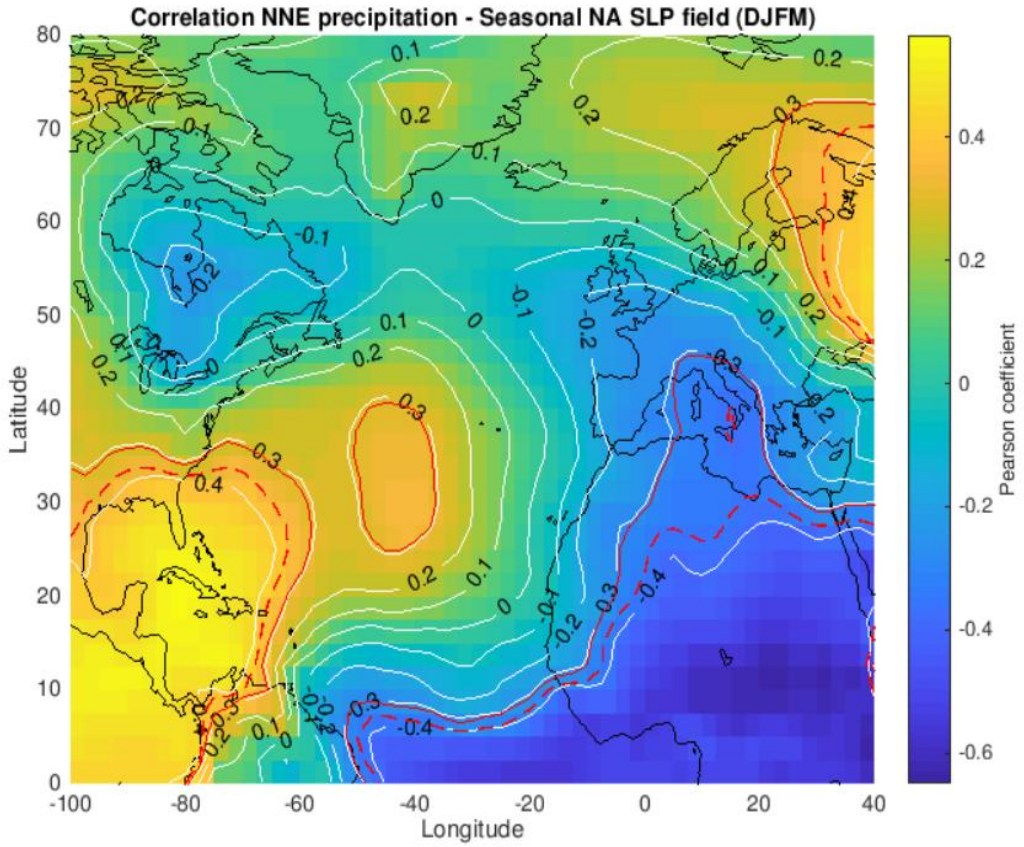

Figure 20. The correlation map between the MAM NNE rainfall and the seasonal SLP (DJFM) field is displayed. The colours in the map represent the correlation level between the two variables in each point of the grid. Colours tending to blue indicate negative correlations while positive ones are shown using colours tending to red. White contours are used to represent the correlation levels. Red continuous and dashed lines surround the areas where the confidence level is above 90% and 95%, respectively.

The results of the spatial composite analysis performed between the NNE rainfall and the North Atlantic SLP field during boreal winter are displaced in the figures 21 (for DJF SLP field), 22 (JFM) and 23 (DJFM). In all the WET+ and WET maps it appears a region in the middle of the North Atlantic Ocean (between 25N-40N and 60W-40W) where the composite differences are significant at 90% confidence level. In this area, there are positive SLP anomalies, i.e. the surface level pressure tends to be higher when the rainy season in NNE is more abundant than normal. The signal is stronger in the first part of the winter, where the composite differences reaches the 95% confidence level, so December seems to take an important stake in the determination of the rainy season quality. The anomalies

pattern of WET and WET+ cases is coherent with that identified in the spatial correlation analysis. In the DRY- composite the are two wide areas of significant anomalies: the first extends from the equator to the middle of the Africa and to the southern and central Europe; the second in located north of Iceland and Scandinavian Peninsula, in the Arctic Ocean. These areas become wider and with higher statistical significance in the last part of the winter. This pattern can be associated to the results showed in the previous section, in which a positive anomaly of the NAO index during the DRY- rainy season was found. However, as in the NAO case, the signal is not repeated in the DRY case.

Looking to the WET+ and WET composite and correlation maps of the SLP field calculated in DJFM, the pressures' pattern resemble very much the "trough" NAO configuration identify by Hurrell et al., (2003) by means of a cluster analysis (Figure 24). In the trough NAO configuration, the southern centre of pressure acts between 25N-40N and 60W-20W, the same area of high correlations and pressure anomalies. So, the statistics found in this area across the middle/topical North Atlantic are possibly related to the anomalous displacement and strength of the southern NAO centre of action. This configuration seems to affect the NNE rainy season and the mechanisms that connect the two phenomena are illustrated in the following paragraph. It's important to remark that these considerations are proposed only for the WET+ and WET years, considering that in the DRY and DRY- cases the same areas don't seem to have the same influence over the NNE precipitation. The same discussion can't be used to the northern centre of action, whose position and strength are not well defined in the space both looking to the composite and correlation map and to the trough pattern.

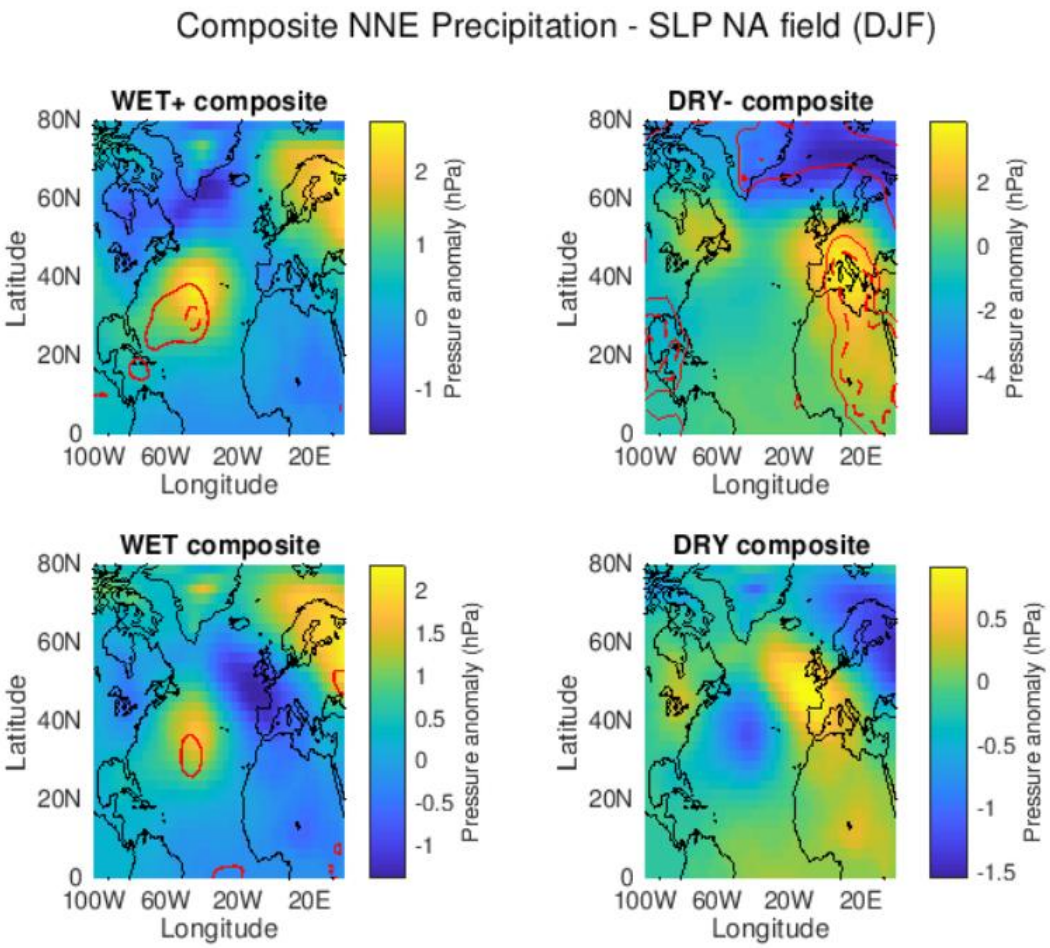

Figure 21. In the figure are displayed four maps corresponding to the WET+ (upper left panel), DRY- (upper right), WET (lower left) and DRY (lower right) composites between the NNE precipitation in MAM and the North Atlantic SLP field calculated in the DJF months. Yellow tending colours means that the area is characterized by positive pressure anomalies; blue tending colours are used to represent negative anomalies. Continuous and dashed red lines are used to represent respectively the areas in which the anomalies are significative ate the 90% and 95% confidence level.

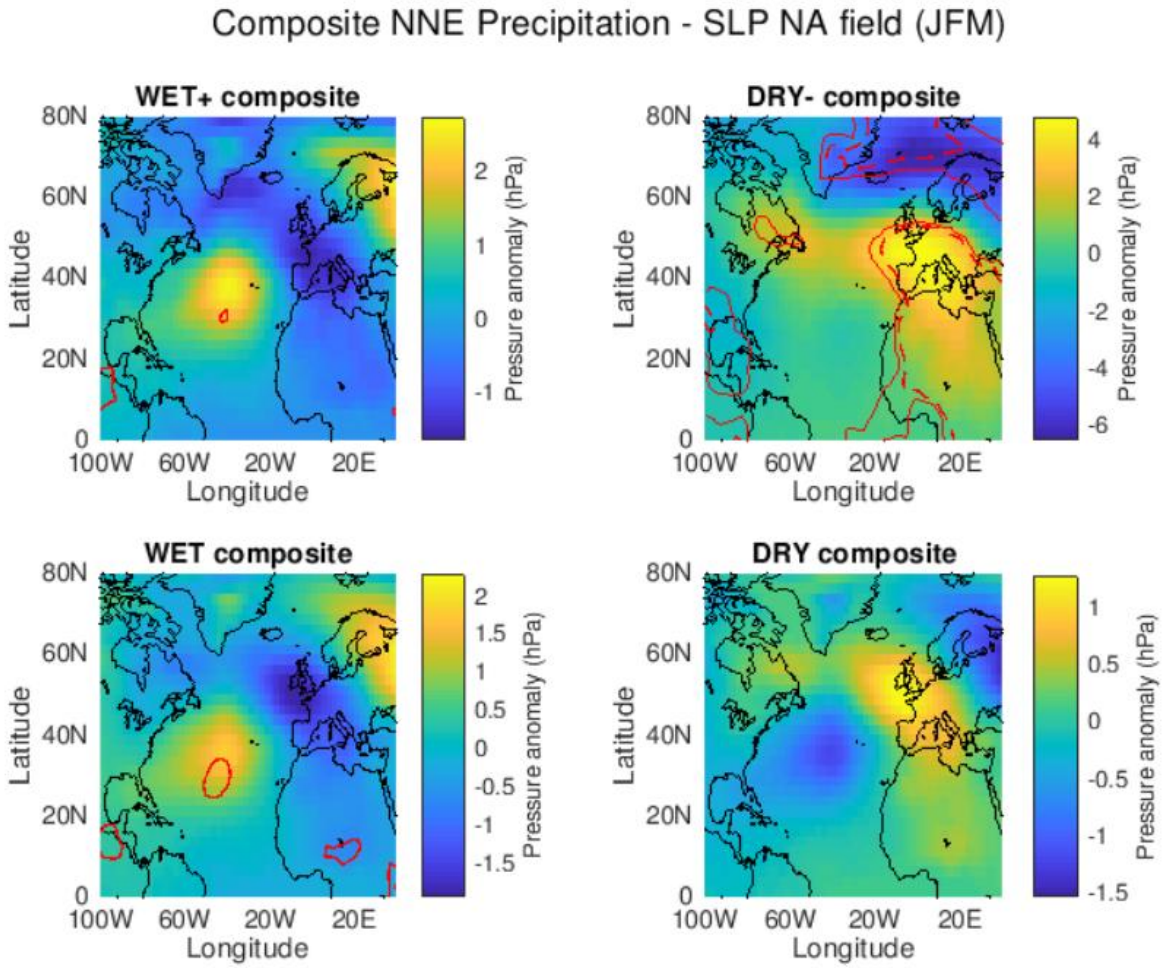

Figure 22. In the figure are displayed four maps corresponding to the WET+ (upper left panel), DRY- (upper right), WET (lower left) and DRY (lower right) composites between the NNE precipitation in MAM and the North Atlantic SLP field calculated in the JFM months. Yellow tending colours means that the area is characterized by positive pressure anomalies; blue tending colours are used to represent negative anomalies. Continuous and dashed red lines are used to represent respectively the areas in which the anomalies are significative ate the 90% and 95% confidence level.

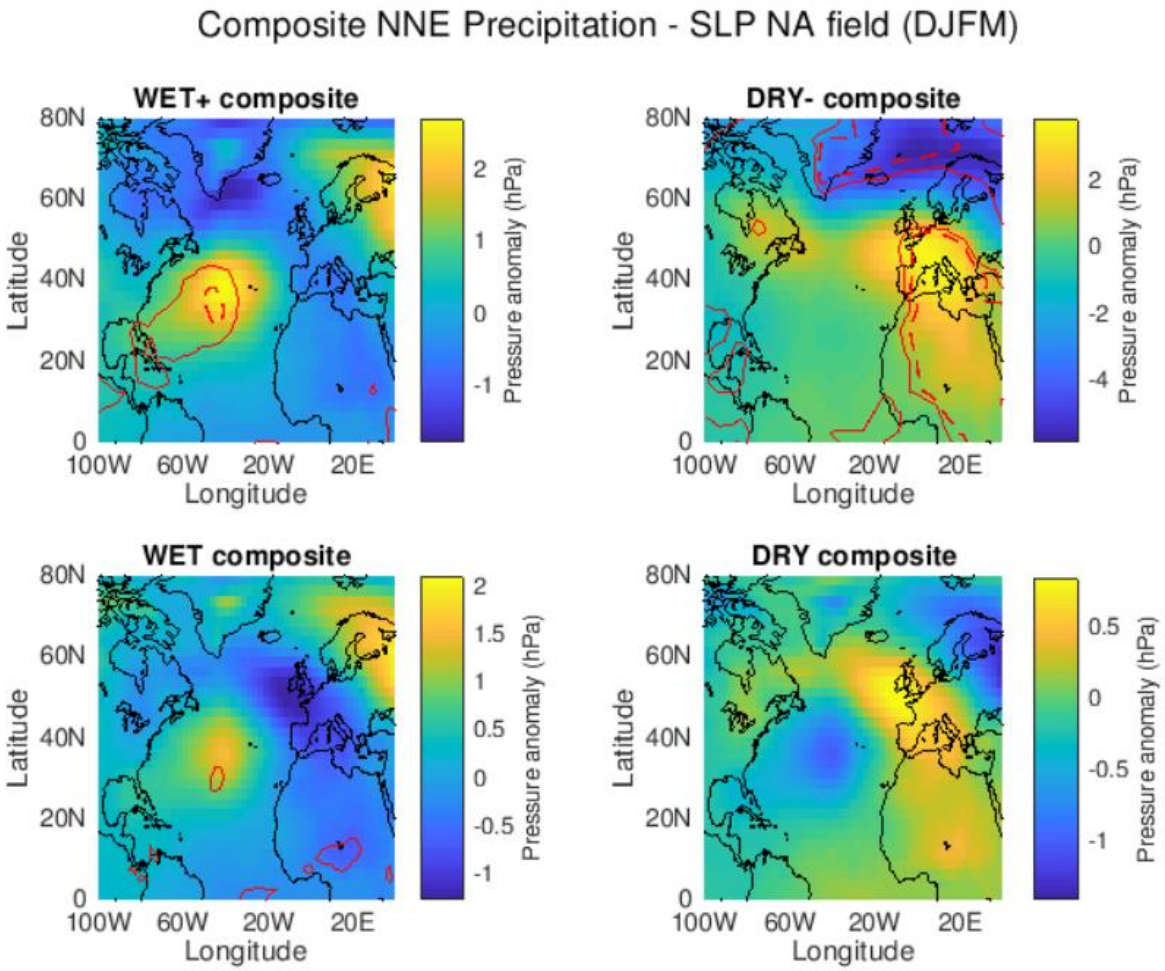

Figure 23. In the figure are displayed four maps corresponding to the WET+ (upper left panel), DRY- (upper right), WET (lower left) and DRY (lower right) composites between the NNE precipitation in MAM and the North Atlantic SLP field calculated in the DJFM months. Yellow tending colours means that the area is characterized by positive pressure anomalies; blue tending colours are used to represent negative anomalies. Continuous and dashed red lines are used to represent respectively the areas in which the anomalies are significative ate the 90% and 95% confidence level.

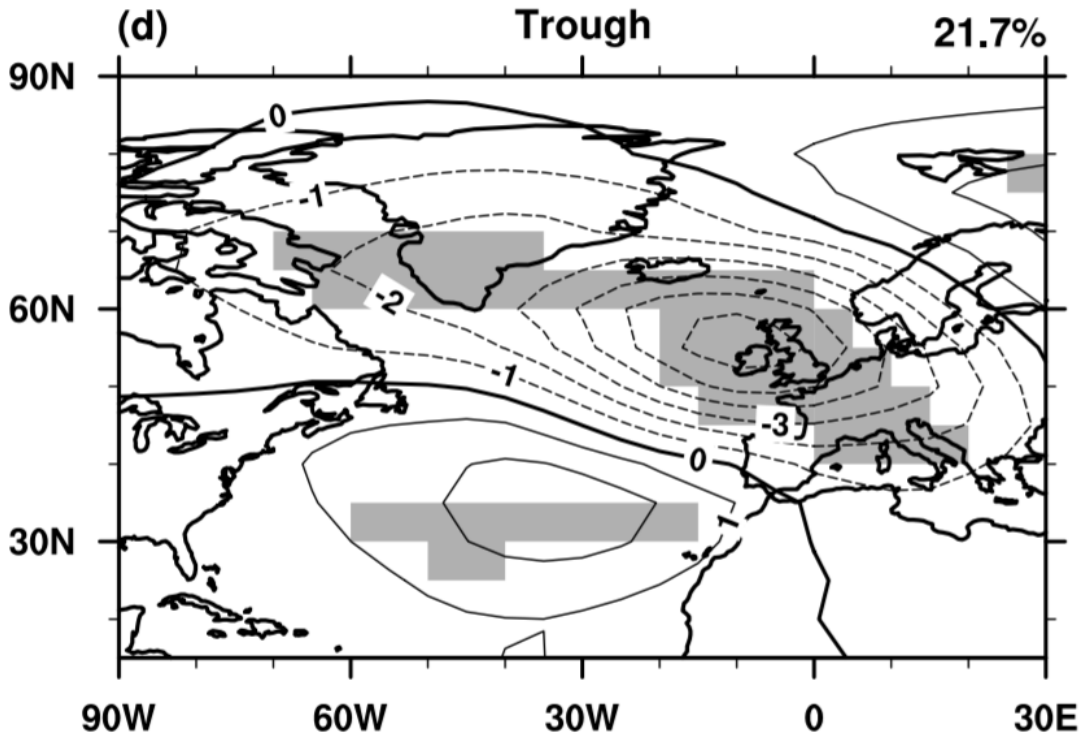

Figure 24. Trough NAO pattern identified by Hurrell et al., (2003) through a cluster analysis of the wintertime mean Surface Level Pressure field calculated from December to March. This pattern characterizes the 21.7% of the North Hemisphere winters and the years used to compose the map range from 1900 to 2001. Shaded areas exceed the 95% confidence level using T and F statistics [see Cassou, 2001]. The contour interval is 1 hPa.

5.3. Surface wind and SST fields associated with NNE precipitation anomalies

In the present section are reported the wind and SST composite maps calculated using a three-month arithmetic mean of the variable considered, starting from the December-January-February average and ending in March-April-May. Also, the DJFM composite is presented.

Let's consider first the WET+ and WET cases in the wind field composite. During boreal winter, there is a strong positive south-westward wind anomaly in the tropical North Atlantic, that spans from 25N to 0 latitude. In the DJF, DJFM and JFM maps Figure 25, 26 and 27), it clearly appears the high-pressure centre from which the surface winds departure; this centre, is in the same position in which the positive SLP anomalies were registered in the SLP composite analysis. That is

coherent with the fact that an increase of the high-pressure centre produces a strengthen in the associated counter clockwise winds. It is possible to observe a difference in the southward extension of the wind anomalies between the WET+ and WET case; in the WET+ case the north easterlies reach the deep equatorial latitudes and the can influence the CESG through its WES positive feedback. In the other case, the wind anomalies reach only the 10N latitude and the effect over the deep tropics is so reduced. Moving to the boreal spring, the tropical North Atlantic wind anomalies are reduced, coherently to the seasonal weakening of the Azores High, resulting from a general decrease of the NAO influence over the Northern Hemisphere. During the boreal spring, represented in the FMA e MAM maps (Figures 28 and 29), the positive north easterlies anomalies, above described, move southward towards the equator, contributing to enhance the CESG. As the same time, it's possible to see a negative anomalous longitudinal band between 0 and 10S, that roughly corresponds to the trough related to the ITCZ position. In these composites maps, the ITCZ stands south of the equator, thus propitiating an above than normal rainy season over NNE.

Looking to the DRY- and DRY composite maps, the biggest difference from the previous case in the boreal winter wind field is the absence of the north easterlies positive anomalies that characterize the North Atlantic basin at the middle and tropical latitudes. Anomalous positive winds are instead recorded over the North of Europe. Boreal spring shows an inverse equatorial SST pattern with respect to the WET+ and WET cases. In fact, instead of the negative wind anomaly that characterize that extend just south of the equator, there is a southward wind anomaly that "pull" northward the trough associated with the ITCZ. The ITCZ band is not well defined as in the previous case by the negative winds anomaly, probably because it's weaker than normal, coherently with the DRY- and DRY precipitation composite.

It's important to underline how the WES feedback works only in WET+ and WET cases. The opposite is not true. In fact, neither in SLP field composite analysis neither in the winds ones was found a centre of pressure in the same position of the one that characterize the WET+ and WET cases. So, a lower than normal pressure

between 25N-40N and 60W-20W doesn't has a significative consequence over the NNE rainy season.

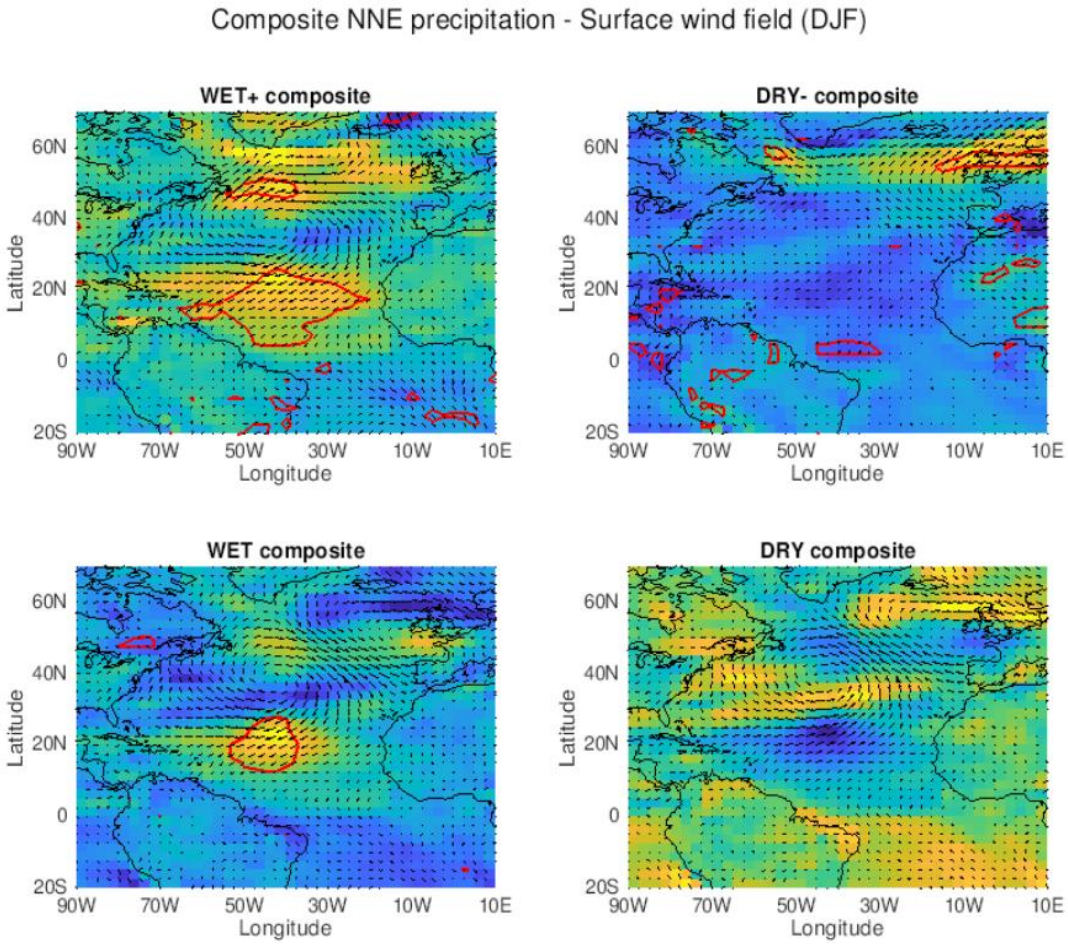

Figure 25. NNE precipitation - surface wind field (DJF) composite analysis. In the figure are displayed four maps, corresponding to the WET+ (upper left panel), DRY- (upper right), WET (lower left) and DRY (lower right) composites. Yellow tonalities are used to represent positive wind anomalies, blue ones indicated negative wind anomalies Black arrows indicate the wind direction. Continuous red line surround areas with anomalies significative ate the 95% confidence level.

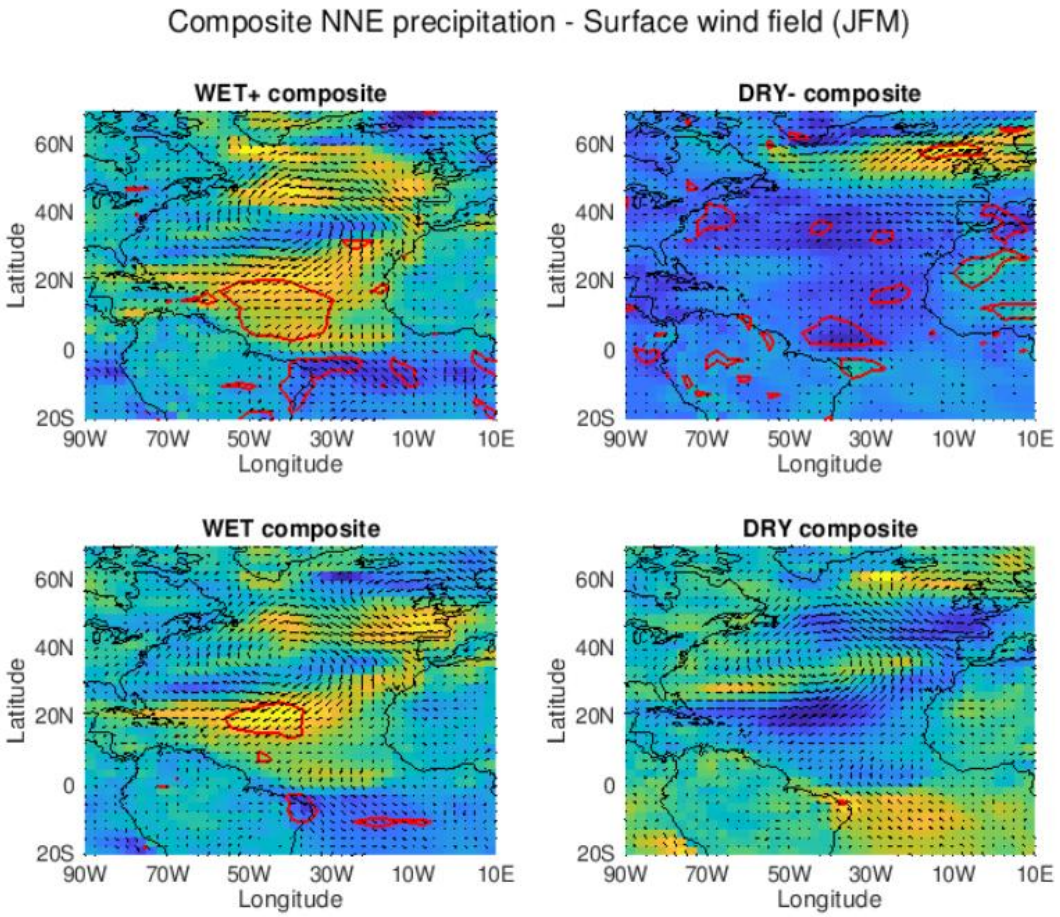

Figure 26. NNE precipitation - surface wind field (JFM) composite analysis. In the figure are displayed four maps, corresponding to the WET+ (upper left panel), DRY- (upper right), WET (lower left) and DRY (lower right) composites. Yellow tonalities are used to represent positive wind anomalies, blue ones indicated negative wind anomalies Black arrows indicate the wind direction. Continuous red line surround areas with anomalies significative ate the 95% confidence level.

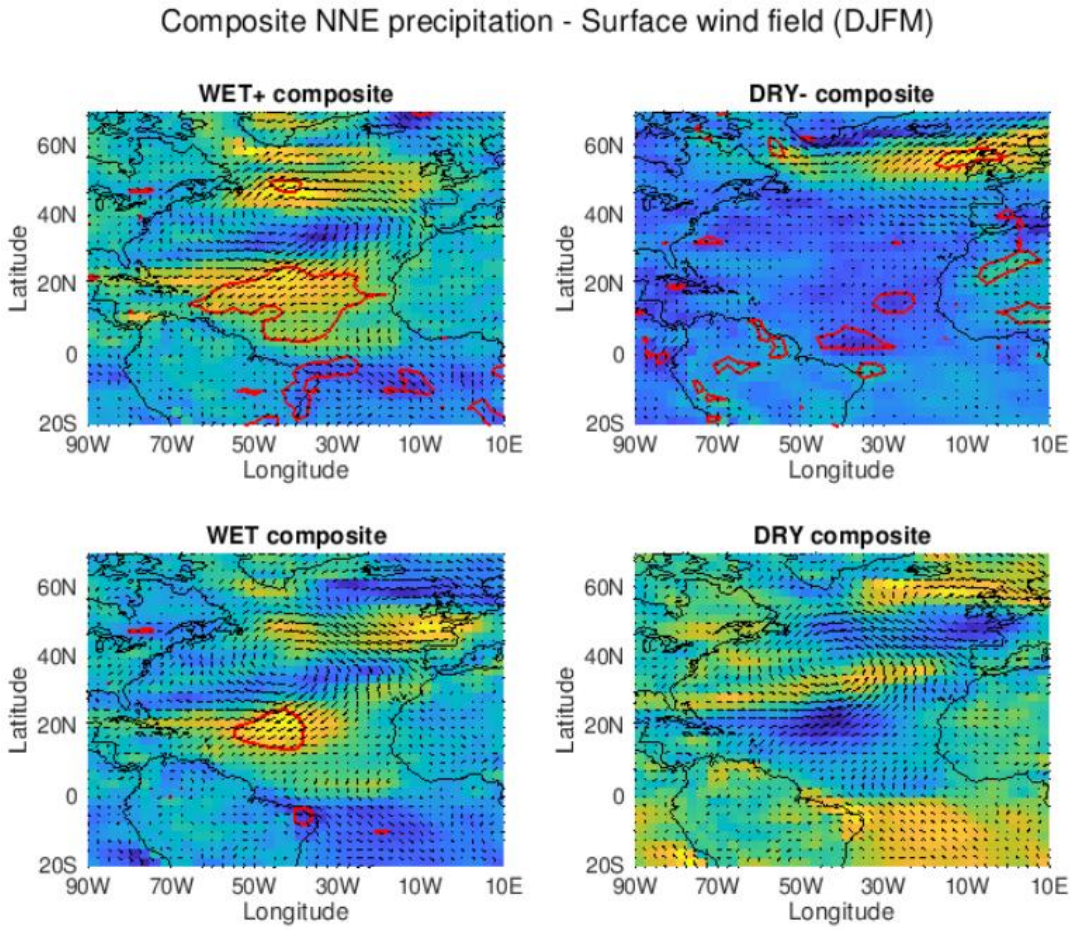

Figure 27. NNE precipitation - surface wind field (DJFM) composite analysis. In the figure are displayed four maps, corresponding to the WET+ (upper left panel), DRY- (upper right), WET (lower left) and DRY (lower right) composites. Yellow tonalities are used to represent positive wind anomalies, blue ones indicated negative wind anomalies Black arrows indicate the wind direction. Continuous red line surround areas with anomalies significative ate the 95% confidence level.

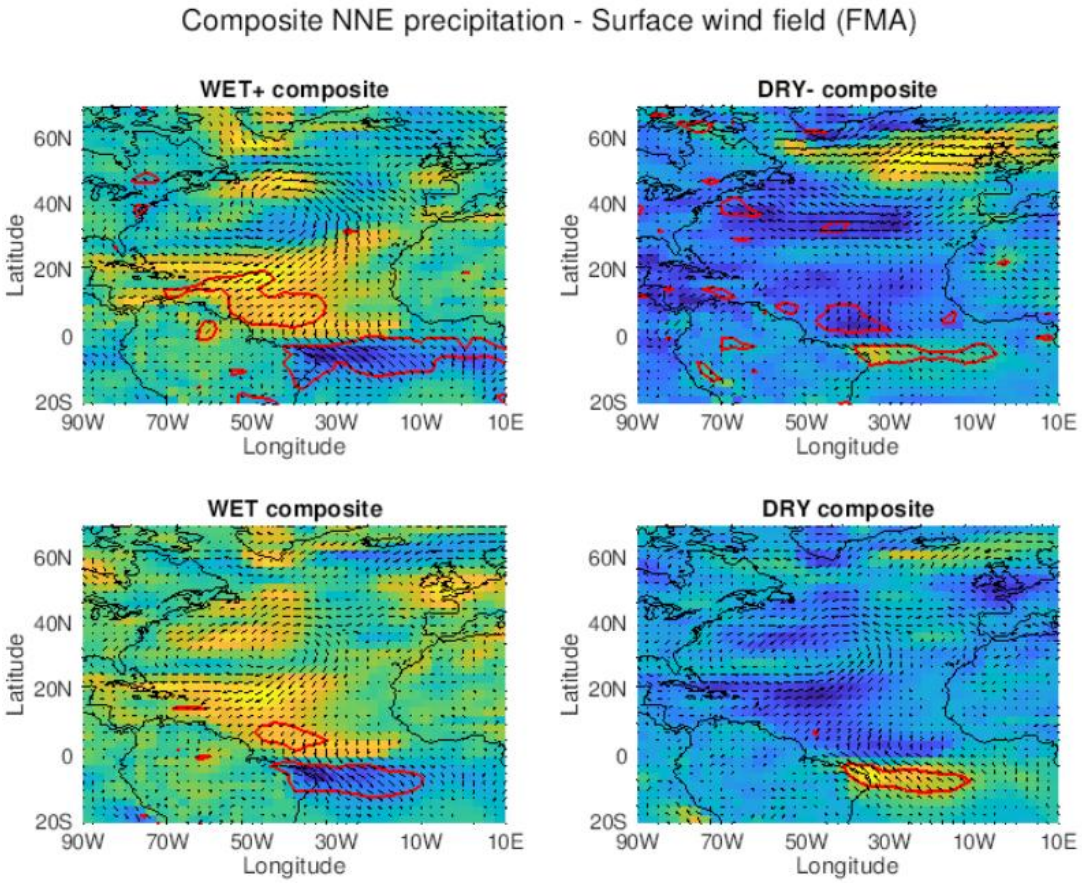

Figure 28. NNE precipitation - surface wind field (FMA) composite analysis. In the figure are displayed four maps, corresponding to the WET+ (upper left panel), DRY- (upper right), WET (lower left) and DRY (lower right) composites. Yellow tonalities are used to represent positive wind anomalies, blue ones indicated negative wind anomalies Black arrows indicate the wind direction. Continuous red line surround areas with anomalies significative ate the 95% confidence level.

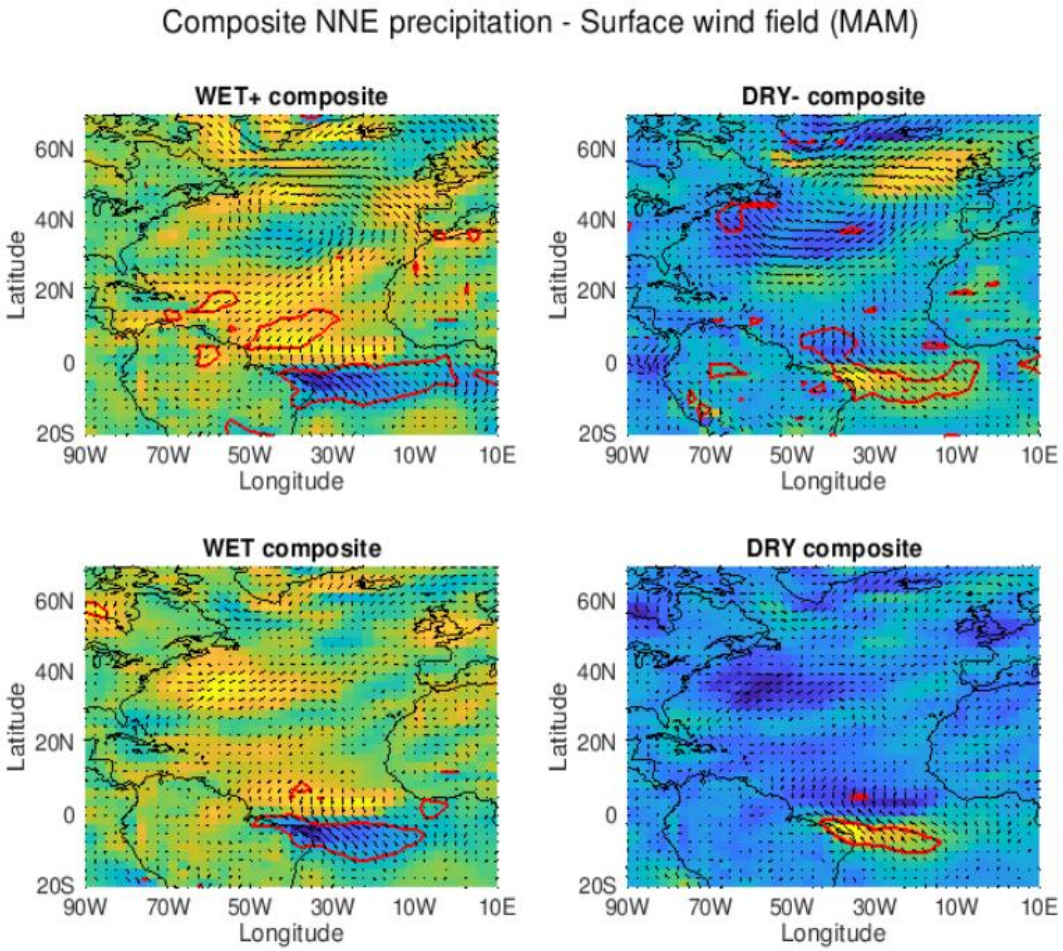

Figure 29. NNE precipitation - surface wind field (MAM) composite analysis. In the figure are displayed four maps, corresponding to the WET+ (upper left panel), DRY- (upper right), WET (lower left) and DRY (lower right) composites. Yellow tonalities are used to represent positive wind anomalies, blue ones indicated negative wind anomalies Black arrows indicate the wind direction. Continuous red line surround areas with anomalies significative ate the 95% confidence level.

The Figures 30, 31, 32, 33 and 34 show the composite maps of the Atlantic SST and the NNE rainfall. Considering only the WET+ composite maps from the boreal winter to spring, it is possible to see the tropical Atlantic SST dipole formation. While the southern lobe is visible in every chart, the northern one increase in intensity and width proceeding from DJF to MAM composites. The SST anomalies grow with some lag with respect to the SLP and wind anomalies. This is coherent with what was illustrated by Nobre and Shukla (1996), that registered a 2-months' time lag between the development of positive north-easterly wind anomalies and negative SST anomalies over tropical North Atlantic. The SST charts, limited to the WET+ and WET case, seems to be consistent to the pattern identified in the

whole research, i.e. an anomalous position of the southern centre of action of the NAO teleconnection determine an increase in the north-easterly trade winds that through the WES feedback force the northern tropical Atlantic SST to decrease, thus creating the conditions for a circulation that is favourable to abundant precipitation over NNE.

The WET composite shows the same pattern as the WET+ ones, but with weaker SST anomalies. It's important to note the negative SST anomalies that characterizes the west Latin America coasts: these are related to the ENSO teleconnection, that without any doubt play a strong part in the NNE precipitation modulation The DRY- composite display weak negative anomalies in each map, with the exception of the area in which the southern centre of pressure identified in the WET+ composites acts, where the negative anomalies are statistically significative. It would be expected, in the DRY- composite, to see an inverted SST pattern with respect to the WET+ and WET case, with the tropical Atlantic SST dipole inverted in sign. Instead, it is remarkable the strong ENSO positive anomaly that extends off the Perú and Colombia coasts. That may strengthen the thesis that the DRY- anomalies are largely influenced by El Niño phenomenon, making the NAO influence less important of that showed in the NAO DRY- composite charts.

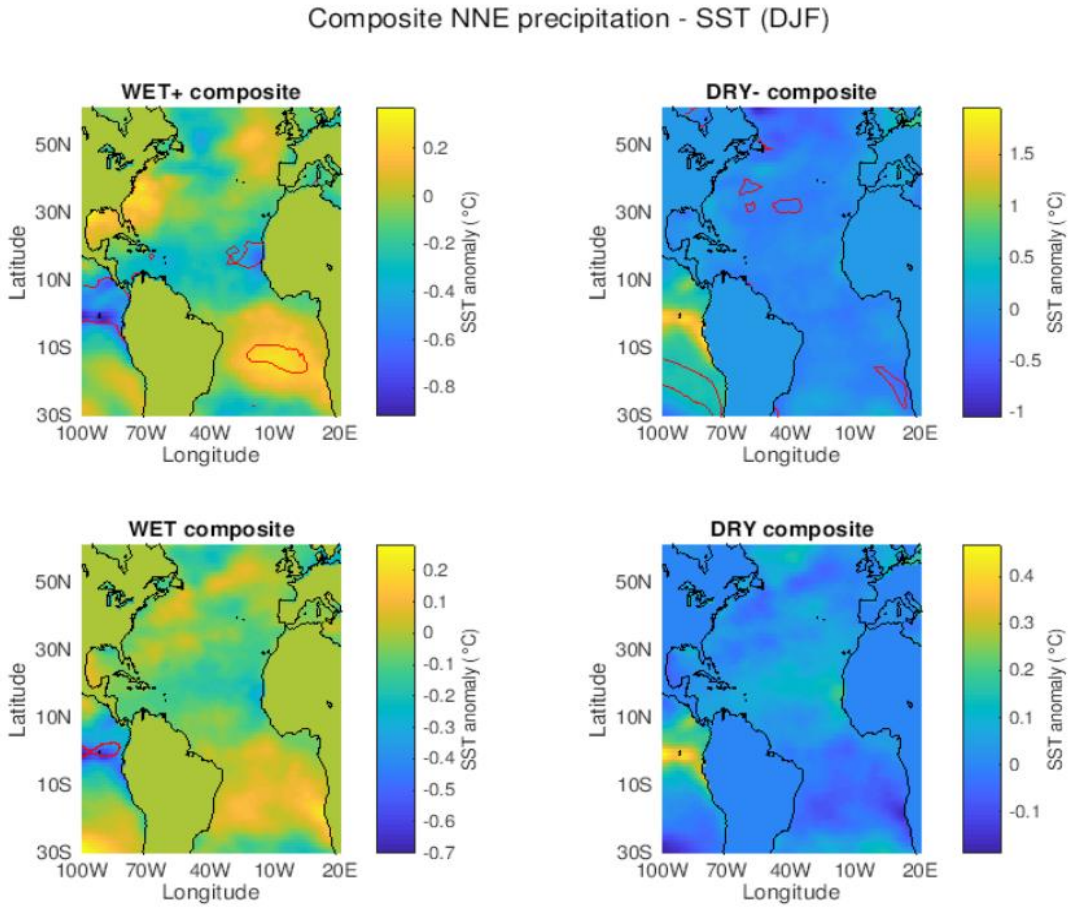

Figure 30. NNE precipitation - SST (DJF) composite maps. In the figure are displayed four maps, corresponding to the WET+ (upper left panel), DRY- (upper right), WET (lower left) and DRY (lower right) composites. Positive and negative anomalies are represented with yellow and blue shades, respectively. Red contours surround areas where SST anomalies are significative at the 95-confidence level.

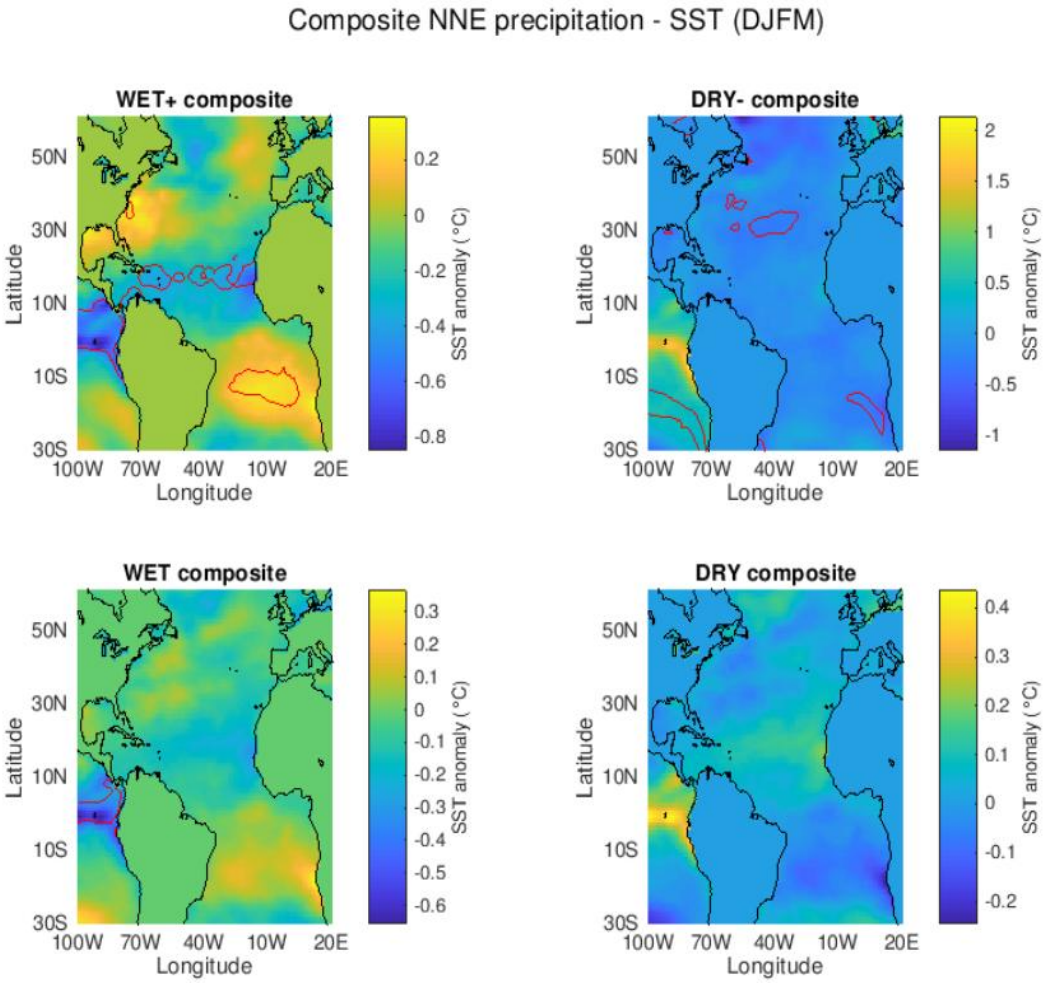

Figure 31. NNE precipitation - SST (DJFM) composite maps. In the figure are displayed four maps, corresponding to the WET+ (upper left panel), DRY- (upper right), WET (lower left) and DRY (lower right) composites. Positive and negative anomalies are represented with yellow and blue shades, respectively. Red contours surround areas where SST anomalies are significative at the 95 confidence level.

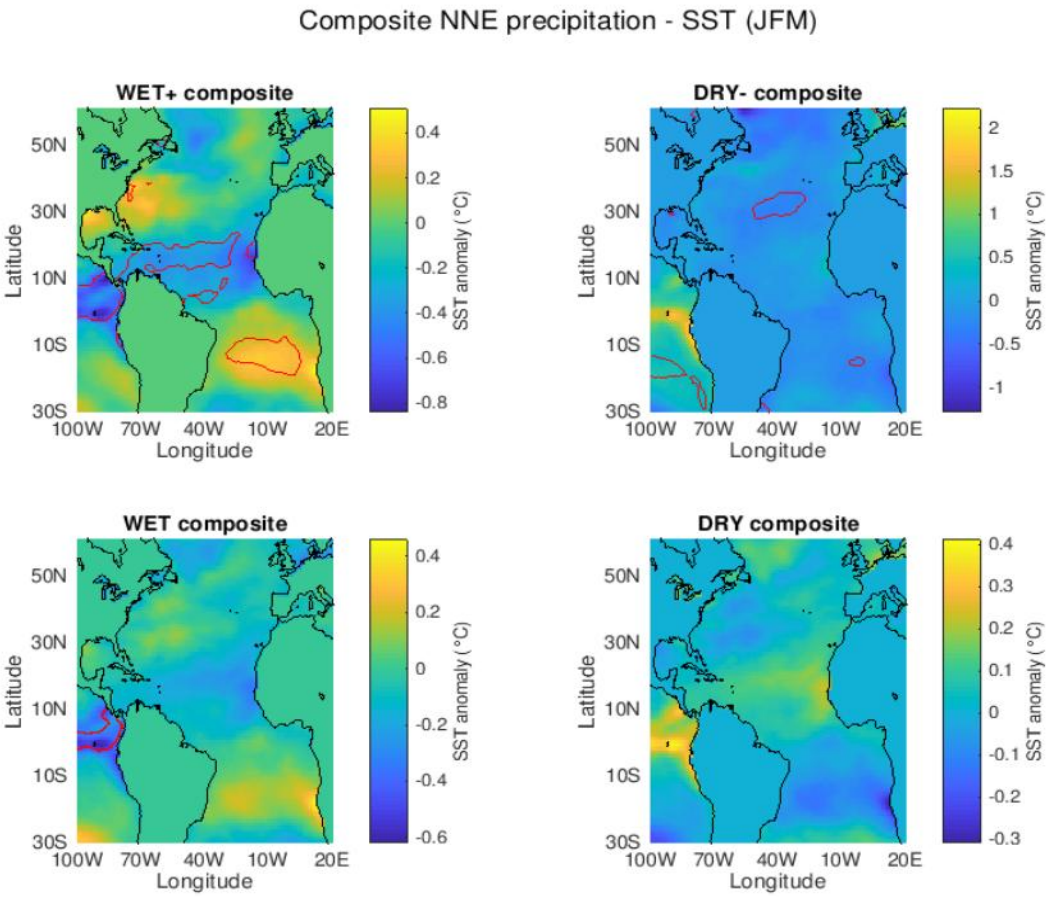

Figura 32. NNE precipitation - SST (JFM) composite maps. In the figure are displayed four maps, corresponding to the WET+ (upper left panel), DRY- (upper right), WET (lower left) and DRY (lower right) composites. Positive and negative anomalies are represented with yellow and blue shades, respectively. Red contours surround areas where SST anomalies are significative at the 95-confidence level.

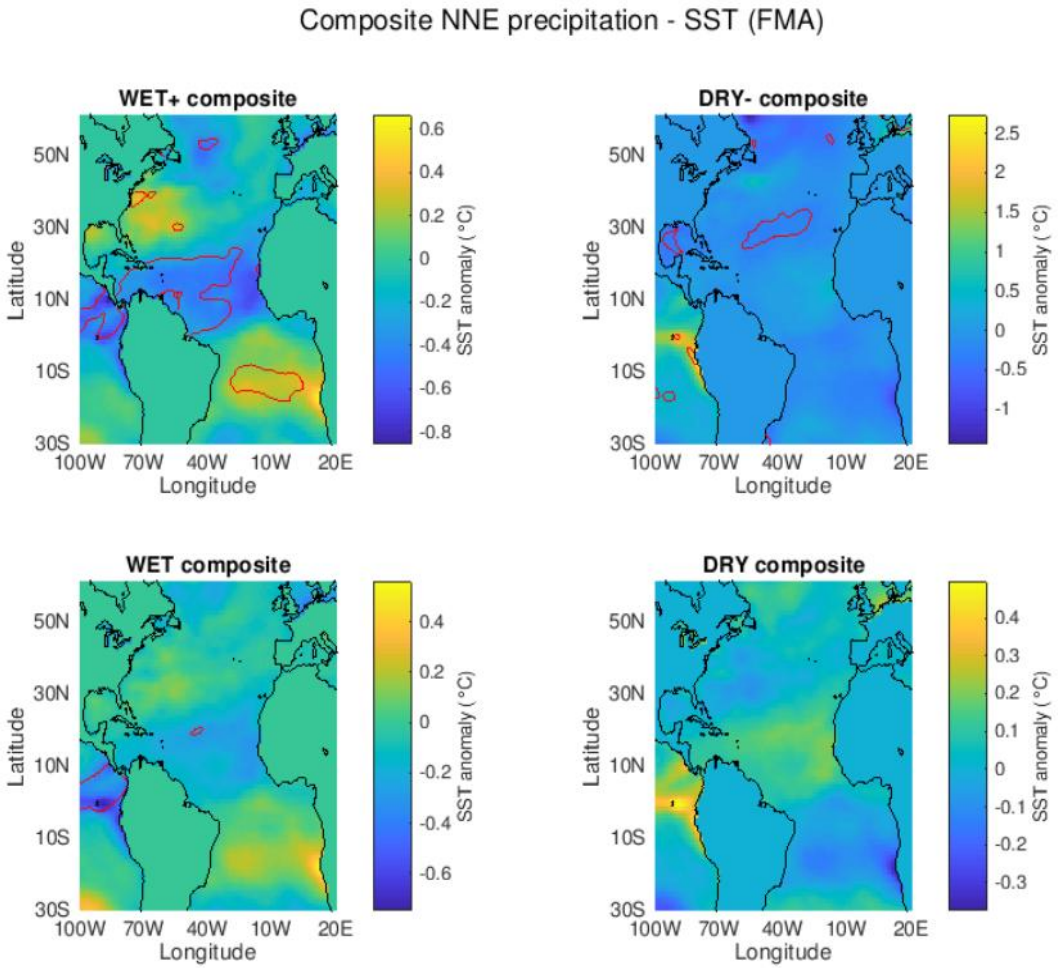

Figura 33. NNE precipitation - SST (FMA) composite maps. In the figure are displayed four maps, corresponding to the WET+ (upper left panel), DRY- (upper right), WET (lower left) and DRY (lower right) composites. Positive and negative anomalies are represented with yellow and blue shades, respectively. Red contours surround areas where SST anomalies are significative at the 95-confidence level.

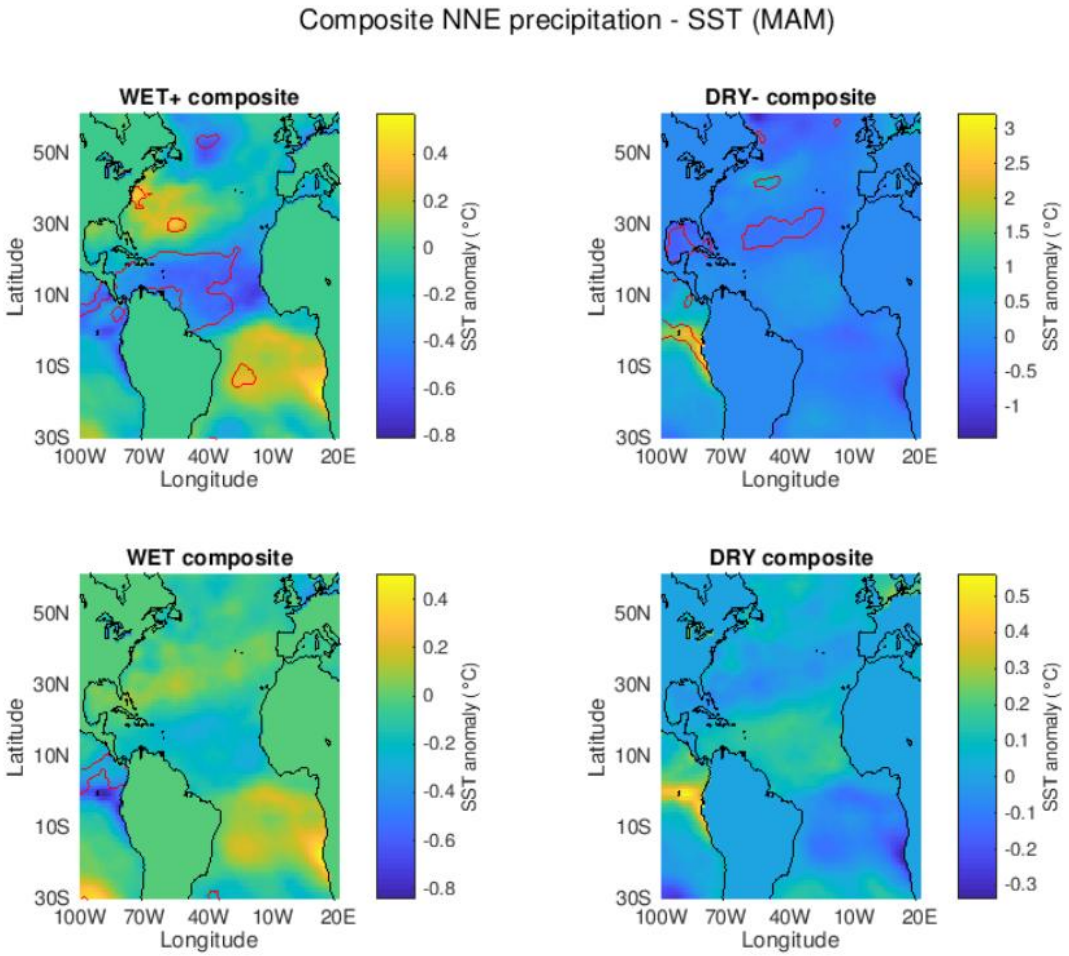

Figure 34. NNE precipitation - SST (MAM) composite maps. In the figure are displayed four maps, corresponding to the WET+ (upper left panel), DRY- (upper right), WET (lower left) and DRY (lower right) composites. Positive and negative anomalies are represented with yellow and blue shades, respectively. Red contours surround areas where SST anomalies are significative at the 95-confidence level.

5.4. NAOcp and naos index

In this paragraph will be shown the results of the analysis made to test the strength of the relationship between new NAO's centres of pressure related indices and the NNE precipitation. Correlation and composite analysis are the tools used to test this relationship. The seasonal NAOcp correlation with the MAM precipitation is shown in the Figure 35. The highest r coefficient is obtained when the index is calculated using the SLP values from December to February, where it is equal to 0.3086 with the 90% significance level. Looking to the scatter plots of the composite analysis showed in the Figure 36, the difference between the climatological mean and the mean of the SLP values of the WET+ years is significative at the 95% confidence level, meaning that the NAOcp index has a good relationship with the NNE precipitation if the season with large precipitation amount are considered. In the other cases of the composite, the influence of the anomalous displacement of the NAO centres of pressure doesn't seem to influence significative the NNE precipitation.

The NAOs index is calculated only considers the area of action of the southern NAO centre of pressure. The idea of discard the northern Atlantic area in the index calculation is due to the observation of the SLP composite and correlation maps above displayed (figures 18, 19, 20, 21, 22, 23): the anomalous displacement of the southern centre of action is well defined in the tropical/middle North Atlantic by significative r coefficient values and composite (WET and WET+ cases) differences. The same thing can't be affirmed where the latitude is higher than 50N. The scatter plots of NAOs seasonal index versus the NNE precipitation is represented in the Figure 37. The NAOs index shows a better relationship with the NNE precipitation if compared to the NAOcp index. In fact, the r coefficient of all the seasonal charts is significative at the 90% significance level, with a peak in the DJF season, where the Pearson coefficient is significant at the 95% level. Also, the composite graphs in Figure 38 indicate a stronger relation between the index and the NNE precipitation. The composite differences of the WET+ and WET cases are both significant at the 95% level. This means that, when the MAM rainy season is above than normal in the NNE Brazil, it is likely that the NAOs index is positive.

Finally, a monthly NAOs correlation analysis is performed to assess the role of every month in the NAOs seasonal calculation. The results are represented in Figure 38. February is the month in which the SLP used to calculate the NAOs index influence greater the NNE precipitation (95% significance level), where March SLP doesn't seem to have a remarkable role over the NNE rainy season amount.

The NAOs index has stronger statistical relationship with the NNE MAM rainy season also compared with the NAO sb and NAO pc indices, both considering the correlation and composite analysis. One point of interest is the comparison between the indices by mean of the composite analysis. Considers the extreme composite cases: the trend that the NAO pc index showed in the DRY- case doesn't extend to the DRY case, where the NAOs index behaviour in the WET+ case is consistent with the WET one. This suggest that the DRY- trend can be the affected and forced by some other phenomenon (like the ENSO), while the NAOs index effectively represents a phenomenon that has a stake over NNE precipitation in a great number of cases.

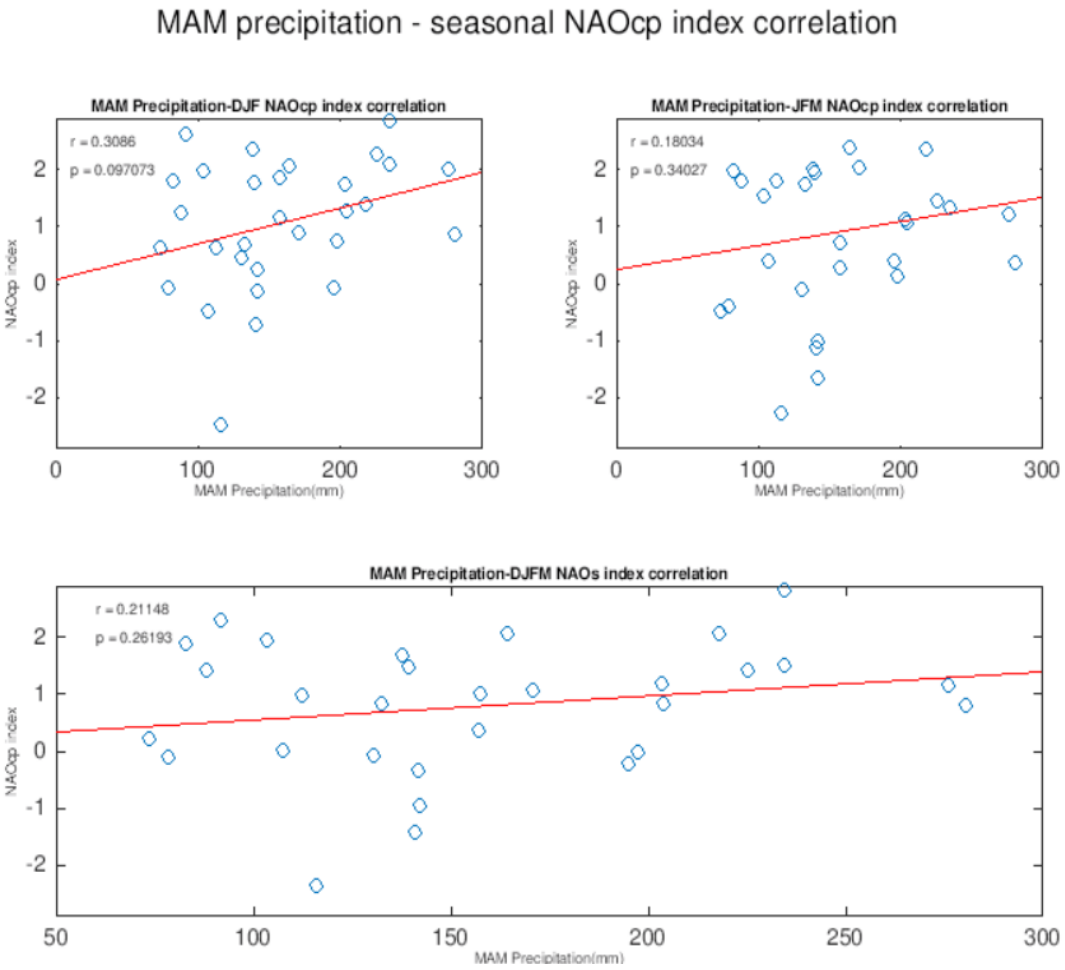

Figure 35. The scatter plots of the seasonal NAOcp index - MAM precipitation are shown. In the panels, the NAOcp seasonal index is calculated using the monthly NAOcp index mean from December to February (upper left), from January to March (upper right) and from December to February (lower one). In each panel, the x and y axis represent the NNE precipitation amount during MAM and the NAOcp index values, respectively. Each blue dot represents the annual value of precipitation and NAOcp index; the red line is the regression line of the data. r and p are, respectively, the seasonal Pearson coefficient and the p value.

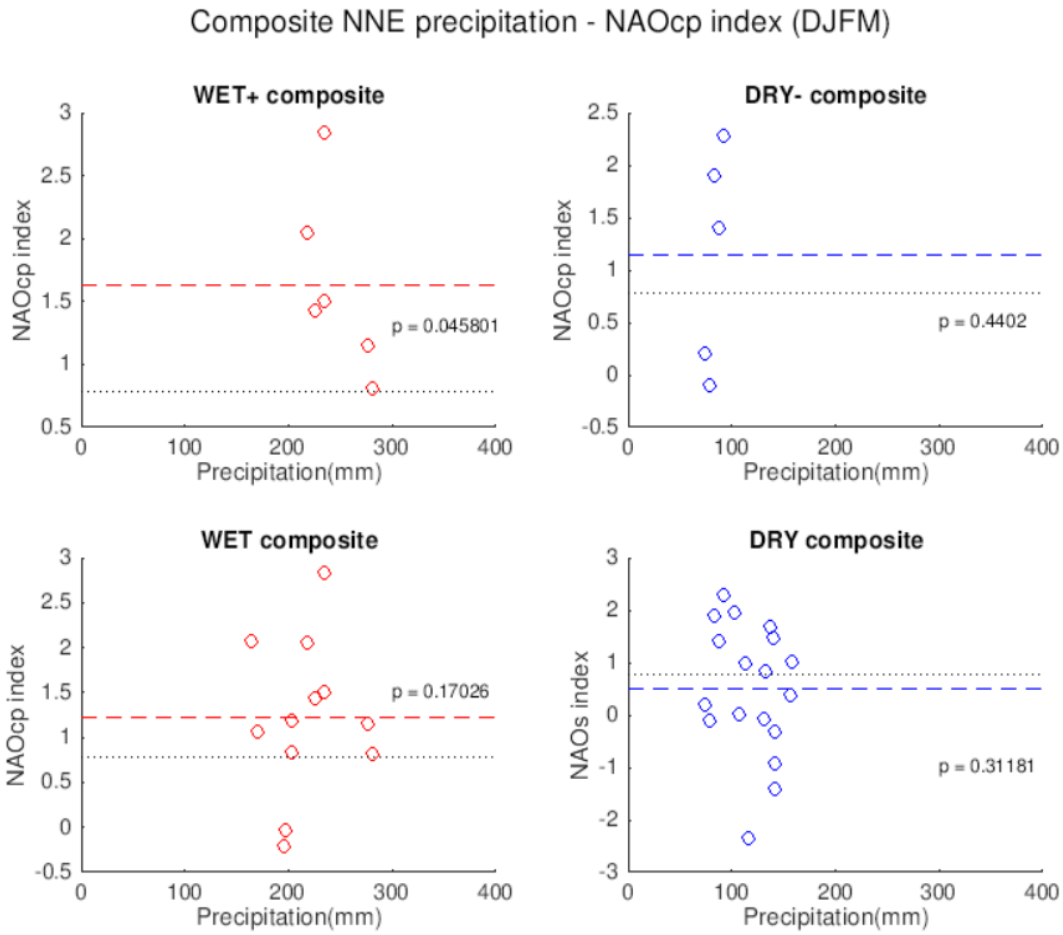

Figure 36: In the figure are displayed four panels representing the results of the composite analysis between NNE precipitation and seasonal (DJFM) NAOcp index. WET+ and DRY- years are represented, respectively, in the left and right upper panels, while WET and DRY years are showed in the bottom panels. Blue color is used in the graphs where precipitation below than normal is involved, red color where precipitation is above than normal. On the x-axis the precipitation range is shown and on the y-axis the NAO index values are displayed. The blue/red dots represent the individual seasonal NAO index value, the blue/red lines represent the mean of the seasonal NAO index considering the years selected in each composite; the black dotted line is the mean of the seasonal NAO index considering all the years from 1981 to 2010.

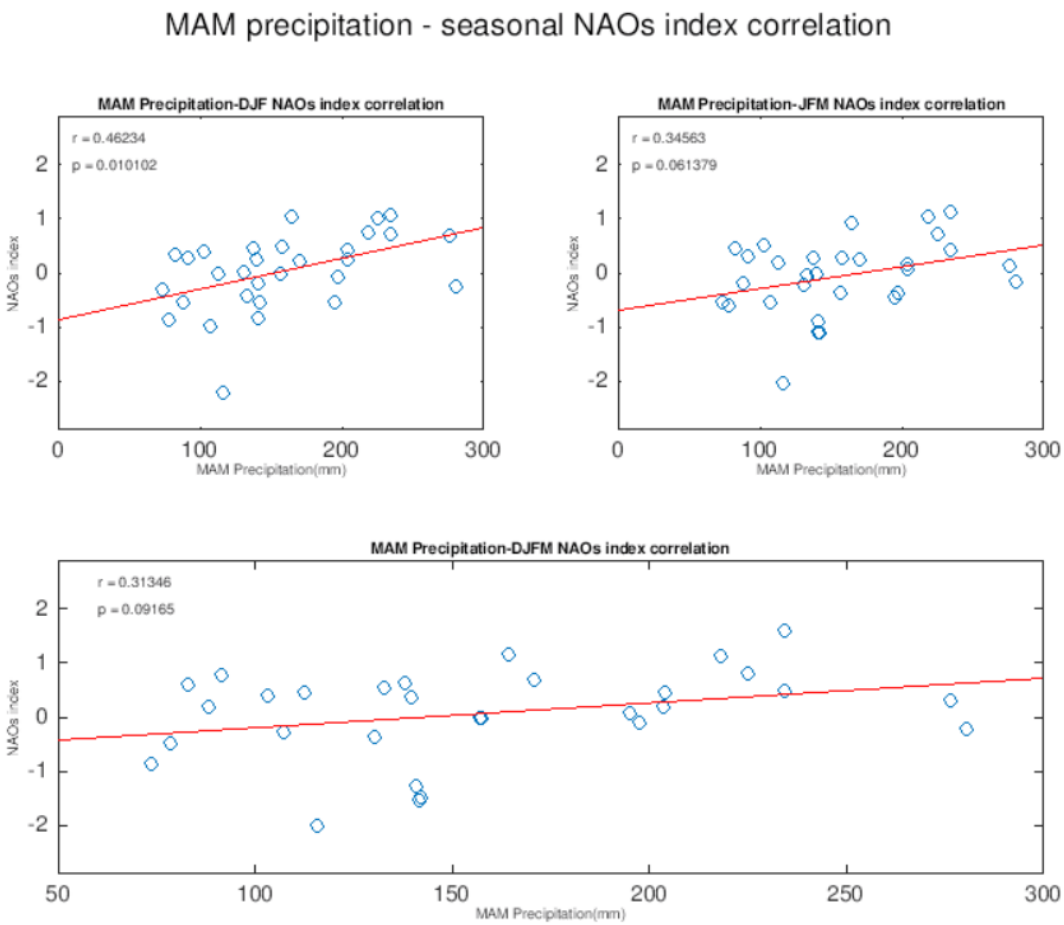

Figure 37. The scatter plots of the seasonal NAOs index - MAM precipitation is shown. In the panels, the NAOs seasonal index is calculated using the monthly NAOs index mean from December to February (upper left), from January to March (upper right) and from December to February (lower one). In each panel, the x and y axis represent the NNE precipitation amount during MAM and the NAOs index values, respectively. Each blue dot represents the annual value of precipitation and NAOs index; the red line is the regression line of the data. r and p are, respectively, the seasonal Pearson coefficient and the p value.

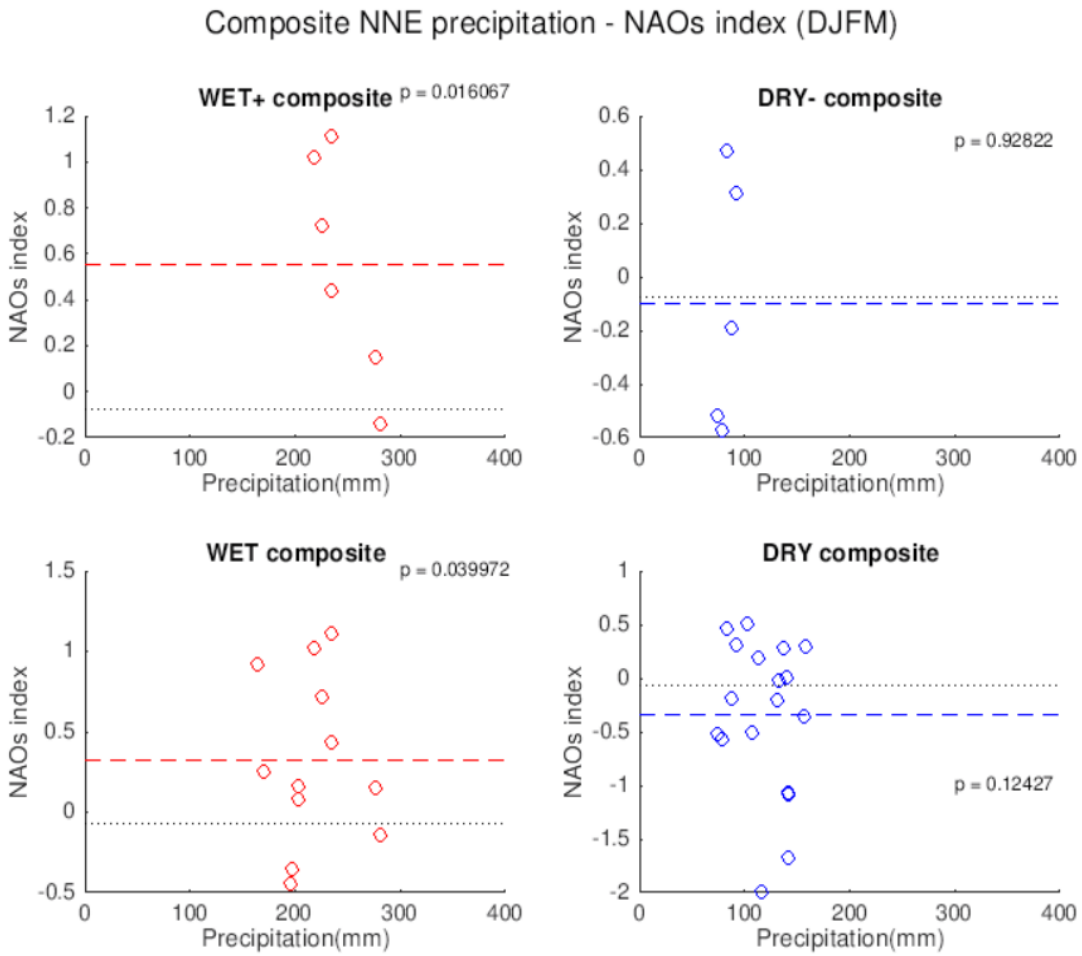

Figure 38. In the figure are displayed four panels representing the results of the composite analysis between NNE precipitation and seasonal (DJFM) NAOs index. WET+ and DRY- years are represented, respectively, in the left and right upper panels, while WET and DRY years are showed in the bottom panels. Blue colour is used in the graphs where precipitation below than normal are involved, red colour where precipitation are above than normal. On the x-axis the precipitation range is shown and on the y-axis the NAO index values are displayed. The blue/red dots represent the individual seasonal NAO index value, the blue/red lines represent the mean of the seasonal NAO index considering the years selected in each composite; the black dotted line is the mean of the seasonal NAO index considering all the years from 1981 to 2010.

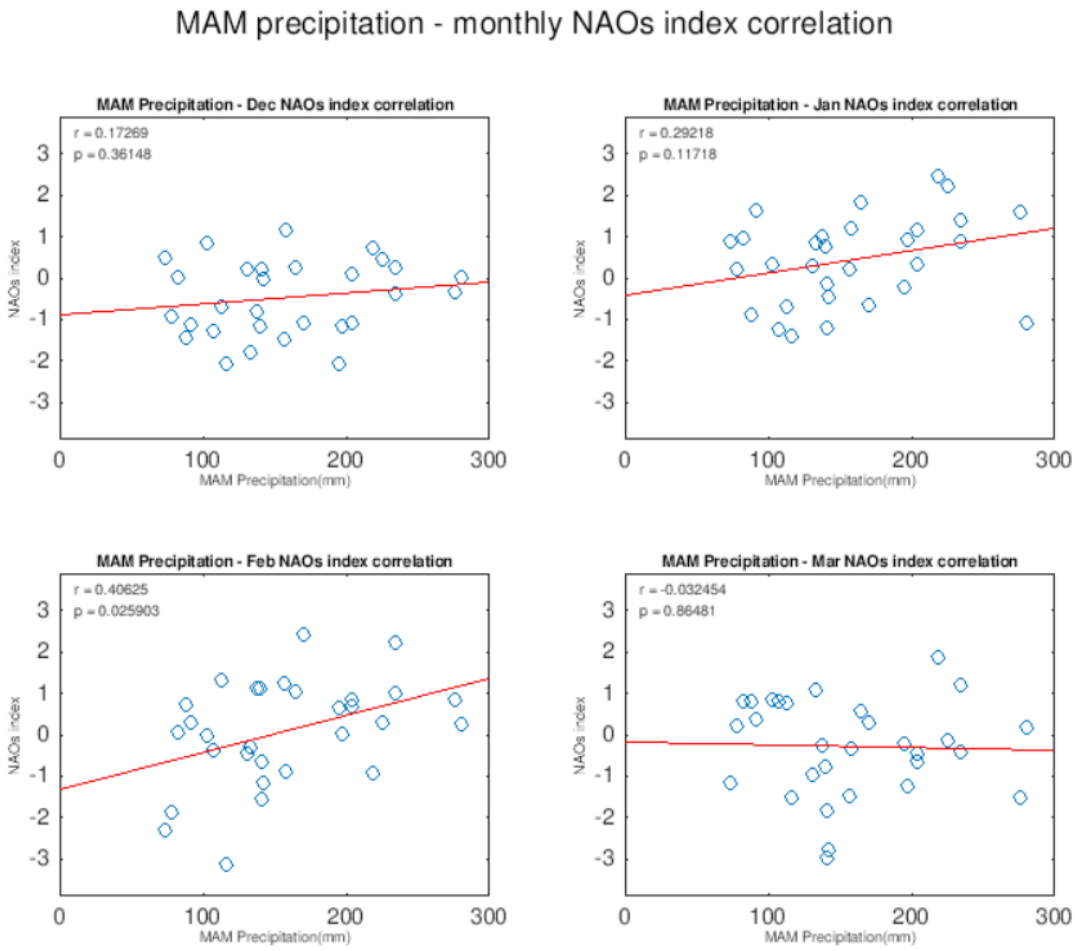

Figure 39. The scatter plots of the monthly NAOs index - MAM precipitation from December to March are shown. Each month in which the NAOs index is calculated is separately displayed in the panels of the figure. In each panel, the x and y axis represent the NNE precipitation amount during MAM and the NAOs index values, respectively. Each blue dot represents the annual values of precipitation and NAOs index; the red line is the regression line of the data. r and p are, respectively, the monthly Pearson coefficient and the p value.

6. CONCLUSIONS

6.1. Final remarks

In the first part of this work, the classical indices by which the NAO teleconnection is expressed are used to find the NAO influence over the NNE rainy season. The NAO station based (NAOsb) index and the NAO index derived using principal component analysis (NAOpc) are considered in this phase. The linear relationship between both indices and the NAO precipitation is not statistically significant. Moreover, a composite analysis over the NNE precipitation is made and a statistically significant relationship, limited only to the NAOpc index, is only obtained in the DRY- cases. However, if we consider that the DRY- composite includes only five years, during which the ENSO teleconnection was in the strong or very-strong phase, it is probable that the results are strongly influenced by the El Niño behaviour. This consideration is strengthened by the fact that the DRY composite does not show the same trend of the DRY- one, thus bounding the anomalous signal only to the extreme dry years.

Better results were found in the relationship between the North Atlantic SLP field and the NNE rainy season. The linear correlation analysis shows an area of positive correlation located between 60W-20W and 25N-40N; in addiction, above than normal SLP values in the WET and WET+ composite cases were found in this area. This suggests that this region may play an important role in determining the quality of the NNE rainy season. This area is approximately the same of that occupied by the southern centre of pressure when the NAO teleconnection takes on a "trough" configuration identified through a cluster analysis of the North Atlantic SLP field during wintertime (Figure 24). The "trough" configuration is a spatial variation of the NAO positive phase, in which the southern NAO centre of pressure is in an anomalous southern and western more position. In this pattern, the northern centre of pressure doesn't present a determined location. The composite analysis presents statistically significant SLP differences only when the NNE precipitation is above normal: in fact, in this case, the high-pressure centre force enhanced south-westward trade winds that, penetrating in the deep tropics, cold the Tropical North Atlantic

SST and contribute to modify the ITCZ position. The opposite is not true, as evidenced by the fact that the results of the DRY and DRY- composite years don't show significant SLP anomalies in the same area. So, this area doesn't have a relevant influence over the NNE rainy season in dry years.

The composites of the wind and SST fields are coherent with the SLP-trade winds-WES mechanism that is related to above than normal precipitation over NNE. In fact, in the WET and WET+ wind composites the north-easterly trade winds coherently blow from the same area in which the Azores anticyclone acts in the years of enhanced rainfall over NNE. It's interesting to observe that the trade wind anomalies shown in the WET+ and WET composites propagate southward passing from boreal winter to spring, reaching the equatorial latitudes. The trade winds seem to be the vector that "transport" the middle latitude circulation anomalies to the deep tropics. In the DRY and DRY- wind composites, the wind field isn't characterized by consistent and significant anomalies. This can be another clue of the fact that the North Atlantic doesn't exert a determinant influence over NNE precipitation during dry years, and other factors may be the drivers of the Sêcas. The same conclusions can be drawn by considering the SST composite maps: in the WET and WET+ composites is clearly visible the formation of the negative SST anomaly over the Tropical North Atlantic, that is more evident in spring than during winter. This is the consequence of the action of the trade winds that, through the WES mechanism, force the decrease of the Tropical NA SST and gradually contribute to generate the negative anomalies in this area.

Finally, an index (NAOs) based on the SLP measured in the region of action of the NAO southern centre of pressure was calculated. This index shows a better relationship with the NNE rainy season with respect to the classical NAO indices. An explanation for this is that the classical NAO indices are created to relate the shifts and variation of the NAO teleconnection to changes in the European or North American climate. However, in the NNE case, they don't seem to represent correctly the influence of the North Atlantic system of pressures over that region. The NAOs index shows a better statistical relation also in comparison with the NAOcp index, that was calculated with the same method of the NAOs index but considering the NAO centres of pressure. So, include the northern NAO centre of pressure weakens

the relation between the signal of the teleconnection and the NNE rainy season. The NAO seems to have a stronger influence over the NNE region when the southern CP is considered individually, analysing its area of action and its intensity.

6.2. Suggestions for future researches

The results obtained in this research can be used as a starting point for future studies. There are three lines of research that can be interesting to explore: make the same procedure adopted in this work to assess if the NAO also influences the precipitation in other regions of the South America; the analysis of other teleconnections in the Boreal Hemisphere that can play a role over the NNE precipitation and the inclusion of the displacement of the southern NAO centre of action in some simulation model.

In the first case, it's interesting to discover if the NAO has a significant relationship with the precipitation in the whole NEB, in the Amazon Forest and in the Pantanal, whose rainy season is also influenced by variation of the ITCZ displacement. Second, in this work we found other areas in which there was a statistically significant correlation with the NNE rainy season. Looking at the Figure 18, it is possible to observe two areas in which the Pearson coefficient reach significant values, located over the West Africa and the East Russia. In these areas, approximately, acts the pressure dipole related to the East Atlantic teleconnection. For this reason, it may be interesting assess the significance of the relationship between the East Atlantic teleconnection and the NNE rainy season. Finally, it's suggested to force a GCM model with the NAO trough configuration order to assess the response of the atmosphere to this anomalous displacement of the NAO related centres of pressure and verify if what was observed in this work is coherent with the model simulation.

REFERENCES

Alves, J. M. B., & Repelli, C. A. (1992). A variabilidade pluviométrica no setor norte do Nordeste e os eventos El Niño-Oscilação Sul (ENOS). *Revista Brasileira de Meteorologia*, 7(2), 583-592.

Barreto, F. A. F. D., NETO, P. D. M. J., & TEBALDI, E. (2001). Desigualdade de renda e crescimento econômico no nordeste brasileiro. *Revista Econômica do Nordeste*, Fortaleza, 32, 842-859.

Bischoff, T., & Schneider, T. (2016). The equatorial energy balance, ITCZ position, and double-ITCZ bifurcations. *Journal of Climate*, 29(8), 2997-3013.

Boschat, G., Simmonds, I., Purich, A., Cowan, T., & Pezza, A. B. (2016). On the use of composite analyses to form physical hypotheses: An example from heat wave–SST associations. *Scientific reports*, 6, 29599.

Broccoli, A. J., Dahl, K. A., & Stouffer, R. J. (2006). Response of the ITCZ to Northern Hemisphere cooling. *Geophysical Research Letters*, 33(1).

Campos, J. N. B., & STUDART, T. D. C. (2001). Secas no Nordeste do Brasil: origens, causas e soluções. *IV Dialógo Interamericano de Gerenciamento de Águas*. ABRH: Foz do Iguaçu.

Chiang, J. C., & Friedman, A. R. (2012). Extratropical cooling, interhemispheric thermal gradients, and tropical climate change. *Annual Review of Earth and Planetary Sciences*, 40.

Chu, P. S. (1983). Diagnostic studies of rainfall anomalies in Northeast Brazil. *Monthly Weather Review*, 111(8), 1655-1664.

Czaja, A., & Frankignoul, C. (2002). Observed impact of Atlantic SST anomalies on the North Atlantic Oscillation. *Journal of Climate*, 15(6), 606-623.

Czaja, A., Robertson, A. W., & Huck, T. (2003). The Role of Atlantic Ocean- Atmosphere Coupling in Affecting North Atlantic Oscillation Variability. *The North Atlantic Oscillation: climatic significance and environmental impact*, 147-172.

de Albuquerque Cavalcanti, I. F. (2015). The influence of extratropical Atlantic Ocean region on wet and dry years in North-Northeastern Brazil. *Frontiers in environmental science*, 3, 34.

De Souza, E. B., & Ambrizzi, T. (2006). Modulation of the intraseasonal rainfall over tropical Brazil by the Madden–Julian oscillation. *International Journal of Climatology*, 26(13), 1759-1776.

De Souza, E. B., Kayano, M. T., & Ambrizzi, T. (2005). Intraseasonal and submonthly variability over the eastern Amazon and Northeast Brazil during the autumn rainy season. *Theoretical and Applied Climatology*, 81(3-4), 177-191.

Hastenrath, S. (1984). Interannual variability and annual cycle: Mechanisms of circulation and climate in the tropical Atlantic sector. *Monthly Weather Review*, 112(6), 1097-1107.

Hastenrath, S. (2006). Circulation and teleconnection mechanisms of Northeast Brazil droughts. *Progress in Oceanography*, 70(2-4), 407-415.

Hastenrath, S. (2012). Exploring the climate problems of Brazil's Nordeste: a review. *Climatic Change*, 112(2), 243-251.

Hastenrath, S., & Greischar, L. (1993). Further work on the prediction of northeast Brazil rainfall anomalies. *Journal of Climate*, 6(4), 743-758.

Hastenrath, S., & Heller, L. (1977). Dynamics of climatic hazards in northeast Brazil. *Quarterly Journal of the Royal Meteorological Society*, 103(435), 77-92.

Hastenrath, S., & Lamb, P. (1977). Some aspects of circulation and climate over the eastern equatorial Atlantic. *Monthly Weather Review*, 105(8), 1019-1023.

Hurrell, J. W., Kushnir, Y., Ottersen, G., & Visbeck, M. (2003). An overview of the North Atlantic oscillation. *The North Atlantic Oscillation: climatic significance and environmental impact*, 1-35.

Kang, S. M., Held, I. M., Frierson, D. M., & Zhao, M. (2008). The response of the ITCZ to extratropical thermal forcing: Idealized slab-ocean experiments with a GCM. *Journal of Climate*, 21(14), 3521-3532.

Kousky, V. E. (1979). Frontal influences on northeast Brazil. *Monthly Weather Review*, 107(9), 1140-1153.

Kousky, V. E., & Alonso Gan, M. (1981). Upper tropospheric cyclonic vortices in the tropical South Atlantic. *Tellus*, 33(6), 538-551.

Kousky, V. E., Kagano, M. T., & Cavalcanti, I. F. (1984). A review of the Southern Oscillation: oceanic- atmospheric circulation changes and related rainfall anomalies. *Tellus A*, 36(5), 490-504.

Mahajan, S., Saravanan, R., & Chang, P. (2010). Free and forced variability of the tropical Atlantic Ocean: Role of the wind–evaporation–sea surface temperature feedback. *Journal of Climate*, 23(22), 5958-5977.

Molion, L. C. B., & Bernardo, S. D. O. (2002). Uma revisão da dinâmica das chuvas no nordeste brasileiro. *Revista Brasileira de Meteorologia*, 17(1), 1-10.

Moura, A. D., & Shukla, J. (1981). On the dynamics of droughts in northeast Brazil: Observations, theory and numerical experiments with a general circulation model. *Journal of the atmospheric sciences*, 38(12), 2653-2675.

Namias, J. (1972). Influence of northern hemisphere general circulation on drought in Northeast Brazil. *Tellus*, 24(4), 336-343.

Nobre, P., & Shukla, J. (1996). Variations of sea surface temperature, wind stress, and rainfall over the tropical Atlantic and South America. *Journal of climate*, 9(10), 2464-2479.

Rajagopalan, B., Kushnir, Y., & Tourre, Y. M. (1998). Observed decadal midlatitude and tropical Atlantic climate variability. *Geophysical Research Letters*, 25(21), 3967-3970.

Souza, E. D., & Ambrizzi, T. (2002). ENSO impacts on the South American rainfall during 1980s: Hadley and Walker circulation. *Atmósfera*, 15(2), 105-120.

Souza, P., & Cavalcanti, I. F. A. (2009). Atmospheric centres of action associated with the Atlantic ITCZ position. *International journal of Climatology*, 29(14), 2091-2105.

Tavares, F. B., & de Araújo Júnior, I. T. (2012). Estrutura Econômica e Distribuição Interpessoal de Renda no Nordeste. *Dissertações de Mestrado*.

Terray, P., Delécluse, P., Labattu, S., & Terray, L. (2003). Sea surface temperature associations with the late Indian summer monsoon. *Climate Dynamics*, 21(7-8), 593-618.

Tomaziello, A. C. N. Variabilidade da Zona de Convergência Intertropical do Atlântico durante as estações seca e chuvosa da América do Sul tropical.

Torres, R. R., & Ferreira, N. J. (2011). Case studies of easterly wave disturbances over Northeast Brazil using the Eta Model. *Weather and Forecasting*, 26(2), 225-235.

Uvo, C. B., Repelli, C. A., Zebiak, S. E., & Kushnir, Y. (1998). The relationships between tropical Pacific and Atlantic SST and northeast Brazil monthly precipitation. *Journal of Climate*, 11(4), 551-562.

Uvo, C. R. B., & Uvo, C. R. B. (1989). A Zona de Convergência Intertropical (ZCIT) e sua relação com a precipitação da Região Norte do Nordeste Brasileiro. INPE.

Van Loon, H., & Rogers, J. C. (1978). The seesaw in winter temperatures between Greenland and northern Europe. Part I: General description. *Monthly Weather Review*, 106(3), 296-310.

Wainer, I., & Soares, J. (1997). North northeast Brazil rainfall and its decadal- scale relationship to wind stress and sea surface temperature. *Geophysical research letters*, 24(3), 277-280.

Walker, G. T. (1928). Ceará (Brazil) famines and the general air movement. *Beitr. Phys. d. Frein. Atmosph*, 14, 88-93.

Xie, S. P., & Carton, J. A. (2004). Tropical Atlantic variability: Patterns, mechanisms, and impacts. *Earth's Climate*, 121-142.

Yu, B., & Lin, H. (2016). Tropical atmospheric forcing of the wintertime North Atlantic Oscillation. *Journal of Climate*, 29(5), 1755-1772.